Carter, R.M., McCave, I.N., Richter, C., Carter, L., et al., 1999
Proceedings of the Ocean Drilling Program, Initial Reports Volume 181

3. Site 1119: Drift Accretion on Canterbury Slope[1]

Shipboard Scientific Party[2]

BACKGROUND AND OBJECTIVES

General Description

Site 1119 is located 96 km east of the eastern South Island shoreline, offshore from Timaru, within the Canterbury Basin (Fig. F1). The site was drilled in a water depth of 393 m on the upper continental slope and 5 km seaward of the edge of the continental shelf, which here lies at a water depth of 150 m. Farther seaward, the slope levels out onto an offshore platform at ~800–1000 m, which continues at a regional level across the tops of the Campbell Plateau and Chatham Rise. The site was located along *Maurice Ewing* multichannel seismic line 1E (Fig. F2), in a position ~5 km upslope from the head of a seafloor mass failure zone. Minor irregularities in the seafloor on either side of Site 1119 indicate that small-scale mass movement is also present in the vicinity of the drill hole, as confirmed by the 3.5-kHz profile through the site (Fig. F3A). These facts notwithstanding, drilling at Site 1119 penetrated through an area of seaward-dipping, continuous sub-bottom reflectors, within which any substrate failure is minor and probably shallowly based.

Multichannel profile Ewing-1E penetrates the complete thickness of the Cretaceous–Holocene Canterbury Basin succession and, below the bottom of Fig. F2, images the top of the inferred graywacke basement clearly. The seismic succession is threefold and comprises an onlapping Cretaceous to late Eocene sequence of nonmarine through shallow marine to offshore marine sediment (Onekakara Group), an Oligocene–earliest Miocene interval of flat-lying greensand and limestones (Kekenodon Group), and a Miocene–Holocene interval of eastward-prograding clinoform strata (Otakou Group). The equivalent stratigraphic intervals

F1. Locality map of Site 1119, p. 32.

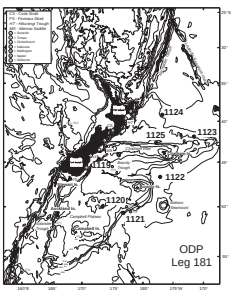

F2. Portion of multichannel seismic line, p. 33.

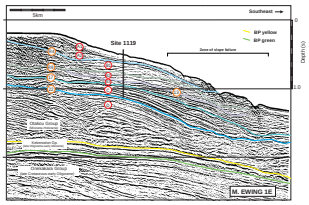

F3. Portion of 3.5-kHz precision depth recorder line, p. 34.

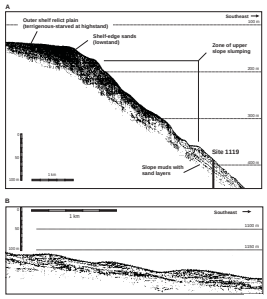

[1]Examples of how to reference the whole or part of this volume.
[2]Shipboard Scientific Party addresses.

Ms 181IR-103

have been well studied in the nearby onland Canterbury Basin (e.g., Carter, 1988; Field and Browne, 1989) and are also known from offshore exploration wells such as Clipper, which is located 40 km west-southwest of Site 1119 (Hawkes and Mound, 1984).

The clinoform reflectors within the Miocene–Holocene Otakou Group show considerable variability on line Ewing-1E, delineating features that superficially resemble nested submarine channels. Fulthorpe and Carter (1991) have shown that this seismic geometry occurs widely within a shore-parallel zone under the mid-Canterbury shelf-edge and that it represents a major field of sediment waves or drifts whose deposition commenced in the early Miocene. Individual drifts initiate at the toe of the slope and prograde landward, resulting in the creation of a shore-parallel gutter between a growing drift and the shelf-edge. Later, the gutter becomes filled, which causes the drift to accrete to the edge of the shelf (Fig. **F4**). Drilling was designed to penetrate the upper part of these drifts.

F4. Schematic development of sediment drifts, **p. 35.**

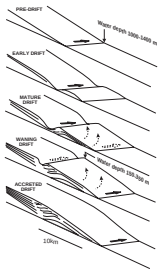

Site Objectives

Site 1119 was drilled to sample the Canterbury sediment drifts. Deposited in estimated paleo–water depths of 400–1000 m, the drifts were probably deposited from northward-flowing Antarctic Intermediate Water (AAIW) and Subantarctic Mode Water (McCartney, 1977), which originate by sinking at the Antarctic Polar Front and proximal to the Subantarctic Front, respectively. Flow may also have been driven by the predecessor current to the Antarctic Circumpolar Current. In either case, a copious source of sediment is required to build the drifts. Individual drift examples attain a relief of >1 km and have a shore-normal width of 15 km. Some drift activity continues today, as evidenced by the presence of 5-km wavelength, low-angle drifts at 1200-m depth on the modern seafloor (Fig. **F3B**). Site 1119 samples will allow the provenance of the Canterbury drift sediments to be established, paleocurrent velocities to be inferred, and the late Miocene–Pliocene history of the important AAIW water mass to be reconstructed. If sand-rich intervals are found in the hole, their presence may imply relative sea-level change during the late Miocene–Pliocene (cf. Fulthorpe and Carter, 1989).

The upper 40 m of sediment at Site 1119, above the conspicuous drift sequence shown on the multichannel seismic profile, appears on 3.5-kHz profiles as a series of transparent layers (muds) separated by thin, parallel reflectors (sands) (Fig. **F3A**). Although minor surficial slumping obscures the detail, the sands apparently thicken upslope, until at the shelf edge they comprise a hard reflecting zone of probable lowstand shoreface origin. The geometric evidence from the seismic profiles indicates a likely depth of deposition for the upper sediments from Site 1119 of ~240 m at lowstand (and therefore ~370 m for any intercalated offshore highstand strata). The glacial intervals in these sediments were thus deposited nearshore, under the influence of lowstand shorelines, and were provided with terrigenous sediment from the Alpine Fault plate boundary in the west. In apparent contrast, the older large sediment drifts were presumably deposited mainly under the control of regional current activity, from sources yet to be established, but which might include a southern, oceanic input. Confirming the provenance of the drifts, and whether or not a regional paleoceanographic change occurred between their deposition and that of the cyclic upper Pleistocene beds, were high-priority drilling objectives at Site 1119. In addi-

tion, continuous hydraulic piston-cores through the probable lowstand sediment wedges will provide an important high-resolution section of the mid-late Pleistocene on the upper slope, allowing its cyclicity and sequence stratigraphy to be established and compared with nearby sites, including DSDP 594 (Kennett et al., 1986), and with similar cyclothemic successions on land (Saul et al., 1999).

OPERATIONS

Sydney to Site 1119

The last line in Sydney cleared the dock at 0839 hr local time on 17 August 1998. The sea voyage to Site 1119 (proposed site SWPAC-1C) required 136.8 hr at an average speed of 9.7 kt. The planned track was to proceed on a southeasterly course, pass through Cook Strait between the North and South Islands of New Zealand, and then proceed directly south to Site 1119. However, because of heavy seas and bad weather that course was abandoned, and the vessel steered a southerly heading, taking the *JOIDES Resolution* around the southern tip of the South Island and then north to the site location.

The sizeable southern swell caused the voyage across the Tasman Sea to be slower than expected (9.6 kt average speed) and less comfortable than hoped for. When the vessel cleared the Foveaux Strait between the South Island and Stewart Island and turned northeast, the seas calmed and the vessel speed increased to 12 kt. Because no seismic survey was required, the vessel proceeded directly to the Global Positioning System coordinates of the location.

Hole 1119A

The positioning beacon was dropped at 0342 hr on 23 August 1998. The advanced hydraulic piston core/extended core barrel (APC/XCB) bottom-hole assembly was assembled, using an 11 7/16-in used RBI C-3 bit with a lockable float valve, and deployed. Hole 1119A was spudded with the APC at 1015 hr on 23 August. The recovery indicated that the water depth referenced to the dual elevator stool was 406.5 meters below rig floor (mbrf), equivalent to 395.50 meters below sea level (mbsl). Hole 1119A is a single-core hole designated for mudline sampling (Table **T1,** also in **ASCII format**).

T1. Site 1119 coring summary, **p. 72.**

Hole 1119B

The second hole of the site was spudded with the APC at 1050 hr on 23 August without offsetting the vessel. The seafloor depth inferred from recovery was 407.8 mbrf (396.8 mbsl). APC coring proceeded to 155.54 meters below seafloor (mbsf) when Core 17H did not achieve full stroke (Table **T1**). Cores were oriented starting with Core 3H. Heat-flow measurements were attempted with the Adara heat-flow shoe at 33.2 mbsf (4H), 61.7 mbsf (7H), 90.2 mbsf (10H), and 118.7 mbsf (13H), but could not be retrieved because the instrument had an electronic failure. The drill bit cleared the seafloor at 0020 hr on 24 August.

Hole 1119C

The vessel was offset 20 m to the east, and the bit was lowered 3 m before the initial mudline attempt to provide stratigraphic overlap in the sedimentary record. The seafloor depth inferred from recovery was 407.2 mbrf (396.2 mbsl). APC coring advanced to 160.3 mbsf, where piston coring was concluded when Core 17H failed to achieve a full stoke. XCB coring deepened the hole to the depth objective of 494.8 mbsf (Table T1). No hole problems were encountered.

Logging Operations at Hole 1119C

After pumping down the aluminum "go-devil," the hole was flushed with 60 barrels of high-viscosity mud. The drill string was pulled back in the hole to logging depth where the bit was positioned at 95.0 mbsf. Three logging measurements were scheduled for this hole. Logging operations began at ~2300 hr on 25 August. Three standard tool-string configurations were run: the triple combination, the Formation MicroScanner (FMS) with a sonic sensor (two passes), and the Geologic High Resolution Magnetic Tool (GHMT) (see **"Downhole Measurements,"** p. 29, in the "Explanatory Notes" chapter). Logging was conducted below the pipe at 80 mbsf to a hole obstruction at ~40 m above the bottom of the hole. The hole quality was poor, with an uneven borehole wall and many breakouts and ledges. The Nuclear Resonance Magnetic Sonde (measuring total magnetic field) on the GHMT suite failed to collect data for unknown reasons.

After logging was concluded by 1330 hr on 26 August, the Schlumberger equipment was dismantled. The drill pipe was lowered to 454 mbsf and the circulating head made up to the pipe. After filling the hole with 170 barrels of 12 pounds per gallon (1438 kg/m^3) heavy mud, the drill string was pulled out of the hole. While the drill string was being retrieved, the beacon was released and recovered, and the hydrophones and thrusters retracted and secured. At 1915 hr on 26 August, the vessel was under way to Site 1120.

LITHOSTRATIGRAPHY

Introduction

The Canterbury continental shelf, and, therefore, the lithology at Site 1119, are strongly influenced by the terrigenous input from New Zealand. Marked uplift of readily erodible rocks along the South Island Alpine Fault, coupled with a vigorous climate, have ensured delivery of large volumes of sediment to the Canterbury shelf (Gibb and Adams, 1982; Griffiths and Glasby, 1985). Much of the modern fluvial load is entrained within an active, along-shelf transport system, and it is mainly under glacial sea-level lowstands that significant quantities of sediment reached the continental slope (e.g., Carter and Herzer, 1979; Carter and Carter, 1993). Thus, at Site 1119 we can anticipate a eustatically controlled supply of terrigenous sediment. In addition, the Canterbury continental margin is swept by coastal and longslope currents, which results in the transport of sediment and subsequent formation of large sediment drifts along the continental slope (Fulthorpe and Carter, 1991). It is against this background of sea-level–controlled, terrigenous supply to a contour current that Site 1119 was drilled.

Description of Lithostratigraphic Units

The sedimentary sequence is divided into three lithostratigraphic units that are identified on the basis of sediment grain size and composition, together with downhole changes in bedding characteristics. The dominant criteria used for recognition of the units are visual observation of the core and estimates of core composition from smear slides (**"Site 1119 Smear Slides,"** p. 70), supported by shipboard measurements of calcium carbonate, physical properties, and bulk mineralogy using x-ray diffraction (XRD). These data, along with biostratigraphic control (see **"Biostratigraphy,"** p. 11), are summarized in Figures **F5** and **F6.** The three lithologic units fit well with the detailed seismic stratigraphy derived from the processed multichannel seismic line run by the *Maurice Ewing* in 1996 (see **"Background and Objectives,"** p. 1). This line also assisted in the subdivision of lithostratigraphic Unit II and in the paleoenvironmental interpretation.

Unit I

Interval: Core 181-1119A-1H; Core 181-1119B-1H through Section 10H-6; Core 181-1119C-1H through Section 10H-3
Depth: 0–6.01 mbsf (Hole 1119A); 0–88.2 mbsf (Hole 1119B); 0–87.3 mbsf (Hole 1119C)
Age: late to middle Pleistocene

Unit I extends from the present seafloor to ~88 mbsf and has a dominant lithology of greenish gray (5GY 5/1 to 5G 5/1) silty clay interbedded with subordinate silty sand and sandy silt. On seismic profiles it appears as a drape resting on a sequence of sediment drifts. The thickness of individual clayey beds is difficult to quantify because of expansion gaps in the core but, where intact, beds are commonly >2 m thick and reach a maximum thickness of 14 m. Sediments are often faintly mottled and banded with darker (greenish gray, 5G 4/1) and lighter (greenish gray, 5GY 6/1) tones (Fig. **F7**). Localized dark staining, associated with concentrations of pyrite, is also a common feature. Trace fossils are ubiquitous with *Asterosoma, Chondrites, Terebellina,* and *Thalassinoides* as the prominent forms. Smear slides reveal a prevalence of quartzofeldspathic silt grains and clay minerals with nannofossils as a prominent accessory. Siliceous sponge spicules are locally abundant. Mica is also present and gives the silty clay a distinctive speckled appearance in hand specimen. Macrofossils are sparsely scattered throughout the beds and include fragments, single and double valves of the mollusks *Tawera spissa* and *Zygochlamys delicatula* (Fig. **F8**), plus fragments of the brachiopod *Neothyris*. The presence of *Zygochlamys delicatula* is particularly important as it signifies cold-water conditions, which is consistent with the subantarctic microfauna of the clays (see **"Biostratigraphy,"** p. 11). Another indication that the silty clays were deposited during glacial periods is their close lithologic and stratigraphic similarity to clays from the offshore Canterbury region, whose glacial paleoclimatic signature has been reliably determined by stable isotopes (e.g., Nelson et al., 1986).

Contrasting with the glacial silty clays are scattered beds of olive-gray (5Y 5/1–5Y 5/2) sandy silt and silty sand. Bed thicknesses are typically <1 m, although in Core 181-1119B-6H a bed reaches 1.8 m (42.7–44.5 mbsf). Basal contacts with the glacial clays are usually, but not invariably, sharp and often include sand-filled *Chondrites* burrows below (Fig. **F9**). The sand-sized fraction is dominated by quartzofeldspathic grains

F5. Site 1119 summary log, **p. 36.**

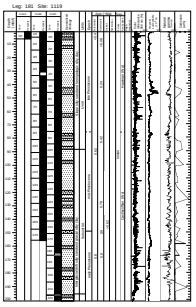

F6. Major components present on XRD profiles, **p. 39.**

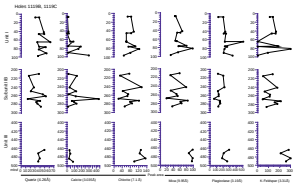

F7. Color banding in greenish gray silty clays, **p. 40.**

F8. Cored section showing intact valves of *Zygochlamys delicatula*, **p. 41.**

F9. Olive-gray silty sand overlying greenish gray silty clay, **p. 42.**

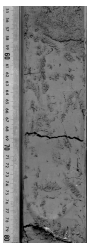

and varying numbers of foraminifers, with accessory quantities of opaque minerals and rock fragments. Nannofossils are conspicuous in the finer fraction. Macrofossils, especially valves of *Tawera spissa,* are also conspicuous. Although paleoenvironmental analysis of the microfaunal content was not carried out, the distinctive olive-gray color of the sediments and their stratigraphic position correlate well with documented interglacial deposits in the Canterbury region (e.g., Griggs et al., 1983; Nelson et al., 1986).

Unit II

Seismic profiles across Site 1119 depict the main bodies of two sediment drifts and the edge of a third. These deposits are represented in the core by lithostratigraphic Unit II, which can be divided into Subunits IIA, IIB, and IIC on the basis of bedding style and lithology.

Subunit IIA

Interval: Sections 181-1119B-10H-6 through 17H-CC; Sections 181-1119C-10H-3 through 21X-6
Depth: 88.2–155.54 mbsf (Hole 1119B); 86–196 mbsf (Hole 1119C)
Age: middle Pleistocene to early Pleistocene

Subunit IIA, corresponding to the youngest drift, extends from ~88 to ~196 mbsf. Its base corresponds to a prominent reflector marking the top of Subunit IIB drift. Cores show that the Subunit IIA drift is a succession of alternating silty clay and shell-bearing silty sand beds with the same color alternations as Unit I. Silty clays are mainly greenish gray (5GY 5/1) and the silty sands are olive gray (5Y 5/1- 5Y 5/2), suggesting that even though they form part of the drift, they nonetheless represent an interglacial/glacial cyclic sedimentation pattern similar to that described for the overlying sediments.

The greenish gray silty clays are the dominant lithology with beds commonly up to 6 m thick (given thickness inaccuracies caused by post-coring expansion of the sediment). Beds tend to have faint color banding and indistinct mottling that is associated with trace fossils such as *Planolites, Thalassinoides,* and *Chondrites*. Like sediments from Unit I, Subunit IIA hand specimens exhibit mica flakes, dark stains associated with pyrite, and scattered shell debris, but the quantities of the last two components are less than in their Unit I counterparts. Nevertheless, there were still sufficiently large fragments to identify the key molluscan species, *Zygochlamys delicatula,* which makes its last appearance (first time upcore) in Core 181-1119C-18X at 168 mbsf. As noted earlier, the presence of this species confirms the dominance of cold-water conditions at the site. In smear slides, the main constituents are clay, quartzofeldspathic silt, and nannofossils with accessory amounts of opaque minerals (?pyrite), foraminifers, mica, and, near the top of the subunit, radiolarians.

While the greenish gray silty clay beds of Unit I and Subunit IIA are similar, the olive-gray (5Y 5/1) silty sand beds of these units are different. Compared to Unit I lithologies, the underlying sand beds of Subunit IIA are more frequent and, on average, are thicker, typically >1 m. Some beds appear to be <1 m but their tops or bottoms are often missing at core voids, suggesting that the weakly consolidated sediments may have been washed out during drilling. Subunit IIA silty sand beds are further distinguished by their normal grading (Fig. **F10**), which may sometimes be repeated within a single bed without an intervening ero-

F10. Dark–light drift couplet in Unit II, **p. 43.**

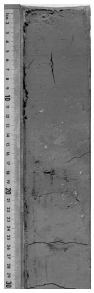

sional contact. Clayey sediments below the bases tend to be strongly bioturbated with olive-gray, sand-filled burrows of *Chondrites* and *Thalassinoides* standing out against the greenish gray, silty clay of the host sediment. These graded sands pass upcore to clayey silts, which have a gradational contact with the overlying greenish gray silty clays. Between 120 and 140 mbsf, the olive-gray beds become finer grained (clayey silt to silty clay), with gradational contacts at the top and bottom of each bed. In hand specimen, these fine-grained deposits are most readily distinguished by color from the greenish gray clays. Coarser, graded silty sand reappears below 140 mbsf. Hand specimen and smear-slide data further highlight differences with the Subunit IIA silty sands, being richer in shell debris, benthic foraminifers, and glauconite, compared to Unit I silty sands. Glauconite, however, still remains in accessory (<5%) amounts—this smear-slide observation is confirmed by XRD data.

Subunit IIB

Interval: Sections 181-1119C-21X-6 through 31X-2
Depth: 196–285.2 mbsf (Hole 1119C)
Age: early Pleistocene

Subunit IIB corresponds to the second drift that extends from ~196 to ~285 mbsf. Nearly all of this drift (~207–~275 mbsf) is early Pleistocene in age with the base possibly extending into the late Pliocene. It carries many of the lithologic features of Subunit IIA: thick beds of greenish gray (5GY 5/1) silty clay intercalated with thinner but nonetheless distinctive graded layers of olive-gray (5Y 5/2) shell-bearing silty sand with gradational tops and bioturbated bases. There is also a downcore change in grain size to finer grained (clayey silt to silty clay) beds with gradational bottoms and tops (274–280 mbsf). The ichnofossil assemblage of both subunits is similar with *Thalassinoides* and *Planolites* as common forms. However, *Chondrites* is less common than in Subunit IIA. Finally, the gross composition of both subunits is similar.

Despite the similarities, sufficient differences exist to warrant designation of the two subunits. The olive-gray drift sands have higher carbonate contents (60%–70% in Subunit IIB compared to <50% in Subunit IIA) that reflect higher concentrations of nannofossils, molluscan shell debris, and benthic foraminifers. Much of the shell material is too comminuted to allow reliable identification of genera. However, a few unbroken mollusks survive, including the bivalve *Limopsis* and the gastropod *Taniella*. In addition, Subunit IIB has higher quantities of mineral carbonate, which coincides with the first development of drilling biscuits, suggesting the sediment is becoming lithified through the formation of carbonate cement.

Of special note is the unique occurrence of a thin fine-sand turbidite in the greenish gray silty clays at 288 mbsf (Core 181-1119C-31X) (Fig. F11). The basal sand is 2 cm thick, but the top of the bed could not be pinpointed, as it merged with the ambient silty clays. Also evident in this core and other silty clay beds throughout Site 1119 is faint color banding. Smear slides of samples from a light-colored band and the overlying greenish gray clay (181-1119C-31X) showed that both sediments had similar compositions, with the notable exception of the light band, which contained only "rare" nannofossils in contrast to the overlying nannofossil-rich clay. The dearth of microfossils in the light band may reflect a turbidite origin either through direct river discharge at lowered sea level or remobilization of rapidly deposited sediment.

F11. Thin fine-sand turbidite, p. 44.

Whatever the case, the compositional differences and the association with a sand turbidite suggest that the color banding is a reflection of mud turbidite deposition.

Subunit IIC

Interval: Sections 181-1119C-31X-2 through 43X-2
Depth: 285.2–401 mbsf (Hole 1119C)
Age: late Pliocene to early Pleistocene

Subunit IIC encompasses a sequence of strong reflectors that represent the landward edge of a large drift as it thins toward the moat at the base of the late Pliocene paleoslope. On the basis of lithology, this subunit lies between ~285 and 401 mbsf. Again, alternations of greenish gray silty clay with olive-gray silty sand dominate the sequence. But, in contrast to the overlying subunits, the silty sand beds of Subunit IIC have (1) a higher concentration of carbonate (reaching 75%) (Fig. F5), and (2) a higher frequency of occurrence, with 16 silty sand beds per 100 m of section compared to 12 beds in Subunit IIA and 10 beds in Subunit IIB (note these numbers are based on the lithostratigraphic summary Figure F5 and, in reality, the numbers of individual beds, as recorded on the visual core logging sheets, will be higher). An abundance of silty sand may also be reflected in the poor core recovery of Subunit IIC, which was the worst of the entire Site 1119 core (Fig. F5). Recovered lithologies were mainly well-consolidated greenish gray silty clay, whereas silty sand beds, when present, were often incomplete. Furthermore, the silty sand typically occupied the core catcher, where it presumably was protected from washing out.

Unit III

Interval: Sections 181-1119C-43X-2 through 52X-CC
Depth: 401–494.8 mbsf (Hole 1119C)
Age: late to mid-Pliocene

The remainder of the cored section, from 401 to 494.8 mbsf, is almost exclusively greenish gray (5GY 5/1) silty clay. This firm sediment has been disrupted by the ubiquitous formation of drilling biscuits. For much of the section, the sediment appears to be moderately bioturbated with *Zoophycos* and a single occurrence of *Chondrites*. Despite sediment reworking, some mud turbidites may be present at 475 and 483 mbsf, as evinced by a rhythmic sequence of <3-cm-thick, greenish gray (5GY 6/1) laminae normally grading up to the typical greenish gray silty clay. Unit III has a mixed terrigenous/pelagic biogenic composition of clay, quartzofeldspathic silt grains, calcareous nannofossils, and minor amounts of foraminifers. Although XRD data points are scattered and semiquantitative, silty clays of Unit III also appear to be richer in mica and chlorite, compared to their Units I and II counterparts.

No glacial/interglacial signature could be discerned from the lithology.

Discussion

Boundaries between the units and subunits at Site 1119 have been identified on the basis of core lithology and with reference to the seismic stratigraphy (Fig. F2; Table T2). Prominent seismic reflectors can be correlated accurately to the cores using seismic velocities measured in

T2. Summary table of depths and thicknesses for seismic units and reflectors at Site 1119, p. 86.

the drill hole during the logging operations. The measured velocity increases downhole from 1375 to 1558 m/s.

In Unit I, we see the classic interglacial/glacial cyclicity found elsewhere in continental slope settings around New Zealand (e.g., Griggs et al., 1983; Nelson et al., 1986). The slope sands are interpreted to have accumulated during interglacial highstands, when the terrigenous supply to the outer continental shelf was reduced by both onshore alluviation and diversion along the shelf by the prevailing storm-forced current regime (Carter and Herzer, 1979). As a result, the shelf and slope were starved and the sand was presumably generated either from sediment reworked and redeposited from the shelf edge, from the reworking of older slope deposits, or from both these processes. Off the modern Canterbury margin, the shelf and slope down to ~400 m is subject to the north-flowing Southland Current and Front (Chiswell, 1996). This flow has a mean speed of ~6 cm/s but may exceed 30 cm/s when forced by storms (Carter and Herzer, 1979), when seasonal changes affect the density stratification of the Southland Front (Chiswell, 1996), and when flood tidal currents, which themselves are intensified by the slope topography, reinforce the current. Combine this with the superimposed effects of large surface waves and internal waves breaking against the shelf edge (Carter and Herzer, 1979), then sediment transport will take place. While observations of the flow regime over the upper slope are sparse, the presence of eroded sediments in 3.5-kHz profiles (Carter et al., 1985; Herzer, 1981) and gravel/sand lags on shelf/slope terraces (Carter et al., 1985), attest to the power of modern currents to erode and move bedload.

In contrast, glacial periods were times of high sediment supply to the shelf edge and slope, as witnessed by the thickness of the greenish gray silty clay beds at Site 1119, and by sedimentation rates measured for various parts of the eastern South Island margin, Carter et al. (unpubl. data), for example, indicate a two- to fourfold increase in the noncarbonate sediment flux in the last glaciation, compared to the Holocene. At times of lowered sea level, South Island rivers extended across the emergent continental shelf and discharged their loads close to the shelf edge (Carter et al., 1986). Fine silt and clay, settling through the water column, together with pelagic biogenic detritus and aeolian dust, contributed a hemipelagic component to bottom sediments. Mud turbidites also may have contributed to the glacial sediment budget, but unequivocal turbidites are scarce in the core. Finally, sediment may have been swept into the area from the south by the ancestral Southland Current. It is unlikely that the current generated fine-grained sediment through reworking of the substrate, as there is a lack of moating in Unit I (see **"Background and Objectives,"** p. 1).

Unit II also accumulated under a climatically controlled sediment supply, as indicated by the alternations of greenish gray silty clays (glacial) and olive-gray silty sands (interglacial). However, compared to the slope drape deposit of Unit I, Unit II accumulated as a series of drift deposits. The seismic architecture of shelfward-migrating, mounded reflectors, with each mound separated from the paleoslope by a moat, identifies the mounds as shelf-parallel drifts (Fulthorpe and Carter, 1991). These authors surmised that the drifts were deposited by a contour current flowing along the Canterbury slope since Miocene times. The moats were identified as zones of either nondeposition or erosion, where the current was topographically intensified against the slope under Coriolis deflection (to the left facing downcurrent in the Southern Hemisphere). Such an inference requires that the current flowed north.

For Site 1119, a key issue is how the lithologic data compare with the seismic interpretation of drift sedimentation by Fulthorpe and Carter (1991). Lithologic characteristics of sandy and muddy drift deposits (contourites) have been summarized by Stow and Holbrook (1984). For "sandy contourites," these authors cite features such as fine irregular layering, extensive bioturbation, poorly sorted silt/sand (although well sorted sands may also occur), and mixed terrigenous and shell-bearing sands. For "muddy contourites," key features are homogeneity with poor or no bedding, rare silt laminae, bioturbation structures, mainly silty mud with <15% sand, and elevated carbonate levels. While these generalized criteria fit the Canterbury slope sediments well, there remains the possibility that some beds, in particular those with well-defined graded intervals, may be (silt or) mud turbidites. Certainly, the presence of a thin (<1 cm), graded, very fine sand bed with a sharp, eroded base indicates an incursion by a turbidity current into the greenish gray silty clay facies of Unit II. Mud turbidites may also have contributed to this facies, as suggested by occasional color banding. However, unless much of the banding has been obliterated by bioturbation, which is unlikely, the influence of turbidites in the glacial silty clay facies appears to be fairly minor. The graded beds in the interglacial silty sand are also discounted as turbidites because (1) they lack any components other than "A" of the classic Bouma sequence, (2) normal graded sequences may be repeated in a single bed without an erosional contact between each sequence, and (3) some normal graded beds are preceded by reverse graded sediments without an obvious break in succession. Such features are more consistent with deposition under a fluctuating current rather than a continuously decelerating turbidity current.

Assuming that a contour current had a significant influence on Unit II sedimentation, the following events are envisaged. During interglacial sea-level highstands, the terrigenous supply of sediment to the upper slope was reduced. Sediment reaching the upper slope was probably a mixture of terrigenous and biogenic shell debris reworked from the shelf edge terraces (e.g., see Carter et al., 1985) and sand winnowed from underlying drift deposits. In each of Subunits IIA and IIB, the resultant olive-gray, shell-bearing, silty sands exhibit a distinctive downcore trend of (1) a succession of single and multiple graded beds with sharp bases that are commonly bioturbated to (2) a succession of finer-grained beds with gradational top and bottom contacts with the glacial silty clays, to (3) a return to the coarser silty sand beds with sharp basal contacts. Such a trend may be related to variations in the local speed of the current and/or to changes in the supply of sediment to the current. Under glacial sea-level lowstands, Site 1119 received large quantities of silt and clay from (1) river discharge near the shelf edge, (2) contour current transport from southern sources, (3) minor turbidity currents, and (4) aeolian detritus swept from the Canterbury Plains (e.g., see Stewart and Neall, 1984; Ives, 1973). Results of XRD suggest a downcore change from calcic to potassic feldspar (Fig. **F6**), possibly indicating a change in source of the clay component. One possibility is that if the potassic feldspar has in part a plutonic source, then it could mean a southerly provenance (e.g., the plutonic complex of Stewart Island). Detailed mineralogical work is required to confirm this. Whether or not climatic fluctuations affected the speed of the contour current itself has yet to be determined.

Unit III, at least in the core section, carries no obvious lithologic signature of the paleoclimatic fluctuations evident in the overlying units.

It is possible that some sand beds may have been lost from Unit III during the coring. Whatever the case, the lithologic and seismic data show the unit is a widespread mud drape overlying a large drift of probable middle to early Pliocene age. Reasons for the change from drift to mud drape require further investigation.

BIOSTRATIGRAPHY

Introduction and Summary

The micropaleontological biostratigraphy of Site 1119 is mostly based on the onboard study of core-catcher samples. Hole 1119B samples were used for the upper part of the section and Hole 1119C samples for the lower part. Additional samples were taken from within selected cores to address specific age and paleoenvironmental questions. The absolute ages assigned to biostratigraphic datums follow the references listed in Tables **T2,** p. 59; **T3,** p. 60; **T4,** p. 63; and **T5,** p. 64; all in the "Explanatory Notes" chapter.

There are no obvious long hiatuses in Site 1119. Using our best fit from the constraining datum levels from all four microfossil groups, we conclude that Site 1119 cored a near-complete section of late Pliocene and Pleistocene sediments (Table **T3**). The Pliocene/Pleistocene boundary (1.8 Ma) is near 300 mbsf, and the base of the section, at 494 mbsf, approximates the middle/late Pliocene boundary (~2.6–2.8 Ma), or is somewhat older (~3.8 Ma) on foraminiferal evidence.

T3. Correlated biostratigraphic events, **p. 87.**

Calcareous Nannofossils

The nannofossil content is variable throughout the site but is generally common or abundant (Table **T4**). The preservation is generally good to moderate in the lowermost part of the section (Cores 181-1119C-46X to 52X) and from Core 181-1119C-33X to the top. The preservation is moderate to poor between Samples 181-1119C-34X-CC and 45X-CC, displaying dissolution, overgrowth, and recrystallization; Samples 181-1119C-40X-CC and 41X-CC are almost barren.

T4. Identification and abundance of nannofossils, **p. 88.**

Emiliania huxleyi is abundant in the uppermost part of the section and dominates the nannofossil assemblages in Samples 181-1119C-1H-CC and 2H-CC. The first occurrence (FO) of this species (0.24 Ma) occurs in Sample 181-1119C-5H-CC. The acme of the same species is recorded in the two uppermost core-catchers. The age of the bottom of this acme zone in the Pacific has been estimated to be at 0.12 Ma or 0.085 Ma (Table **T1**). *Pseudoemiliania lacunosa* has a sporadic distribution and very low abundance throughout the section. The last occurrence (LO) of this species (0.42 Ma) occurs in Sample 181-1119C-9X-CC.

Medium-sized *Gephyrocapsa* (which includes specimens with a maximum length between 3.5 and 5.5 µm and diagonal bridge: *Gephyrocapsa oceanica* s.s., *Gephyrocapsa caribbeanica, Gephyrocapsa sinuosa*) are common or abundant from the top of the section down to Sample 181-1119C-17X-CC. Gephyrocapsiids with a crossbar aligned to the short axis of the central opening, identified as *Gephyrocapsa parallela* in this study, occur in intervals from Samples 181-1119B-14X-CC to 17X-CC. The FO of *G. parallela* has been calibrated to the uppermost Matuyama Chron around the Jaramillo Event (Takayama, 1993). The top of the acme of *G. parallela* is reported as 0.78 Ma, around the Matuyama/

Brunhes boundary in the northwestern Pacific.

The nannofossil assemblage is dominated by small *Gephyrocapsa* (specimens <3.5 µm in size) in the interval between Samples 181-1119C-18X-CC and 26X-CC; in this interval medium-sized *Gephyrocapsa* are virtually absent. A major change occurs in Sample 181-1119C-27X-CC, where large *Gephyrocapsa* (specimens >5.5 µm) are abundant. Large *Gephyrocapsa* occur from Samples 181-1119C-27X-CC to 29X-CC (~1.24 to ~1.46 Ma). Medium-sized *Gephyrocapsa* are common again below Sample 181-1119C-29X-CC.

The LO of *Helicosphaera sellii* occurs in Sample 181-1119C-27X-CC. Different values for the absolute age are given for this event (all between 1.2 and 1.65 Ma). The last appearance of *H. sellii* appears to be time transgressive from tropical to mid-latitudes, with a range from 1.5 to 1.2 Ma. For the time being, we have adopted an age of 1.26 Ma for the LO of *H. sellii*.

The FO of medium-sized *Gephyrocapsa* is recorded in Sample 181-1119C-32X-CC. This event should correspond to the FO of *Gephyrocapsa oceanica* s.l. (1.7 Ma), the FO of *G. caribbeanica* (1.66 Ma), the FO of *Gephyrocapsa* >4 µm (1.71 Ma), and to the FO of *Gephyrocapsa sinuosa* (~1.75–1.8 Ma). This event has been detected to be slightly above the top of the Olduvai Event, and has been used as a good marker for the Pliocene/Pleistocene boundary (1.81 Ma).

Dictyococcites productus is common or abundant throughout the section, but becomes dominant in the lower part, below the FO of medium-sized *Gephyrocapsa*. The genus *Calcidiscus,* represented mostly by *C. leptoporus,* is sporadic throughout the section. *Calcidiscus macintyrei* is present only in two samples (Samples 181-1119C-29X-CC and 49X-CC), and thus in this section the LO of this species cannot be used for biostratigraphic correlation.

Only one specimen, not well preserved, of *Discoaster asymmetricus,* is recorded in Sample 181-1119C-52X-CC. Its LO is reported to be close to that of *D. tamalis,* tied to at an absolute age of ~2.8 Ma. Nevertheless, the paucity of discoasterids in the temperate and subantarctic area in the Southwest Pacific during the Pliocene (Lohman, 1986) hampers the recognition of any reliable markers to date the Pliocene sequences below Core 181-1119C-32X.

Reworked nannofossils are sporadic throughout the section—*Cyclicargolithus floridanus, C. abisectus, Dictyococcites bisectus,* and *Discoaster deflandrei,* from the late Eocene–early Miocene—are the most common. Miocene species, such as *Helicosphaera ampliaperta, Reticulofenestra pseudoumbilicus, Sphenolithus moriformis, S. neoabies,* and *S. heteromorphus,* occur in a few samples.

Foraminifers

Foraminiferal assemblages are generally rich and well preserved, and planktonic forms compose 60%–95% of the total. Less well-preserved, slightly recrystallized, and glauconite-filled assemblages occur in the sandy, micritic horizons lower in the section (e.g., in Sample 181-1119C-38X-1, 64–68 cm) (Tables **T5, T6**). Throughout the section the assemblages are dominated by *Globigerina bulloides, G. quinqueloba,* and other small *Globigerina* species. *Neogloboquadrina pachyderma* (mostly sinistrally coiled) is present throughout, generally being more common higher in the section. *Globorotalia scitula* is present in low numbers throughout most of the section. One specimen of *Globorotalia hirsuta*

T5. Identification and abundance of planktonic foraminifers, **p. 89.**

T6. Identification and abundance of benthic foraminifers, **p. 90.**

(FO 0.45 Ma) is present in Sample 181-1119B-1H-CC and it occurs no lower.

Typical 3- to 3.5-chambered *Globorotalia inflata* is the dominant globorotaliid down to Sample 181-1119C-18X-CC; below this level the morphotype becomes more rounded and smaller, with the taxon present in lower numbers. The highest occurrence of a compressed form of *Globorotalia puncticulata,* locally called *Globorotalia puncticuloides,* is in Sample 181-1119C-18X-CC. It replaces *G. inflata* as the most common globorotaliid from Sample 181-1119C-19X-CC to almost the bottom of the section. The LO datum of *G. puncticuloides* in this region is not well tied to an absolute age (~2 Ma in DSDP Hole 593; ~0.7–0.8 Ma in DSDP Hole 284; ~0.8 Ma in DSDP Hole 594). It is just above the Brunhes/Matuyama boundary (0.78 Ma) at Site 1122.

Globorotalia truncatulinoides occurs sporadically in low numbers down to 181-1119C-18X-CC, but no lower. Although the Atlantic and Pacific FO datum of *G. truncatulinoides* morphotypes is 2.6 Ma, it is known to be sparse or absent at southern, austral latitudes through most of the Pliocene and in the lower Brunhes Chron interval in DSDP Holes 284 and 594 (Hornibrook and Jenkins, 1994). Thus, a local FO at Site 1119 near 0.8 Ma is not surprising. No specimens of its ancestor, *Globorotalia tosaensis,* were found. Similar to nearby DSDP Site 594, the LO of *G. puncticuloides* overlaps one core with the FO of *G. truncatulinoides,* at the base of the local *G. truncatulinoides* zone (Hornibrook and Jenkins, 1994) and near the base of the Brunhes polarity interval (0.78 Ma).

Globorotalia crassula (FO 2.6 Ma) occurs in low numbers down to Sample 181-1119C-41X-CC. The FO of related *G. crassacarina,* as far as may be determined from its rare presence, is in Core 31X, confirming an age younger than 2.6 Ma (late Pliocene). Unkeeled sinistral *Globorotalia crassaformis* morphotypes occur sporadically throughout the lower half of the section with a narrow dextral zone (2.1–3.0 Ma) in Sample 181-1119C-41X-CC. Thus, this sample is dated as late Pliocene (2.1–2.6 Ma, early Nukumaruan Stage). Unit III (Cores 181-1119C-43X to 52X) appears to be below the dextral *A. crassaformis* zone (2.1–3.0 Ma) but all, except 52X-CC, are dominated by *Globorotalia puncticuloides* (FO 3.6 Ma) and are dated as mid-Pliocene (3.0–3.6 Ma). The lowest sample (Sample 181-1119C-52X-CC) has dominant *Globorotalia puncticulata* (LO 3.7 Ma) and is presumably ~3.7–4.0 Ma, mid-Pliocene (late Opoitian Stage).

In on-land sections from New Zealand of late Neogene age, a number of benthic foraminifer first and last occurrences have been documented (Hornibrook et al., 1989), which are of potential stratigraphic value, although undoubtedly diachronous because of local paleoenvironmental changes that are difficult to gauge. One of the best documented biostratigraphic datums is the FO of *Saidovina karrerianum* (Haweran [Wq]–Holocene, <0.4 Ma); unfortunately, the species appears not to be present at Site 1119. Of a number of species documented with LO datums in the Nukumaruan Stage (Wn, 2.6–1.1 Ma), five are recorded in Site 1119 samples: *Plectofrondicularia pellucida* (LO in Sample 181-1119B-13H-CC), *Bolivina affiliata* (LO in Sample 181-1119B-15H-CC), *Anomalinoides parvumbilius* (LO in Sample 181-1119C-18-CC), *Haeuslerella pliocenica* (LO in Sample 181-1119C-36X-CC), and *Karreriella cylindrica* (LO in Sample 181-1119C-38X-1, 64–68). We consider that the first three events are probable upward extensions of their local stratigraphic ranges into the Castlecliffian Stage (Wc, <1.1 Ma). *Haeuslerella* is an endemic New Zealand genus that is common in shelf to upper-

most bathyal facies in the Neogene, and its on-land absence from Castlecliffian strata is well tested and probably reliable. We are therefore confident that the LO of *Haeuslerella* in Sample 181-1119C-36X-CC is not younger than latest Nukumaruan (Wn, >1.1 Ma). An examination of its recorded occurrence in the New Zealand fossil record system indicates that it becomes extinct within the Nukumaruan at a level estimated by G.H. Scott (pers. comm., 1998) of ~2 Ma, an age remarkably coincident for this level with the evidence from other microfossil groups.

The extinction of *Plectofrondicularia advena* (~0.62 Ma) is one of the events recorded worldwide in the *Stilostomella* Extinction Event. Its last occurrence here is in Sample 181-1119B-10H-CC.

In Unit II (Cores 181-1119C-28X through 1119C-44X), the *Globigerina* ooze assemblage is more indurated, with micritic aggregates, encrusted mollusk and echinoid stems, and much glauconite. This level possibly reflects a brief stratigraphic hiatus or condensed section in the late Pliocene.

Diatoms

Diatoms are present in varying amounts through the Pliocene and Pleistocene sedimentary record recovered at this relatively shallow site (Table T7). Their overall abundance is low because of strong dilution with terrigenous detritus at this location. The preservation of the diatoms is generally good.

T7. Identification and abundance of diatoms, p. 92.

Species used in the low-latitude zonal scheme are completely absent from the sediments at this site. Of those species used in zonal schemes for the Antarctic–subantarctic region, only three species were encountered. *Actinocyclus ingens* is present below Sample 181-1119B-15-CC, giving an age for these sediments of >0.65 Ma. A single, poorly preserved specimen of *Nitzschia weaveri* was found in Sample 181-1119C-48-CC, which suggests an age older than 2.74 Ma. The third species is *Nitzschia praeinterfrigidaria*. It occurs only in Sample 181-1119C-38-CC, though in this sample relatively frequently. Following Harwood and Maruyama (1992), this species indicates an age between 3.7 and 4.9 Ma. The preservation of the valves and the composition of the diatom assemblage does not indicate that these specimens of *N. praeinterfrigidaria* are reworked. Nevertheless, the presence of this species at this core depth definitely disagrees with the other fossil datums found for this Hole.

Radiolarians

Throughout the section, radiolarians are rare, and, because of terrigenous dilution, numbers per slide do not exceed 50. Radiolarian faunas are more prevalent in the upper part of the section, but diversity is consistently low (Table T8). Samples from the section lower than Core 181-1119C-23X are mostly barren, except Samples 181-1119C-25X-5, 111–113 cm, and 181-1119C-38X-2,110–111 cm.

T8. Identification and abundance of radiolarians, p. 94.

In the upper part of the section, the predominant species are those characteristic of Antarctic/subantarctic waters (e.g., *Antarctissa strelkovi, A. cylindrica,* and *A. denticulata*). *Spongotrochus glacialis, Triceraspyris antarctica,* and *Phorticium clevei* are also present high in the section.

Lithelius nautiloides (FO 1.93 Ma) occurs sporadically from Samples 181-1119B-4H-CC to 181-1119C-31X-CC. *Pterocanium trilobum* (LO 0.83 Ma) occurs in Sample 181-1119C-25X-5, 111–113 cm. A typical form of

Eucyrtidium calvertense (LO 1.92 Ma) is present in Sample 181-1119C-38X-2, 110–111 cm.

Paleoenvironment

Calcareous Nannofossils

Throughout the core, the nannofossil assemblages consist mainly of subantarctic flora with a few temperate forms. Subtropical species are virtually absent. The ratio of *Calcidiscus leptoporus* + *Helicosphaera* spp. to *Coccolithus pelagicus* appears to be a good indicator of sea-surface temperature in the subantarctic waters in this area: the higher the ratio, the warmer the sea-surface water mass (Hiramatsu and De Deckker, 1997a).

A detailed study of Core 181-1119C-25X's succession of nannofossil assemblages in a depositional cycle spanning ~6 m was conducted. At the base of the cycle, sediments consist mainly of silt enriched in carbonate particles. Nannofossils are generally abundant and diverse. They are dominated by the subantarctic flora, but species that are more or less characteristic of temperate water masses, such as *Helicosphaera carteri, H. sellii,* and *Syracosphaera* spp. (Hiramatsu and De Deckker, 1997b), have been added to the assemblage. The sizes of small placoliths (*Reticulofenestra, Dictyococcites*) are bigger than those deposited in the finer sediments within the cycle. The coarseness of the sediments, the occurrence of tunicate spicules, and bioclastic materials imply that the sediment was transported downslope from the edge of the adjacent continental shelf. However, very few reworked nannofossils are present. We interpret the basal part of the cycle (characterized by coarser sediment) as being deposited during a warmer interglacial period when sea level was at a highstand.

In contrast, in intervals of fine sediment, nannofossil assemblages are enriched with cold-water–dwelling species, such as *Coccolithus pelagicus, Calcidiscus leptoporus,* and small gephyrocapsids (Hiramatsu and De Deckker, 1997a). The assemblages show low abundance and low diversity of indigenous species but contain reworked Cenozoic nannofossils, such as *Cyclicargolithus floridanus, Dictyococcites bisectus, Reticulofenestra pseudoumbilica,* and occasionally discoasterids as well as sphenoliths. The low abundance of nannofossils is considered to be a result of the dilution effect of the increased influx of terrigenous sediments during glacial periods. *Pontosphaera* species generally only occur in the fine-sediment intervals. The size of small placoliths (*Reticulofenestra minutula, R. minuta, Dictyococcites productus, D. perplexa*) is smaller than those deposited during the warm sea-level highstand. The small-sized placoliths are generally considered to be r-selected species, indicative of eutrophic conditions (Young et al., 1994). Some of the fine sediment samples contain abundant pyrite and/or rhombohedral dolomite plates, indicative of strong sulfate reduction. The low diversity and r-selected nannoflora, together with high degree of sulfate reduction (and, therefore, high content of organic matter) suggests that the sediments were deposited in a nearshore setting with high nutrient content. We consider that this part of the cycle was deposited during glacial intervals while sea level was low. The nannoflora is indicative of a coastal eutrophic environment.

Foraminifers

Foraminifer assemblages at Site 1119 consistently are rich in planktonic taxa (60%–95% of foraminifer faunas), indicative of the open-marine, normal salinity environment expected at the site, which at present is situated ~96 km from land. Throughout the section, globigerinid taxa prevail; turborotaliids are rare to common; semi-keeled to keeled globorotaliids and also *Orbulina* are rare; *Globigerinoides* is absent. Hence, the assemblage overall is indicative of a cool to temperate surface water mass (see below). At many levels, the assemblage, and in fact the sediment as a whole, may be characterized as a *Globigerina* ooze, with a consistent admixture of silt-sized, angular quartz, and mica wafers. The most common globigerinid taxa include *Neogloboquadrina pachyderma* (mostly sinistrally coiled), *Globigerina quinqueloba, G. umbilicata, G. bulloides,* and "nondescript" *Globigerina* spp., with less common *Globigerinita glutinata, G. uvula,* and rare *Globigerinella aequilateralis*.

In lithostratigraphic Units I and II (between 181-1119B-1H and 181-1119C-27X-CC), there is an alternation between assemblages that are characterized by (1) globigerinid-dominant fauna with micromollusks and quinqueloculinid benthic forms (including large *Pyrgo anomala*) and, at Sample 181-1119B-17H-CC, masses of siliceous sponge spicules, and (2) the same globigerinid assemblage with consistently more temperate water mass indicators like *Orbulina universa, Globorotalia inflata, G. truncatulinoides, G. crassula,* and *G. scitula*. The latter assemblage also contains (benthic) *Planulina wuellerstorfi, Discanomalina semipunctata,* and common *Globocassidulina curvata,* indicative of upper bathyal or deeper conditions. This contrasting alternation of the two assemblages is seen in core-catcher samples between Cores 181-1119B-1H to 181-1119C-19X, with the warmer and deeper marine component in the coarser lithologies, and the colder and likely shallower assemblage, more tolerant of a neritic water mass and coastal conditions, in the finer lithologies. The finding suggests a systematic pattern reflecting shallower and colder glacial conditions alternating with warmer and deeper interglacial ones in an outer shelf to upper bathyal setting, consistent with the seismic geometry of the site.

To further test this finding, a set of samples was taken from within Core 181-1119C-25X, from fine and coarse horizons:

1. Two samples were taken from near the top of a thick, fining-upward cycle, in a hemipelagic clay (Samples 181-1119C-25X-2, 123–125 cm, and 25X-2, 140–146 cm). This fine interval has a low abundance of foraminifers per unit volume of sediment. It has more abundant *N. pachyderma* than the coarse interval, but far less common globorotaliids, and a slightly lower percentage of benthic foraminifers. The assemblage lacks the deeper marine *Uvigerina* and *Melonis,* has a virtual absence of *Planulina,* but includes *Plectofrondicularia* and *Bulimina;* in addition, there is an abundance of smooth-shelled ostracodes. Among the planktonic forms, there are also more *Globigerinita uvula* and *G. glutinata,* which are tolerant of coastal water masses. We interpret the assemblage as indicative of shallower marine, probably outer shelf to uppermost bathyal conditions, influenced more by cool surface water masses. The low abundance of foraminifers suggests more rapid sedimentation than in the coarser interval.

2. Two decimeter-thick, coarse-grained, sandy levels (Samples 181-1119C-25X-2, 33–37 cm, and 25X-6, 56–58 cm) were sampled, above and below the fine interval, at the base of two consecutive cycles. This coarse interval is rich in molluscan and echinoderm debris and in benthic foraminifers including *Quinqueloculina* spp., *Notorotalia* spp., *Pyrgo anomala, Planulina ariminensis, Anomalinoides sphericus, Discanomalina semipunctatus, Sphaeroidina bulloides, Nonionellina flemingi, Melonis barleanum, Uvigerina peregrina,* and *Bolivinita pliozea,* with rare *Epistominella exigua*. The dominant globigerinid assemblage is enriched with *Globorotalia puncticuloides* (common), *Globorotalia crassicarina–G. crassula, G. inflata,* and frequent ornamented ostracodes. The assemblage as a whole contains a second component consisting of dark-colored, abraded tests with glauconite fill, likely reworked from slightly older levels. This assemblage in the coarse interval likely indicates an upper bathyal (200–400 m) setting with temperate water-mass incursions in agreement with an interglacial highstand period. The number of foraminiferal tests per unit volume of sediment is ~20 to 50 times greater than in the adjacent fine unit, suggesting sediment starvation during accumulation of the coarse unit and possibly also higher surface-water productivity.

The analysis of samples at the bottom and top of a fining-upward sediment cycle was repeated in a sample pair from Core 181-1119C-38X. Here the coarse horizon (Sample 181-1119C-38X-1, 64–68 cm) is a green, micritic, glauconitic, foraminiferal sand with a rich and diverse, though less well preserved, planktonic and benthic foraminiferal fauna. The fine horizon (Sample 181-1119C-38X-2, 100–107 cm) is a gray hemipelagic mud from near the top of a thick, fining-upward unit and has a sparse fauna of small planktonic and benthic foraminifers. These faunal differences are very similar to those documented in the higher cycle. We conclude that the coarser beds represent higher energy, deeper marine, sediment-starved, well-oxygenated, interglacial conditions, with the fining-upward muddy part of the sediment cycle indicating colder and shallower marine conditions, with higher sedimentation rates, when sea level dropped toward the peak of each glacial period.

In lithostratigraphic Unit III, in the lower parts of the section (below Core 181-1119C-44X), the sediment is dominantly hemipelagic clay containing low concentrations of a rich and diversified planktonic and benthic foraminiferal assemblage, very similar to the coarse intervals of Unit II (above), with the consistent addition of *Cibicidoides pachyderma* and *C.* aff. *pachyderma* (LO in Core 181-1119C-41X-CC). The benthic fauna is dominated by a mixture of *Astrononion novozelandicum, Cassidulina carinata, Discorbinella bertheloti, Epistominella exigua, Nonionellina flemingi,* and *Notorotalia* spp. In late Pliocene time, a deeper upper bathyal (~300–600 m water depth) setting is inferred for Unit III at Site 1119.

Diatoms

The dominant diatom species found are cosmopolitan neritic species. Subantarctic species are subordinate and generally occur in higher numbers only in samples rich in diatoms from the gray, clayey silts deposited during glacial periods (compare the species in Samples 181-1119C-16H-8, 60–61 cm, 17H-5, 97–98 cm, 18X-CC, 21X-CC, 22X-CC,

28X-CC, 31X-CC, 32X-CC, 35X-CC, 38X-CC, 48X-CC). Occurrence of subantarctic species in the olive-gray, sandy interglacial sediments (e.g., Sample 181-1119C-17H-CC) is rare and restricted to intervals with generally higher biogenic silica. The abundance of diatoms is controlled by productivity. As productivity is highest during periods of increased terrigenous input, the changes in diatom abundance can be expected to reflect changes in overall sedimentation rates. Using this relationship, higher sedimentation rates can be postulated for the times documented in core intervals between 130–210, 240–260, and 310–390 mbsf at Site 1119 (Fig. F12).

A study of the diatoms in five samples through one sedimentary cycle in Core 181-1119C-25X showed the following pattern. Diatoms were absent from the glauconitic, interglacial sands at the base of the cycle. A low-diversity flora, dominated by neritic, cosmopolitan taxa with just a few subantarctic species, occurs in the gray clayey silts. It is inferred to have been deposited during a glacial period with increased productivity. Higher up in the gray silty clays, the abundance of diatoms in the sediment decreases. The samples from the upper part of the cycle contain only traces of diatoms.

F12. Relative abundance of diatom valves vs. core depth at Site 1119, p. 45.

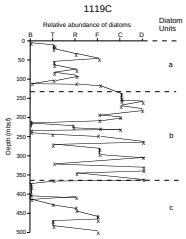

Mollusks

Fossil mollusks occur commonly throughout the upper parts of cores from Site 1119, especially in Units I and II. Single valves of *Tawera spissa* and, at deeper levels, *Limposis peteri,* are the dominant macrofossil in the inferred interglacial (highstand) sand intervals, and in situ double valves of *Zygochlamys delicatula* occur frequently in the inferred glacial (lowstand) silt beds. The glacial silts also contain archibenthal gastropods, including *Cominella* (*Eucominia*) *alertae, Aeneator* (*Ellicea*) *recens, Provocator mirabilis,* and *Pliconacca denticulifera* (Table T9). This molluscan fauna is similar to the upper bathyal fauna that occurs today on mud substrates on the New Zealand upper slope.

T9. List of fossil mollusks from Site 1119, p. 96.

Paleoenvironment Summary

Site 1119 microfossils appear to document a slight overall shallowing through the late Pliocene and Pleistocene, from deeper upper bathyal (300–600 m) to uppermost bathyal-outer shelf (100–400 m) depths. The cycles of coarse and fine sedimentation in the upper two-thirds of the section contain alternating assemblages. The fine-grained intervals contain assemblages with dominantly cool, neritic, shallow-water affinities and were presumably deposited in glacial periods. The coarse-grained intervals contain similar assemblages, but with variable additions of temperate planktonic taxa and benthic foraminiferal indications of slightly deeper water; these were presumably deposited in interglacial periods.

PALEOMAGNETISM

All core archive halves from Holes 1119A and 1119B and those between 131.80 and 494.80 mbsf of Hole 1119C were measured on the shipboard pass-through cryogenic magnetometer. Declination, inclination, and intensity of natural remanent magnetization (NRM) and a 20-mT alternating field (AF) demagnetization step were routinely measured at 10-cm intervals. When time permitted, a 10-mT demagnetiza-

tion step was also measured and some core sections were measured at 5-cm intervals. In situ tensor tool data were collected at the tops of APC cores in an attempt to determine azimuthal orientation of the core to 160 mbsf. The measurements, however, proved inconsistent and therefore only inclination could be used to determine magnetic polarity for both the hydraulic piston and extended core barrel cores. At least two oriented discrete samples were collected from the working half of each core interval for progressive AF and thermal demagnetization and rock magnetic studies. Whole-core magnetic susceptibility was routinely measured on all cores, using a Bartington susceptibility loop on the automated multisensor track (MST).

NRM intensities were generally very low (~10^{-4} A/m on average) and ranged between 10^{-2} and 10^{-5} A/m (Figs. **F13, F14**). Intervals with higher NRM intensities are generally correlative with higher levels of magnetic susceptibility, suggesting that the larger order of magnetic susceptibility variation is caused by the ferrimagnetic component of the sediments. Smaller order variations in NRM intensity and magnetic susceptibility do not appear to be correlated.

Most NRM measurements displayed steeply positive (downcore) inclinations ranging between +60° and +80°, consistent with a drill-string overprint induced during coring (Stokking et al., 1993; Roberts et al., 1996; Fuller et al., 1998). The 20-mT AF demagnetization step was only partly effective in removing the drill-string overprint to the normal inclination of –60° expected for 45°S latitude in the vicinity of New Zealand. In general, the inclination signal at 20 mT of demagnetization was too noisy and random to reliably ascertain polarity, so a suite of discrete samples were stepwise AF demagnetized to 60 mT to determine if the noise level of the data could be reduced by increased levels of demagnetization (Figs. **F15A, F15B, F15C**). In some cases the positive drill-string overprint was observed to be effectively removed to a stable polarity with only 5- to 10-mT alternating fields (e.g., Fig. **F15B**) but, in most cases, AF demagnetization was ineffective in establishing a remanence direction for discrete specimens (e.g., Figs. **F15A, F15C**).

Discrete samples from ~290 mbsf in Hole 1119C were subjected to stepwise thermal demagnetization (e.g., Figs. **F15E, F15F**) to ascertain if the drill-string overprint was being effectively cleaned by the 20-mT step in the pass-through cryogenic magnetometer. This interval was chosen because it retained a positive inclination after 20 mT of demagnetization (Fig. **F14**) and it had high susceptibility and NRM intensity values relative to the rest of the core. Thermal demagnetization was 100% effective in removing the drill-string overprint (Fig. **F15**), demonstrating that AF demagnetization was generally ineffective. Unfortunately, mineral alteration at temperatures above 400°C (demonstrated by sharp increases in susceptibility) prevented the establishment of a stable endpoint or determining if the negative inclinations were caused by a Brunhes normal-field overprint. Saturation isothermal remanent magnetization (SIRM) and backfield SIRM were measured for several discrete samples from Hole 1119B to determine magnetic mineralogy. In all cases, remanence did not become saturated until applied fields of 300–500 mT and B_{cr} values were between 50 and 75 mT (Fig. **F16**). These values, combined with the low unblocking temperature (250°–300°C; Figs. **F15E, F15F**), suggest that the main carrier of remanence is a ferrimagnetic iron sulfide mineral present in relatively low concentrations (SIRM intensities are generally less than 10^{-2} A/m). This is not unexpected as the sediments have an ubiquitous pyrite presence (see **"Lithostratigraphy,"** p. 4). Similar IRM acquisition values were found

F13. Whole-core magnetic susceptibility for Hole 1119B, **p. 46.**

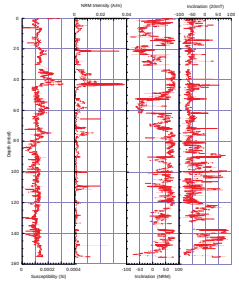

F14. Whole-core magnetic susceptibility for Hole 1119C, **p. 47.**

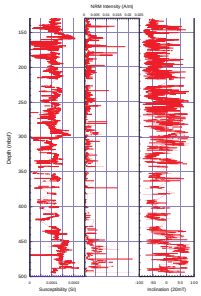

F15. Demagnetization of discrete samples from Site 1119, **p. 48.**

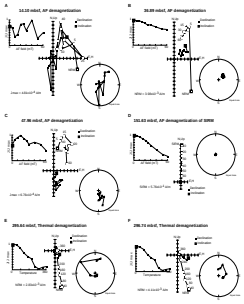

F16. Isothermal remanent magnetization and backfield acquisition curves, **p. 49.**

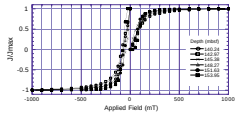

in late Neogene New Zealand sediments containing pyrrhotite (Roberts and Turner, 1993). Similar Pleistocene sediments from the Wanganui Basin, New Zealand, were found to contain reasonable quantities of titanomagnetite; however, SIRM values were <150 mT (Roberts and Pillans, 1993).

It was not possible to determine a magnetic polarity stratigraphy for the sequence cored by Holes 1119B and 1119C. From paleontologic and cyclic sedimentation information (see **"Biostratigraphy,"** p. 11, and **"Lithostratigraphy,"** p. 4) it was expected that the Brunhes/Matuyama boundary should occur at ~150 mbsf and that the interval between 150 and 495 mbsf ranges in age from mid-Pliocene at the base to middle Pleistocene at 150 mbsf. No consistent behavior was observed in the inclination of the cores to reliably identify any of the several reversals that should occur in this interval. Intensity of remanence was measurable throughout the core (Figs. **F13, F14**), and it is the magnetic mineralogy that has prevented isolation of primary remanence from shipboard measurements. However, it appears from shipboard experiments that targeted thermal demagnetization, guided by the paleontology, should allow identification of key magnetostratigraphic reversals in shore-based studies.

COMPOSITE DEPTHS

The composite section for Site 1119 was constructed using data from Holes 1119B and 1119C, which penetrated to 155.54 and 494.40 mbsf, respectively. Magnetic susceptibility (MS) and natural gamma-ray intensity (NGR), both measured on whole cores on the MST, formed the primary data sets used for correlation. Other high-resolution data sets were unsuitable for correlations at this site. The *P*-wave velocity measurements suffered from pervasive gas voids and were determined consistently only in the APC cores from Hole 1119C. GRAPE values showed low-amplitude variation and were difficult to correlate among holes. Split-core reflectance measurements displayed considerable mean offsets between holes as well as poor reproducibility.

The composite section was constructed by aligning the unsmoothed MS data (measured at 4-cm intervals) for Cores 181-1119B-1H to 12H and 181-1119C-1H to 12H. Below this, to the base of Hole 1119B, unsmoothed NGR data (measured at 14- to 16-cm intervals) provided an extra guide to correlation (Cores 181-1119B-13H to 17H and 181-1119C-13H to 17H). Figure **F17** illustrates the final composite section alignments. Documented continuous overlap between the two holes extends down to 90 meters composite depth (mcd). Gaps in the sedimentary sequence, with no overlap between holes, occurred between Cores 181-1119C-9H and 10H, 181-1119C-10H and 11H, 181-1119C-15H and 16H, and 181-1119C-16H and 17H (Fig. **F17**). In these cases, we assigned the top of the deeper core in one hole an mcd value equal to that at the base of the overlying core in the other hole. Table **T10** (also in **ASCII format**) contains the offsets between the mbsf and mcd scales resulting from composite section construction. In general, the offsets roughly follow a linear downhole trend, with mcd depths increasing at a rate of ~10% over mbsf depths (Fig. **F18**). Composite depth sections commonly display such "stretching" on the order of 10% (e.g., Curry, Shackleton, Richter, et al., 1995).

The spliced record (Fig. **F19**), defining a nearly complete sedimentary sequence, extends to 172 mcd. Wherever possible, splice tie points

F17. Composite sections for magnetic susceptibility and natural gamma ray, **p. 50.**

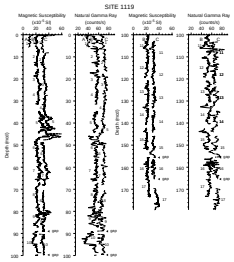

T10. Composite depth section, **p. 97.**

F18. Downhole depth offsets, **p. 51.**

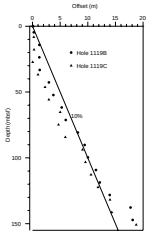

F19. Spliced record for Site 1119, **p. 52.**

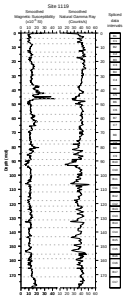

(Table T11, also in ASCII format) were picked at well-defined maxima or minima where the overlap in data from Holes 1119B and 1119C are correlated. Typically parameter values differed by less than 10% at tie levels and the correlation coefficient within a 2-m window often exceeded 0.6. In all cases, ties were selected so that the spliced record was as free from noise (high-frequency variability) as possible.

T11. Splice tie points, p. 105.

AGE MODELS AND SEDIMENTATION RATES

The combined nannofossil, foraminifer, diatom, and radiolarian biostratigraphy yielded 10 FO events and 11 LO events (Table T3) with age significance, using the shipboard stratigraphic framework (see the "Explanatory Notes" chapter). First occurrence events may have been estimated to be too shallow, based on limited sampling. The position of arrows in Figure F20 reflect the possibility that further work may extend these datums downhole. Last occurrence events may be too deep, again as a result of the limited sampling interval. The position of arrows in Figure F20 reflect the possibility that further work may extend these datums uphole. The LO of small nannofossils and diatoms that are prone to reworking have not been used to compile age-depth information.

F20. Age-depth curve using multiple microfossil datums for Site 1119, p. 53.

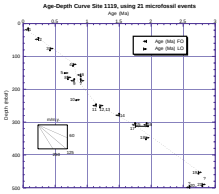

The more reliable events, from the point of view of stratigraphic ranges established at the site and for the age-depth plot (Fig. F20), are listed in Table T3. While the FO of *Globorotalia crassula* in the base of Hole 1119C cannot be shown to be a true FO, the age of its FO (see "Biostratigraphy," p. 10, in the "Explanatory Notes" chapter) affords useful constraint, hence its inclusion here. Equally, the LO of *Discoaster asymmetricus* in the base of Hole 1119C may be a result of reworking, but it still affords useful age constraint for the base of Hole 1119C.

Summarizing the data and taking into account the above uncertainties, the lower 200 m of Hole 1119C is Pliocene, and we find relatively moderate sedimentation rates, ~140 m/m.y. from the bottom of the hole to 300 mbsf. The sedimentation rate then decreases to ~100 m/m.y. from 300 to 250 mbsf in the lowermost Pleistocene. In the lower Pleistocene the rate is ~250 m/m.y. (250–120 mbsf), and middle to upper Pleistocene rates decline to ~125 m/m.y. (upper 120 mbsf). The biostratigraphic data do not indicate obvious stratigraphic disconformities, but resolution is limited using shipboard data. In particular, it must be observed that only the LO acme *G. parallela* (Event 4) defines the slower/faster/slower sedimentation rate motif above 300 mbsf. These varying sedimentation rates may be linked to the progradation and accretion of sediment drifts onto this margin.

INORGANIC GEOCHEMISTRY

Interstitial Waters

Twenty-five interstitial-water samples were collected at Site 1119: 13 samples from Hole 1119B at depths ranging from 2.95 to 153.10 mbsf and 12 from Hole 1119C from 156.70 mbsf to 472.30 mbsf (Table T12, also in ASCII format). Sampling frequency was one per every 10 m for the upper 100 m and one per every 30 m thereafter. Results from these two holes are considered to constitute a single depth profile in this report and the data are plotted together in Figure F21.

T12. Composition of interstitial waters, p. 106.

F21. Depth profiles of interstitial-water constituents at Site 1119, p. 54.

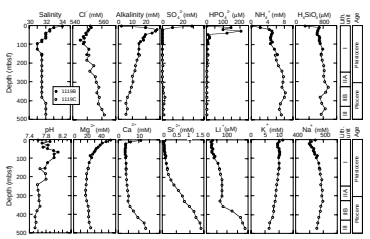

Salinity, Chloride, and pH

Salinities of the interstitial-water samples range from 31.0 to 34.0. The topmost samples show slightly higher values; below 100 mbsf, salinity remains relatively uniform (Fig. F21). Chloride (Cl^-) concentrations in the upper 80 mbsf show a decreasing trend with depth, from the subsurface value of 552 mM to a minimum value of 545 mM at 77.05 mbsf. The concentrations then increase steadily to the bottom. A possible explanation for the occurrence of low chloride concentrations at 77.05 mbsf is freshwater penetration from the land through permeable sandy sediments (Gieskes, 1981). Interstitial-water pH values vary from 7.53 to 8.09. The highest pH is measured at 67.60 mbsf, which coincides with the minima of salinity and chloride. Below 77.05 mbsf, pH values decrease toward the bottom.

Alkalinity, Sulfate, Phosphate, Ammonium, and Dissolved Silica

Interstitial-water alkalinity increases rapidly in the upper few tens of meters of the hole, reaching a maximum of 26.7 mM at 29.65 mbsf. Concentrations then decrease to 14.9 mM at 96.10 mbsf, below which the alkalinity continues to decrease steadily downhole to a minimum value of 5.4 mM at 472.30 mbsf.

Sulfate (SO_4^{2-}) reduction is evidenced by the rapid decrease in sulfate concentration from 28.6 mM at 2.95 mbsf to zero at 20.15 mbsf. Sulfate concentration remains near zero from 20.15 to ~300 mbsf. Below 328.20 mbsf, the sulfate concentrations are slightly raised (<2.4 mM), which is probably caused by contamination from the drilling process. Sulfate is removed by sulfate-reducing bacteria in these rapidly deposited sediments, even though the organic carbon contents of the sediments in this site are relatively low (see "Organic Geochemistry," p. 24). The observed alkalinity increase can be attributed to the production of bicarbonate (HCO_3^-) ions in the sulfate reduction zone.

Phosphate (HPO_4^{2-}) also increases from the uppermost sample (4.5 µM at 2.95 mbsf) to a maximum value of 206 µM at 29.65 mbsf, which is located just below the alkalinity maximum and the top of the sulfate-depleted layer. The phosphate concentrations decrease from ~50 mbsf, presumably because of coprecipitation into carbonate. Below 50 mbsf, phosphate concentrations generally remain less than 10 µM.

Ammonium (NH_4^+) concentrations increase with depth from 0.1 mM at 2.95 mbsf to 5.1 mM at 39.05 mbsf. The rapid increase of ammonium concentration is also related to sulfate reduction. Ammonium values then remain between 4 and 5 mM from 39.05 to 96.10 mbsf. Below 96.10 mbsf, concentrations again increase gradually to a maximum of 8.2 mM at 357.00 mbsf.

Dissolved silica (H_4SiO_4) concentrations increase from a near-seawater value of 281 µM at 2.95 mbsf to 944 µM at 10.65 mbsf, as a result of pore-fluid migration and/or diffusion driven by the concentration difference between seawater and the sediments. From 10.65 to 96.10 mbsf, concentrations are measured within a relatively narrow range, between 682 and 710 µM. The values of samples below 96.10 mbsf are more variable, ranging from 723 to 944 µM. A positive correlation can be seen between the concentration of dissolved silica and the relative abundance of diatoms, especially below 100 mbsf. This is consistent with the dissolution of siliceous tests in the sediments (see "Biostratigraphy," p. 11).

Calcium, Magnesium, and Strontium

Calcium (Ca^{2+}) concentrations are near-seawater values in the shallowest sample (10.8 mM at 2.95 mbsf), and decrease rapidly to under 4 mM by 20.15 mbsf. Magnesium (Mg^{2+}) shows a very gradual decrease from near-seawater values in the shallowest sample to a minimum value of 17.2 mM at 270.70 mbsf. The decrease in calcium and magnesium at 20.15 mbsf (the depth of the sulfate minimum) suggests precipitation of diagenetic carbonate promoted by the rapid increase in alkalinity during sulfate reduction (Compton, 1988). Calcium values remain between 3.2 and 4.1 mM in the interval between 2.95 and 328.20 mbsf. Below this depth, calcium concentration increases to a maximum value of 13.26 mM at 472.30 mbsf, which is close to the seawater value. Generally, the interval of increasing calcium concentrations corresponds to lithostratigraphic Subunit IIB (see **"Lithostratigraphy,"** p. 4), which contains significant amounts of broken shells, benthic foraminifers, and calcareous nannofossils, suggesting effects of carbonate dissolution in interstitial waters.

Potassium, Lithium, and Sodium

The potassium (K^{+}) concentration remains fairly constant in the interval shallower than ~160 mbsf. A minimum value of 9.4 mM at 20.15 mbsf may correspond to the ammonium maximum, suggesting cation exchange has occurred between the pore water and clay minerals. Below 160 mbsf, potassium decreases gradually to a value of 7.6 mM at 414.90 mbsf. In the bottom part of the hole, a small decrease in potassium concentration can be seen between samples at 414.90 and 443.80 mbsf, which corresponds to the boundary between lithostratigraphic Units II and III (428.2 mbsf).

Concentrations of lithium (Li^{+}) exhibit little change in the first 70 mbsf of Hole 1119B, and subsequently increase to ~80 µM by 357 mbsf. Below this depth, lithium concentrations increase rapidly to the maximum value of 184.5 µM at 472.30 mbsf. The interval of rapidly increasing lithium concentrations is coincident with lithostratigraphic Subunit IIB (see **"Lithostratigraphy,"** p. 4). The general trend of the Li^{+} concentration profile is similar to that of Ca^{2+}, suggesting possible control by recrystallization of biogenic carbonate.

Concentrations of sodium (Na^{+}) show a minimum value of 453 mM at 29.65 mbsf. Values subsequently increase to a maximum of 498 mM at 328.20 mbsf, before decreasing further downhole.

Summary of Interstitial-Water Results

The profiles of interstitial-water constituents at Site 1119 reflect the sulfate reduction of organic matter by microbial activity, the recrystallization of biogenic carbonate, and silica diagenesis.

A sulfate-depleted layer occurs at the shallow depth of 20 mbsf. Alkalinity, ammonium, and phosphate increase in the sulfate reduction zone. These increases are all controlled by the degradation of sedimentary organic matter in the shallow burial environment. Sulfate concentrations are near zero from 20.15 mbsf through to the bottom of the hole, suggesting enhanced diagenetic processes occurred throughout the sequence, perhaps including the dissolution of magnetic minerals.

Evidence of carbonate remineralization at Site 1119 is derived from variations in the Mg^{2+}/Ca^{2+} ratio (Fig. **F22**). The significant increase in

F22. Depth profiles of Sr^{2+}/Ca^{2+} and Mg^{2+}/Ca^{2+}, **p. 55.**

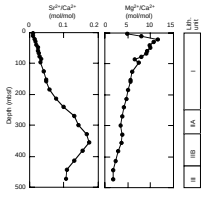

the Mg^{2+}/Ca^{2+} ratio in the sulfate reduction zone may indicate the dissolution of high-magnesium calcite. The decreases in calcium and magnesium concentrations below the sulfate reduction zone might be attributed to the precipitation of diagenetic carbonate promoted by a rapid increase in alkalinity.

ORGANIC GEOCHEMISTRY

Volatile Hydrocarbons

As part of the shipboard safety and pollution-prevention monitoring program, hydrocarbon gases were analyzed by the headspace technique in each core of Hole 1119B and in each core below 150 mbsf of Hole 1119C. When gas was encountered, analyses were made by vacutainer sampling. The headspace methane concentrations increase rapidly below the sediment surface to a maximum value of 36,400 ppm at 20.23 mbsf (Fig. F23). Below this depth, methane concentrations decrease to 3,155 ppm at 96.20 mbsf and fluctuate in the range between 1,500 and 8,000 ppm in the deeper parts of Holes 1119B and 1119C, respectively. However, between 110 and 160 mbsf, three distinct maxima occur with concentrations over 10,000 ppm. C_1/C_2 values are high in all samples, indicating a biogenic source of methane; ratios decrease with depth from values over 10,000 ppm to values of ~500 ppm. In summary, methane concentrations are moderate in headspace samples and hydrocarbons of lower volatility (C_{2+}) could only be recognized in trace amounts. Vacutainer methane concentrations are much higher than in the headspace samples, showing the effect of different sampling techniques. The values are in the range 500,000 to 1,000,000 ppm. C_1/C_2 values are fairly constant (480–650 ppm) and decrease only slightly with depth.

F23. Headspace methane concentrations, p. 56.

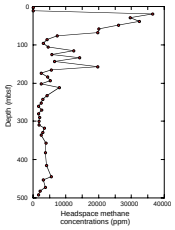

T13. Organic chemistry data, p. 107.

Carbonate and Organic Carbon

The abundances of total, inorganic, and organic carbon and of calcium carbonate in sediments from Holes 1119B and 1119C are summarized in Table T13 (also in ASCII format). Random sampling of all lithologies was performed for carbonate analysis, and for organic carbon measurements one sample per core was analyzed.

Carbonate contents are highly variable throughout the sediment sequence and range from 0.9 to 72.7 wt% (Fig. F24). High carbonate concentrations occur at sediment depths between 300 and 420 mbsf, whereas contents are relatively low below 420 mbsf to the bottom of the hole. Above 300 mbsf, most of the samples have contents below 15 wt%. The range in carbonate content reflects a varying combination of fluctuating biological productivity, dilution by noncalcareous sedimentary components, and postdepositional carbonate dissolution forced by oxidation of organic matter.

Sediments at Site 1119 average 0.34 wt% TOC (Fig. F25), which is low for coastal sediments. This suggests varying environmental conditions in which (1) during deposition of carbonate ooze–rich sediments most of the organic matter is degraded and (2) during periods of low carbonate production the organic matter is diluted by siliciclastic sediments. Consequently, there is no correlation between carbonate and organic matter contents and between organic matter content and depth.

F24. Calcium carbonate contents, p. 57.

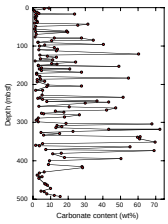

F25. Total organic carbon contents in sediments from Holes 1119B and 1119C, p. 58.

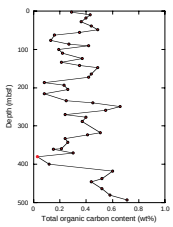

Organic Matter Source Characterization

Organic carbon/nitrogen values were calculated for Site 1119 samples using TOC and total nitrogen concentrations to help identify the origin of the organic matter. The ratios vary from 0.2 to 9.0 with an average of 4.2 (Table T13). These low ratios are not accurate indicators of organic matter source. They may be an artifact of the low organic carbon content, combined with the tendency of clay minerals to adsorb ammonium ions generated during degradation of organic matter (Müller, 1977). This interpretation is supported by (1) constant total nitrogen concentrations and (2) very low atomic $[C/N]_a$ ratios below 4.0 for organic carbon-poor samples (<0.3 wt%).

Rock-Eval analyses were not carried out because of low organic carbon contents (see "Organic Geochemistry," p. 22, in the "Explanatory Notes" chapter).

PHYSICAL PROPERTIES

Index Properties

Index properties measurements were made on one sample per section in the first 17 cores in Hole 1119B and below this on an average of three per core to the total depth in Hole 1119C. Index properties were determined by a gravimetric method (see "Physical Properties," p. 24, in the "Explanatory Notes" chapter). Values of measured index properties (void ratio, porosity, water content, bulk density, and grain density) are presented in Table T14 (also in ASCII format). The properties show little variation downcore, indicating a fairly homogeneous section, with the few variations most likely corresponding to lithologic responses to climatic (glacial-interglacial) signals (Fig. F26).

Multisensor Track Measurements

The shipboard physical properties program at Site 1119 included nondestructive measurements of bulk density, magnetic susceptibility, and natural gamma-ray activity on whole sections of all cores using the multisensor track (MST) (Fig. F27). Magnetic susceptibility was measured at 4-cm intervals and at a high sensitivity (4-s measurement time) in all Site 1119 holes. Magnetic susceptibility is generally low but shows pronounced cyclicity. Extremely low values may be associated with voids. Gamma-ray attenuation porosity evaluator (GRAPE) bulk density measurements were made at 4-cm intervals at all Site 1119 holes. Cyclic increases and decreases in GRAPE density are most likely a result of varying lithologies caused by climatic (glacial-interglacial) fluctuations. A comparison of GRAPE density with the wet-bulk density determined from discrete samples shows general agreement, although overall GRAPE density values are lower than bulk density values obtained by index property measurements (Fig. F28). This may result from the fact that index properties sample preparation involves some water loss and that GRAPE density is measured in undrained cores. In Hole 1119B (0 to 150 mbsf), the wet-bulk density is consistently greater than the GRAPE density. Agreement between these two parameters occurs in the lower part of the section (>190 mbsf). Possible reasons for the discrepancy in the upper part of the core (<190 mbsf) include differences in the handling time of the cores, loss of fluids because of increased hydrostatic

T14. List of index properties measured, p. 110.

F26. Index properties measurements, p. 59.

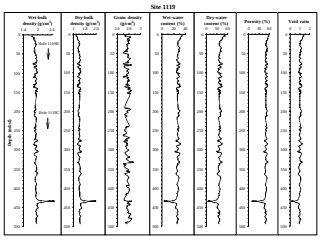

F27. Multisensor track measurements, p. 60.

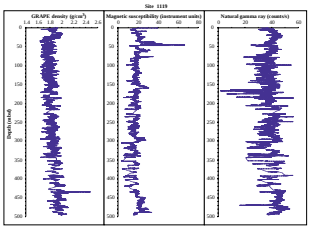

F28. Wet-bulk density measurements, p. 61.

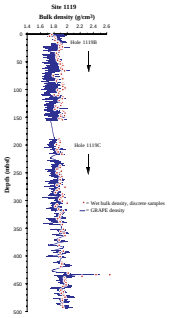

pressure with depth, and the use of different coring methods for the two sections. In the case of handling time, the time interval between splitting the core and the processing of samples tends to increase with core depth as a result of the backlog of accumulating core materials to be processed. As for the increasing pressure downhole, this factor was magnified by a high gas content in the core, and increased effects of gas expansion were observed in the deeper cores as they equilibrated to surface temperature and pressure conditions. This could have allowed more moisture loss, resulting in better agreement in the deeper cores. The upper part of the section was collected using the APC coring method, whereas the deeper part of the section was cored using the XCB method. It is generally accepted that the XCB method causes greater disturbance in the cored materials than the APC method. This factor could also have made a contribution to the differing moisture content estimates. Increased GRAPE densities between 430 and 436 mbsf suggest a significant lithologic change in this interval. The *P*-wave velocity measurements (PWL) were made at 4-cm intervals but gave poor results because of signal attenuation and sediment cracking resulting from high gas content (see **"Organic Geochemistry,"** p. 24). PWL measurements were not collected after Section 181-1119B-3H-1 and for the entire Hole 1119C. Natural gamma-ray activity was measured with a 15-s count every 14 cm in Holes 1119B and 1119C.

Shear Strength

Measurements of shear strength, using a mechanical vane, were made on split cores from Hole 1119B (Fig. **F29**). Samples were generally taken in fine-grained sediments at a resolution of one per section in Hole 1119B. No samples were taken from XCB cores. Increased sand content in the sediment results in lower shear strength values. Values range from 10 to 70 kPa (maximum value 67.5 kPa at 152 mbsf) and generally increase with depth. Low values may be associated with the presence of sand-rich intervals (see **"Lithostratigraphy,"** p. 4). Two significant increases occur at 88 and 129 mbsf after intervals of gradually decreasing shear strength. Shear strength values for Hole 1119C were obtained using the Torvane method. These data correlate well with those from the vane shear results from Hole 1119B (Fig. **F28**).

F29. Shear strength measurements, **p. 62.**

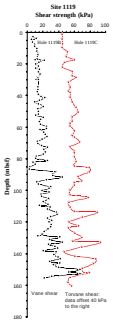

Compressional-Wave Velocity

Compressional-wave velocity was measured parallel and normal to the core axis on split cores from Hole 1119B using the digital sound velocimeter system. The measurements gave poor results because of signal attenuation and sediment cracking resulting from high gas content (see **"Organic Geochemistry,"** p. 24), and, therefore, all the velocity measurements were rejected at Site 1119.

Thermal Conductivity

Four downhole temperature measurements with the Adara temperature tool were taken in Cores 181-1119B-4H, 7H, 10H, and 13H. Thermal conductivity was measured in cores where the Adara temperature tool was used, at an average of three or four per core for both Holes 1119B and 1119C. The Adara temperature tool yielded poor results at the site, which precluded the determination of heat flow. Downhole distribution of thermal conductivity at Holes 1119B and 1119C is

shown in Figure F30. The data collected from cores from these two holes generally agree. The overall trend of the values measured is similar, but absolute values are generally higher in Hole 1119C.

DOWNHOLE MEASUREMENTS

Logging Operations

Downhole logging was performed in Hole 1119C. The drill string was placed at 100 mbsf as the logging tools were lowered to the bottom of the hole. Before logging, the drill string was raised to 80 mbsf. The drill string had to be maintained at 80 mbsf to keep the upper hole wall from collapsing.

Three tool string configurations were run in Hole 1119C, in the following order: the triple combination, the FMS-sonic, and the GHMT (see "Downhole Measurements," p. 29, in the "Explanatory Notes" chapter). A repeat interval was measured with the triple combination, and two full passes were made with the FMS-sonic. Logging speeds are shown in Figure F31. Logging operations began at 2300 hr on 25 August 1998 and finished at 1300 hr on 26 August 1998. Weather conditions were excellent, with less than 1 m of heave throughout. The wireline heave compensator was used during all measurements.

The hole conditions, however, were poor, with an uneven borehole wall, many breakouts, and occasional ledges. The borehole diameter frequently exceeded 18 in and in places (e.g., 364 mbsf) was as narrow as 5 in (Fig. F32A).

The bottom of the borehole was particularly narrow, and became progressively more constricted with each logging run. This was probably because of the influence of swelling clays and cave ins. Deteriorating conditions at the bottom of the hole restricted logging to a maximum depth of 486 mbsf for the triple combination, 470 mbsf for the first pass of the FMS-sonic, 465 mbsf for second pass of the FMS-sonic, and 461 mbsf for the GHMT (Fig. F31). The NMRS tool on the GHMT tool string failed to work.

Data Quality

The quality of some of the data was substantially reduced by poor borehole conditions (Figs. F32A, F32B). The lithodensity (HLDS) and neutron porosity (APS) tools on the triple combination are particularly sensitive to hole conditions, as both tools must be pressed up against the hole wall in order to make a reading. When the hole is of a constantly varying diameter, it is impossible for these tools to maintain wall contact. The other tools on the triple combination, the hostile environment natural gamma (HNGS), resistivity (DIT), and temperature tools (TLT), are less affected by borehole conditions.

Lithodensity and neutron porosity data were edited against the caliper log to remove features that were artifacts of the borehole conditions. Comparison of the lithodensity log data with index properties (see "Physical Properties," p. 25) shows that the log data correlate well with results from the core (Fig. F33). Log-based lithodensity values increase at a greater rate with depth than index bulk density values obtained from the core (Fig. F33). This can be attributed to expansion of the index samples after retrieval of the cores. The log data represent in situ conditions.

F30. Thermal conductivity measurements, p. 63.

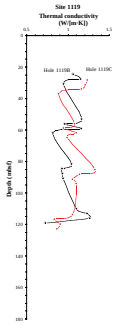

F31. Summary of logging operations at Hole 1119C, p. 64.

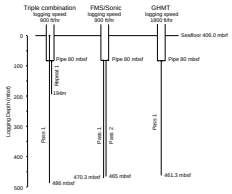

F32. Results from the downhole logging tools, p. 65.

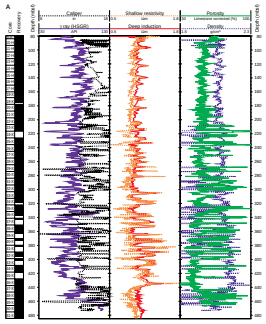

F33. A comparison of log and core index bulk density measurements, p. 67.

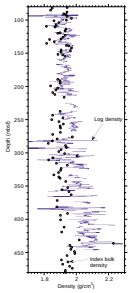

The FMS data were also affected by poor borehole conditions. The pads of this tool have a maximum expansion of 15 in. The hole diameter frequently exceeds 15 in Hole 1119C, and where this occurs the FMS cannot image the borehole wall.

The magnetic susceptibility data from the GHMT tool string is of good quality. There is not much variation in the susceptibility signal, but it correlates well with core-based susceptibility (Fig. F34).

Correlation between the resistivity, susceptibility, and gamma-ray logs and core lithology (see "Lithostratigraphy," p. 4) indicates that lower gamma-ray values, higher resistivities, and lower susceptibilities are indicative of the sandy intervals. It is difficult, however, to assess the significance of the edited bulk density and neutron porosity logs, although a sharp increase in both resistivity and bulk density at ~435 mbsf correlates with an interval of high core-based bulk density values (Fig. F33). This horizon contains a siltstone bed (see "Lithostratigraphy," p. 4).

F34. A comparison of log and core magnetic susceptibility measurements, p. 68.

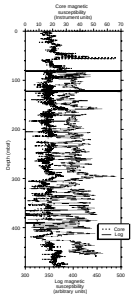

Logging Units

The poor hole conditions and the associated decrease in data quality in the HLDS and APS measurements make it difficult to assign distinct logging units to this hole. In addition, the amplitudes of fluctuations in the data are relatively minor. For example, over the entire section logged, deep resistivity (IDPH) values only vary between 0.8 and 1.5 Ωm, and magnetic susceptibility values vary between 300 and 500 (arbitrary units). Typically, both of these parameters can vary downhole by an order of magnitude. Nevertheless, logging units can be defined in Hole 1119C, mainly on the basis of fluctuations in the resistivity, magnetic susceptibility, and natural gamma-ray values (Fig. F35). Highs in the resistivity values can generally be correlated with lows in the magnetic susceptibility and gamma data. Downhole variations in porosity, calculated from the edited bulk density values (see "Downhole Measurements," p. 29, in the "Explanatory Notes" chapter), are also useful as a guide to changes in lithology.

F35. Downhole variations in natural gamma ray, resistivity, and magnetic susceptibility, p. 69.

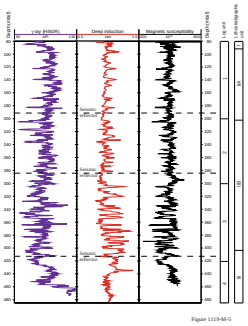

The logging units seem to correlate quite well with major seismic reflectors and the lithostratigraphic units (Fig. F35). Differences in the depths between the logging units and the lithostratigraphic units are relatively small (Fig. F35), and can possibly be attributed to inconsistencies between logging-based depths and core-based depths that arise because of core expansion.

Log Unit 1: Base of Pipe to 200 mbsf

This unit is characterized by low-amplitude, rhythmic variations in the resistivity, magnetic susceptibility, and gamma-ray values (Fig. F35). Porosities are typically 43% to 50%.

Log Unit 2: 200–300 mbsf

Fluctuations in the resistivity, magnetic susceptibility, and gamma-ray values in this section are comparable in amplitude to log Unit 1, but have an increased frequency (Fig. F35). Porosity values again range between 43% and 50%.

Log Unit 3: 300–420 mbsf

Fluctuations in the resistivity, magnetic susceptibility, and gamma-ray values in this unit have a greater amplitude than those recorded above, although their frequency is similar to that seen in log Unit 2 (Fig. F35). Porosity values are more variable, ranging between 28% and 57%.

Log Unit 4: 420–485 mbsf

Within this unit less variability can be seen in the resistivity, magnetic susceptibility, and gamma-ray values (Fig. F35). Porosities tend to be relatively low, with an overall range of 27% to 46%.

FMS Results

Two FMS images are shown for pass 2 (Fig. F36): one with dynamic normalization and one with static normalization. Static normalization takes the white of the most resistive bed and the black of the most conductive bed (see "Downhole Measurements," p. 29, in the "Explanatory Notes" chapter and Schlumberger, 1989) in the entire pass and normalizes the entire image to those extremes. It is a better representation of the absolute range of resistivities in the FMS and allows correlations to be made between horizons. Dynamic normalization does the same thing, but only within a sliding 2-m window. This enhances the visual resolution of the image but does not allow accurate matching of resistivity values over the entire image because each level is independently normalized.

The FMS images are affected by regular washouts of the borehole wall. The images were, however, repeatable between both runs. Where the FMS data are reliable, the sedimentary structure is characterized by horizontal planar bedding and lamination. Also, the images often appear speckled, which is indicative of bioturbation (Fig. F36A). Toward the base of the section (415–426 mbsf), thin (0.1–0.2 m) resistive sand beds can be seen, with a spacing of ~2 m (Fig. F36B).

F36. Example of the FMS images from Hole 1119C, p. 70.

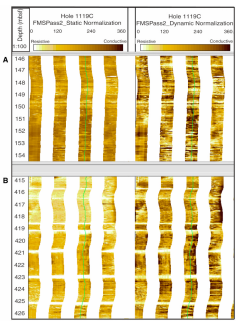

Downhole Temperature

The Temperature Logging Tool (TLT; see "Downhole Measurements," p. 29, in the "Explanatory Notes" chapter) recorded the temperature of the fluid in Hole 1119C. These data can be used to estimate the downhole thermal gradient (Fig. F37). The temperature results suggest a thermal gradient of 16.5°C/km for the slow thermistor. The uphole measurements are between 0.5 and 2°C greater than the downhole measurements, showing that the borehole was still equilibrating during data acquisition. These temperatures do not represent in situ formation temperatures.

F37. Downhole variations in borehole temperature, p. 71.

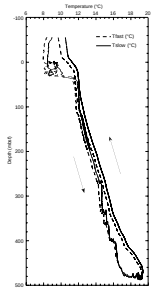

REFERENCES

Carter, L., and Carter, R.M., 1993. Sedimentary evolution of the Bounty Trough: a Cretaceous rift basin, Southwestern Pacific Ocean. *In* Ballance, P. (Ed.), *Sedimentary Basins of the World—South Pacific:* Amsterdam (Elsevier), 51–67.

Carter, L., and Herzer, R.H., 1979. The hydraulic regime and its potential to transport sediment on the Canterbury continental shelf. *Mem.— N. Z. Oceanogr. Inst.*, 83:1–33.

Carter, R.M., 1988. Post-breakup stratigraphy of the Kaikoura Synthem (Cretaceous–Cenozoic), continental margin, southeastern New Zealand. *N. Z. J. Geol. Geophys.,* 31:405–429.

Carter, R.M., Carter, L., and Johnson, D., 1986. Submerged shorelines in the SW Pacific: evidence for an episodic post-glacial transgression. *Sedimentology,* 33:629–649.

Carter, R.M., Carter, L., Williams, J.J., and Landis, C.A., 1985. Modern and relict sedimentation on the South Otago continental shelf, New Zealand. *Mem. N. Z. Oceanogr. Inst.,* 93.

Chiswell, S.M., 1996. Variability in the Southland Current, New Zealand. *N. Z. J. Mar. Freshwater Res.,* 30:1–17.

Compton, J.S., 1988. Degree of supersaturation and precipitation of organogenic dolomite. *Geology,* 16:318–321.

Curry, W.B., Shackleton, N.J., Richter, C., et al., 1995. *Proc. ODP, Init. Repts.,* 154: College Station, TX (Ocean Drilling Program).

Field, B.D., and Browne, G.H., 1989. *Cretaceous and Cenozoic Sedimentary Basins and Geological Evolution of Canterbury Region, South Island, New Zealand*. N. Z. Geol. Surv., Basin Stud., 2.

Fuller, M., Hastedt, M., and Herr, B., 1998. Coring-induced magnetization of recovered sediment. *In* Weaver, P.P.E., Schmincke, H.-U., Firth, J.V., and Duffield, W. (Eds.), *Proc. ODP, Sci. Results,* 157: College Station, TX (Ocean Drilling Program), 47–56.

Fulthorpe, C.S., and Carter, R.M., 1989. Test of seismic sequence methodology on a Southern Hemisphere passive margin: the Canterbury Basin, New Zealand. *Mar. Pet. Geol.,* 6:348–359.

————, 1991. Continental shelf progradation by sediment drift accretion. *Geol. Soc. Am. Bull.,* 103:300–309.

Gibb, J.G., and Adams, J., 1982. A sediment budget for the east coast between Oamaru and Banks Peninsula, South Island, New Zealand. *N. Z. J. Geol. Geophys.,* 25:335–352.

Gieskes, J.M., 1981. Deep-sea drilling interstitial water studies: implications for chemical alteration of the oceanic crust, layers I and II. *In* Warme, J.E., Douglas, R.G., and Winterer, E.L. (Eds.), *The Deep Sea Drilling Project: A Decade of Progress*. Spec. Publ.—Soc. Econ. Paleontol. Mineral., 32:149–167.

Griffiths, G.A., and Glasby, G.P., 1985. Input of river-derived sediment to the New Zealand continental shelf: I. Mass. *Estuar. Coast. Shelf Sci.,* 21:773–787.

Griggs, G.B., Carter, L., and Kennett, J.P., and Carter, R.M., 1983. Late Quaternary marine stratigraphy southeast of New Zealand. *Bull. Geol. Soc. Am.,* 94:791–797.

Harwood, D.M., and Maruyama, T., 1992. Middle Eocene to Pleistocene diatom biostratigraphy of Southern Ocean sediments from the Kerguelen Plateau, Leg 120. *In* Wise, S.W., Jr., Schlich, R., et al., *Proc. ODP, Sci. Results,* 120: College Station, TX (Ocean Drilling Program), 683–733.

Hawkes, P.W., and Mound, D.G., 1984. Clipper-1 geological completion report. *N. Z. Geol. Surv. Open-File Rep.,* 1036.

Herzer, R.H., 1981. Late Quaternary stratigraphy and sedimentation of the Canterbury continental shelf, New Zealand. *N. Z. Oceanogr. Inst. Mem.,* 89:1–71.

Hiramatsu, C., and De Deckker, P., 1997a. The calcareous nannoplankton assemblages of surface sediments in the Tasman and Coral Seas. *Palaeogeogr., Palaeoclimatol., Palaeoecol.,* 131:257–285.

————, 1997b. The late Quaternary calcareous nannoplankton assemblages from three cores from the Tasman Sea. *Palaeogeogr., Palaeoclimatol., Palaeoecol.,* 131:391–412.

Hornibrook, N. de B., Brazier, R.C., and Strong, C.P., 1989. Manual of New Zealand Permian to Pleistocene foraminiferal biostratigraphy. *Paleontol. Bull. N. Z. Geol. Surv.,* 56:1–175.

Hornibrook, N. de B, and Jenkins, D.G., 1994. DSDP 594, Chatham Rise, New Zealand—Late Neogene planktonic foraminiferal biostratigraphy revisited. *J. Micropalaeontol.,* 13:93–101.

Ives, D., 1973. Nature and distribution of loess in Canterbury, New Zealand. *N. Z. J. Geol. Geophys.,* 16:587–610.

Kennett, J.P., von der Borch, C.C., et al., 1986. *Init. Repts. DSDP,* 90: Washington (U.S. Govt. Printing Office).

Lohman, W.H., 1986. Calcareous nannoplankton biostratigraphy of the southern Coral Sea, Tasman Sea, and Southwestern Pacific Ocean, Deep Sea Drilling Project Leg 90: Neogene and Quaternary. *In* Kennett, J.P., von der Borch, C.C., et al., *Init. Repts. DSDP,* 90: Washington (U.S. Govt. Printing Office), 763–793.

McCartney, M.S., 1977. Subantarctic mode water. *In* Angel, M. (Ed.), *A Voyage of Discovery: George Deacon 70th Anniversary Volume*. Deep Sea Res., 24:103–119.

Müller, P.J., 1977. C/N ratios in Pacific deep sea sediments: effect of inorganic ammonium and organic nitrogen compounds sorbed by clays. *Geochim. Cosmochim. Acta,* 41:765–776.

Nelson, C.S., Hendy, C.H., Cuthbertson, A.M., and Jarrett, G.R.,1986. Late Quaternary carbonate and isotope stratigraphy, subantarctic Site 594, Southwest Pacific. *In* Kennett, J.P., von der Borch, C.C., et al., *Init. Repts. DSDP,* 90: Washington (U.S.Govt. Printing Office), 1425–1436.

Roberts, A.P., and Pillans, B.J., 1993. Rock magnetism of lower/middle Pleistocene marine sediments, Wanganui Basin, New Zealand. *Geophys. Res. Lett.,* 20:839–842.

Roberts, A.P., Stoner, J.S., and Richter, C., 1996. Coring induced magnetic overprints and limitations of the long-core paleomagnetic measurements technique: some observations from Leg 160, eastern Mediterranean Sea. *In* Emeis, K.-C., Robertson, A.H.F., Richter, C., et al., *Proc. ODP, Init. Repts.,* 160: College Station, TX (Ocean Drilling Program), 497–505.

Roberts, A.P., and Turner, G.M., 1993. Diagenetic formation of ferrimagnetic iron sulphide minerals in rapidly deposited marine sediments, South Island, New Zealand. *Earth Planet. Sci. Lett.,* 115:257–273.

Saul, G., Naish, T.R., Abbott, S.T., and Carter, R.M., 1999. Sedimentary cyclity in the marine Pliocene–Pleistocene of the Wanganui basin (New Zealand): sequence stratigraphic motifs characteristic of the last 2.5 m.y. *Geol. Soc. Am. Bull.,* 111:524–537.

Schlumberger, 1989. *Formation MicroScanner Image Interpretation:* Houston, TX (Schlumberger Educ. Services).

Stewart, R.B., and Neall, V.E., 1984. Chronology of palaeoclimatic change at the end of the last glaciation. *Nature,* 311:47–48.

Stokking, L.B., Musgrave R.J., Bontempo, D., and Autio, W., 1993. Handbook for Shipboard Paleomagnetists. *ODP Tech. Note,* 18: College Station, TX (Ocean Drilling Program).

Stow, D.A.V., and Holbrook, J.A., 1984. North Atlantic contourites—an overview. *In* Stow, D.A.V., and Piper, D.J.W. (Eds.), *Fine-Grained Sediments: Deep Water Processes and Facies*. Geol. Soc. Spec. Publ. London, 15:245–256.

Takayama, T., 1993. Notes on Neogene calcareous nannofossil biostratigraphy of the Ontong Java Plateau and size variations of *Reticulofenestra* coccoliths. *In* Berger, W.H., Kroenke, L.W., Mayer, L.A., et al., *Proc. ODP, Sci. Results,* 130: College Station, TX (Ocean Drilling Program), 179–229.

Young, J.R., Flores, J.-A., and Wei, W., 1994. A summary chart of Neogene nannofossil magnetobiostratigraphy. *J. Nannoplankton Res.,* 16:21–27.

Figure F1. Locality map for Site 1119, showing location of seismic line Ewing 1E of Figure F2, p. 33.

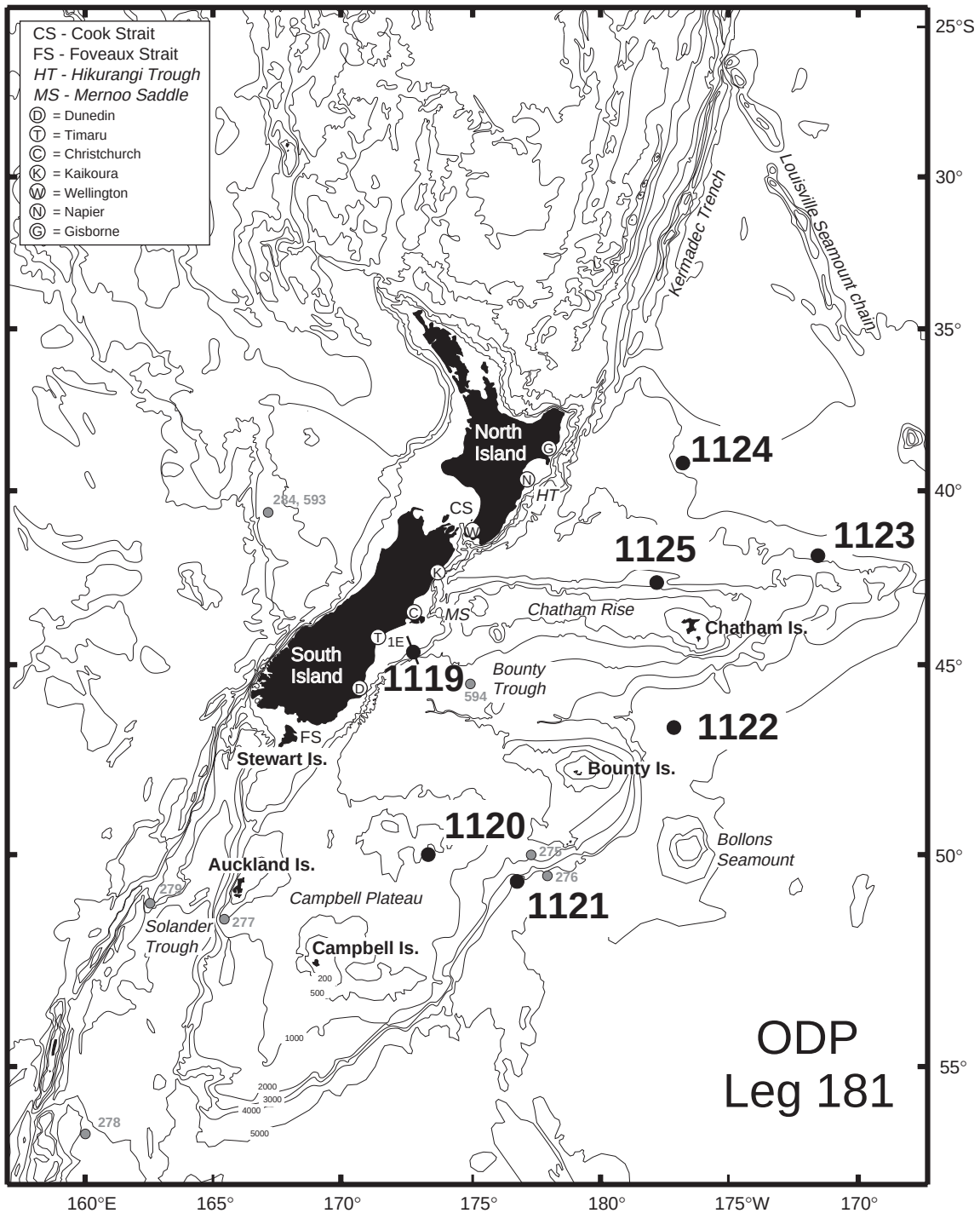

Figure F2. Portion of multichannel seismic line Ewing 1E through Site 1119.

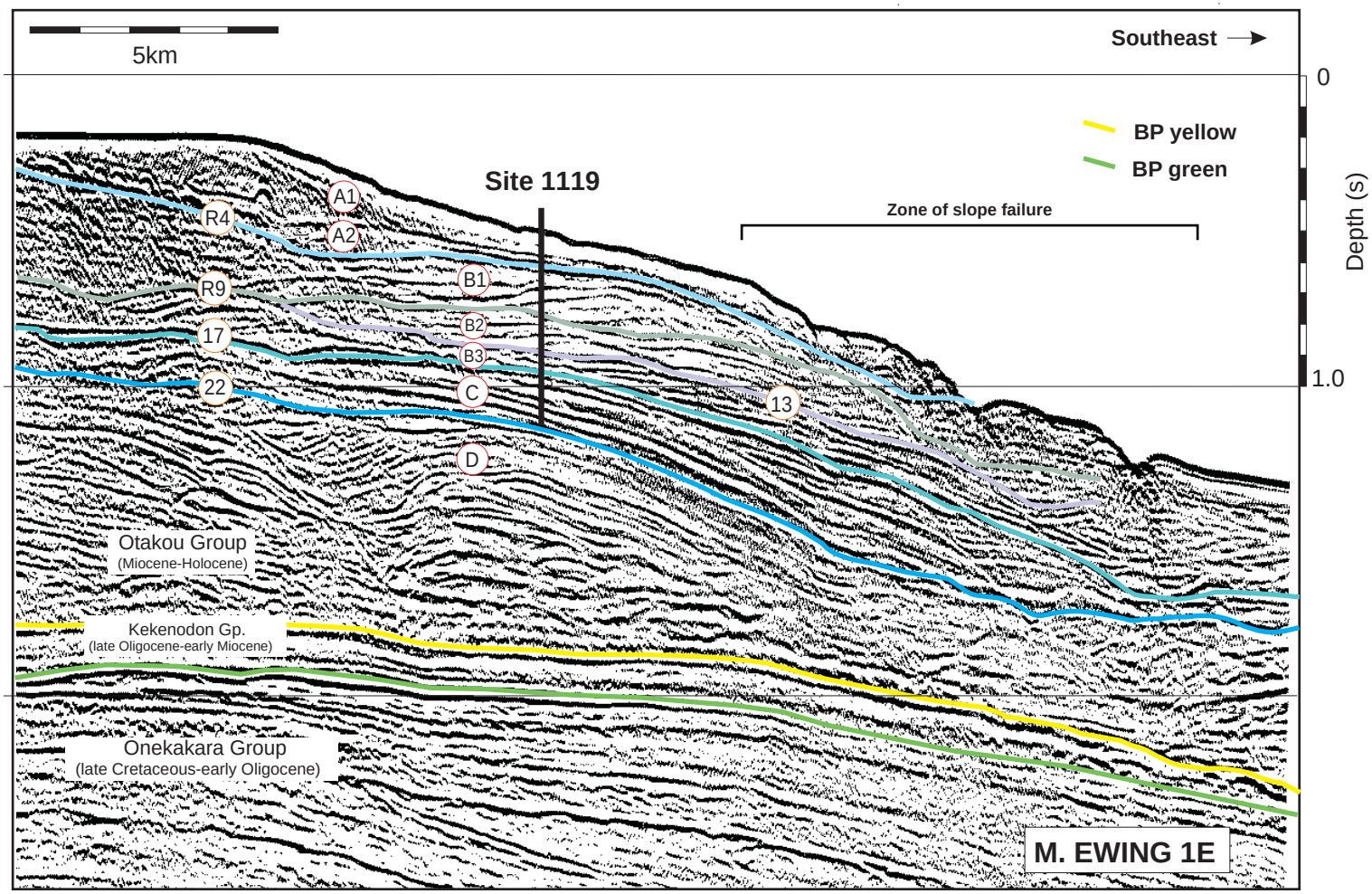

Figure F3. Portions of 3.5-kHz precision depth recorder line Ewing 1E (**A**) through Site 1119, and (**B**) downslope from the position of Site 1119.

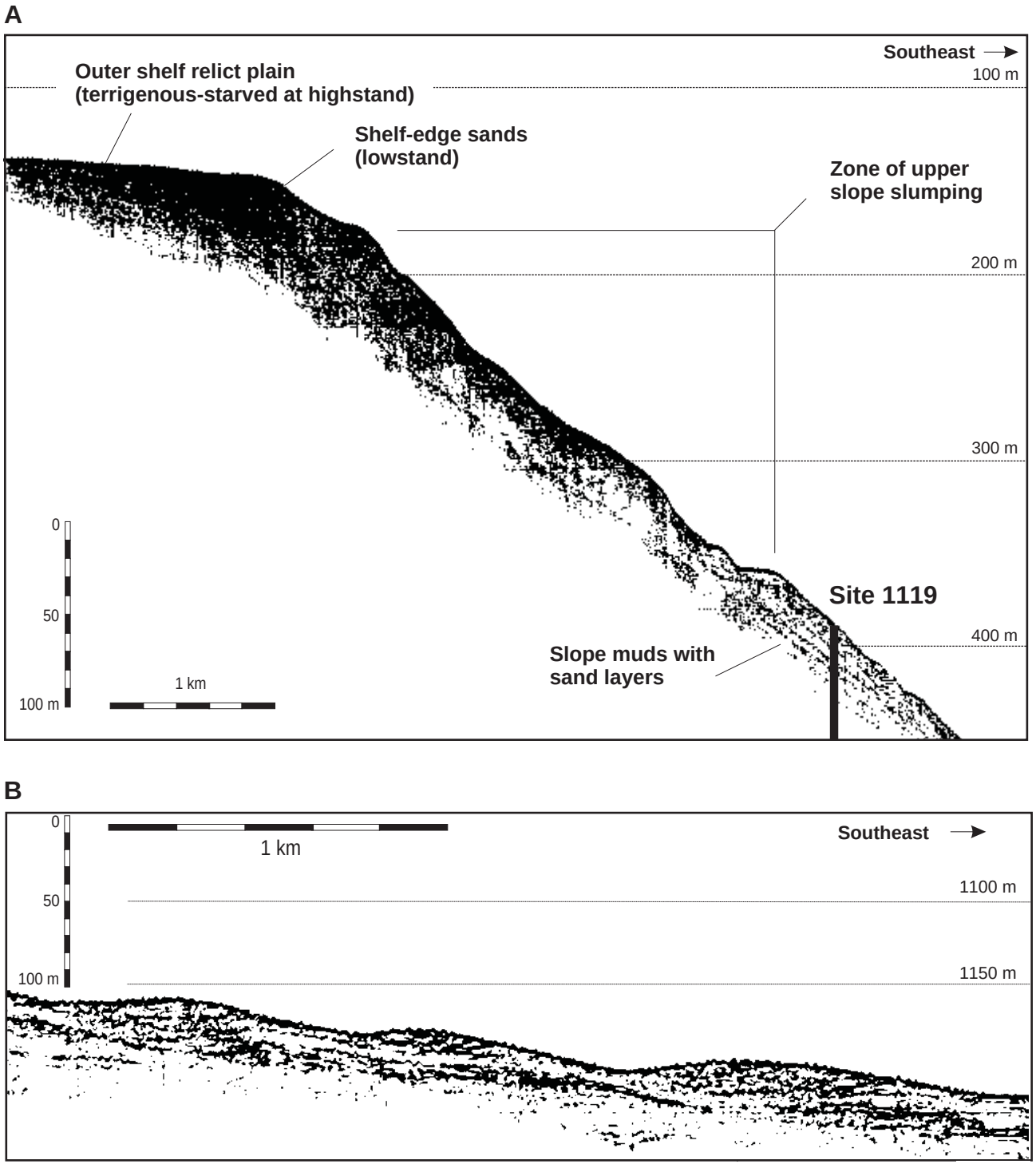

Figure F4. Schematic diagram showing (from top to bottom) the method of development of sediment drifts as they accrete at the outer edge of the continental shelf sediment wedge (after Fulthorpe and Carter, 1989).

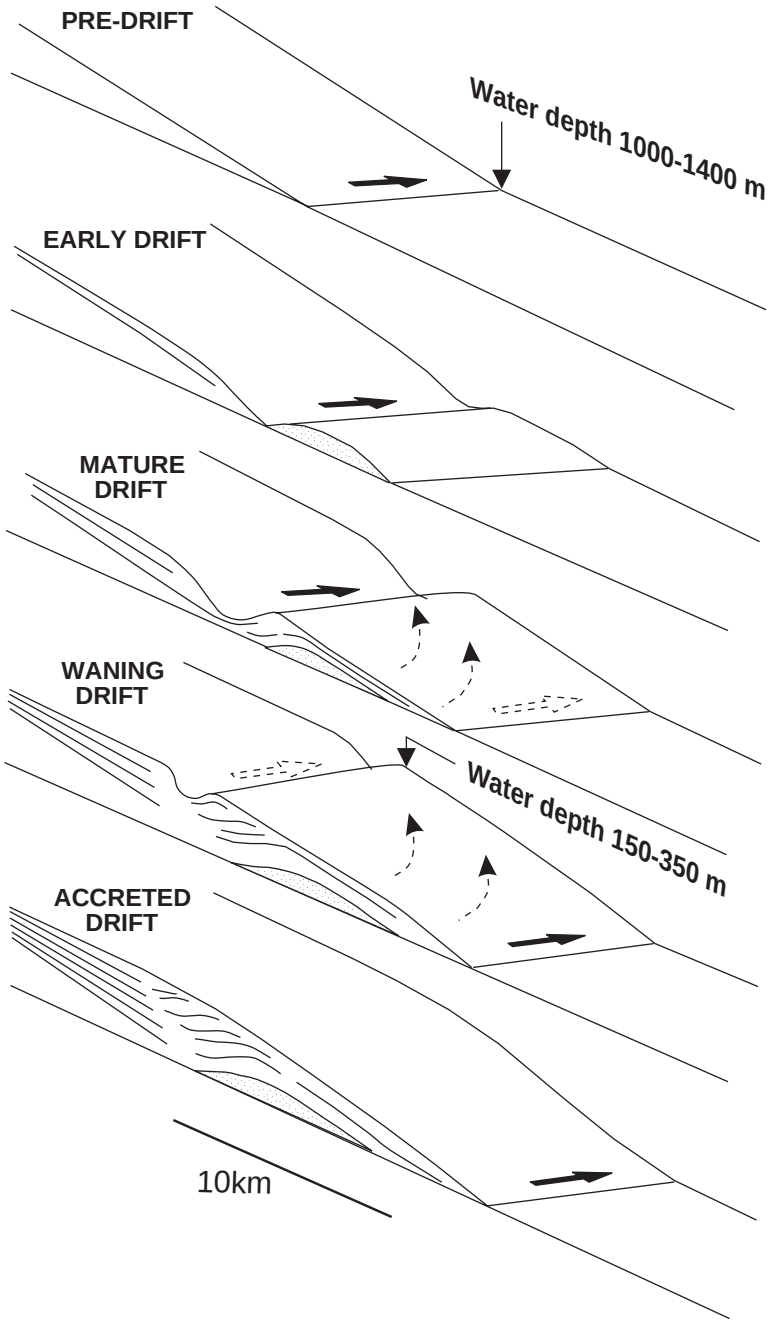

Figure F5. Summary log for Site 1119. (Continued on next two pages.)

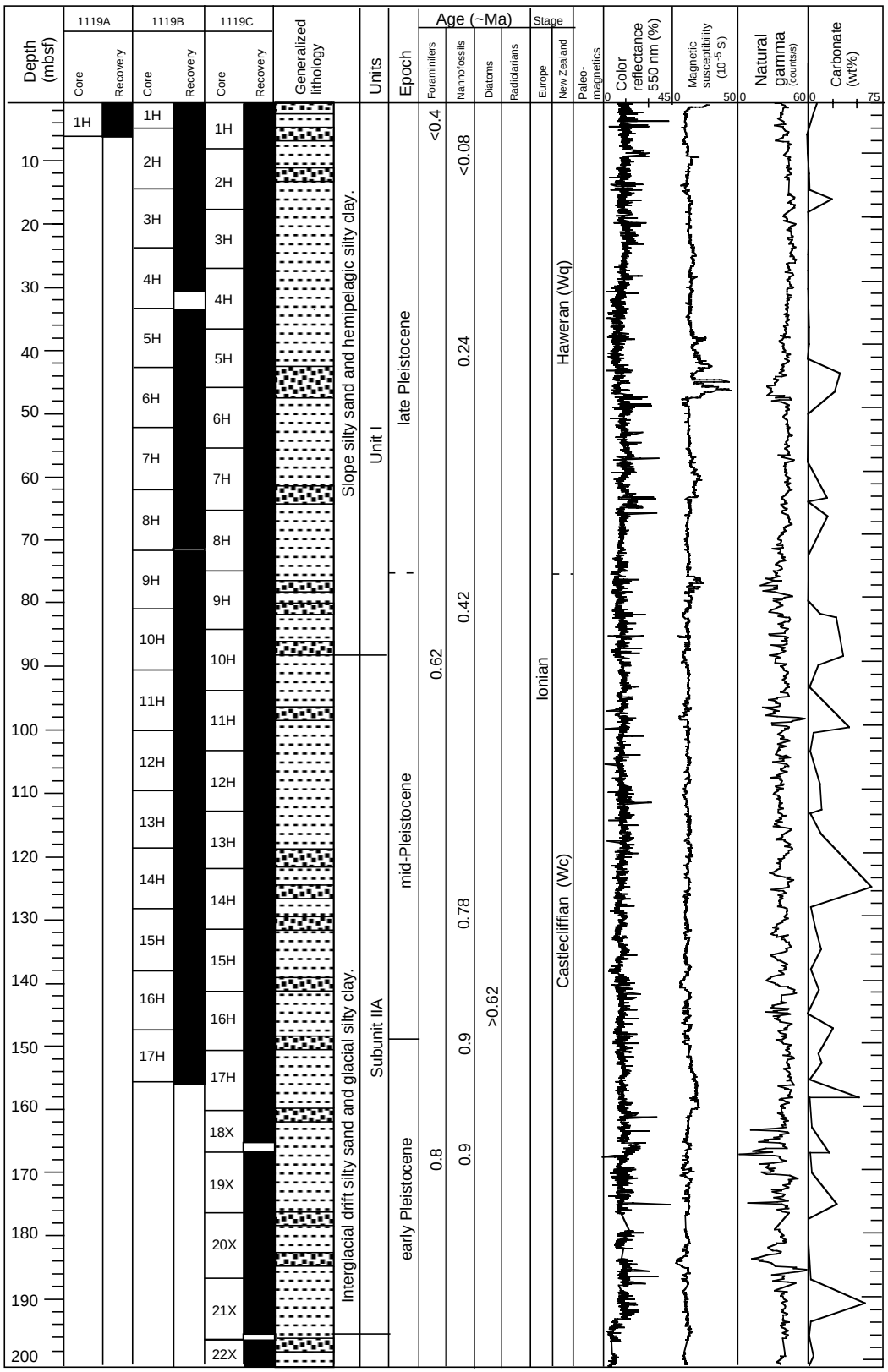

Figure F5 (continued).

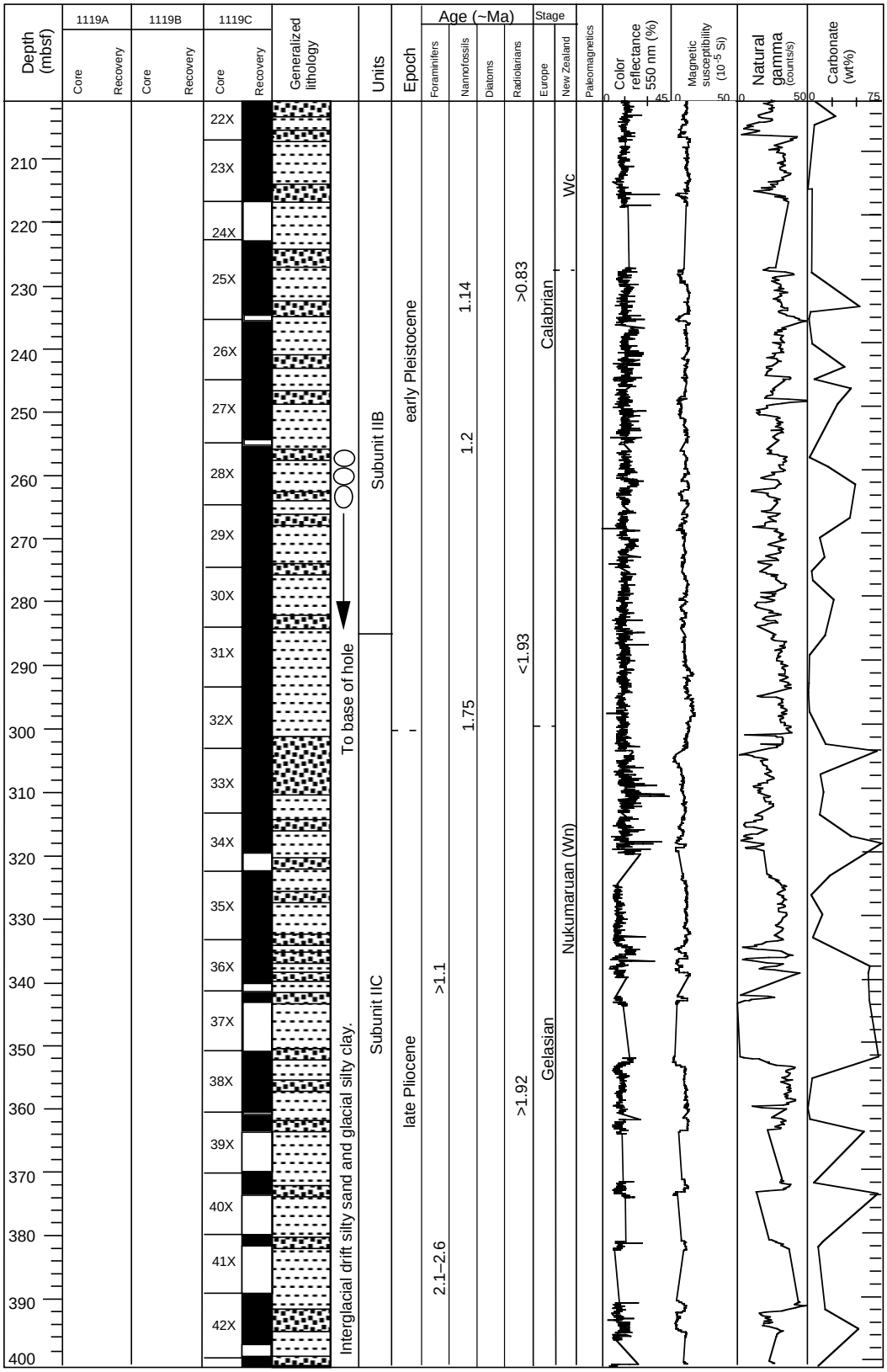

Figure F5 (continued).

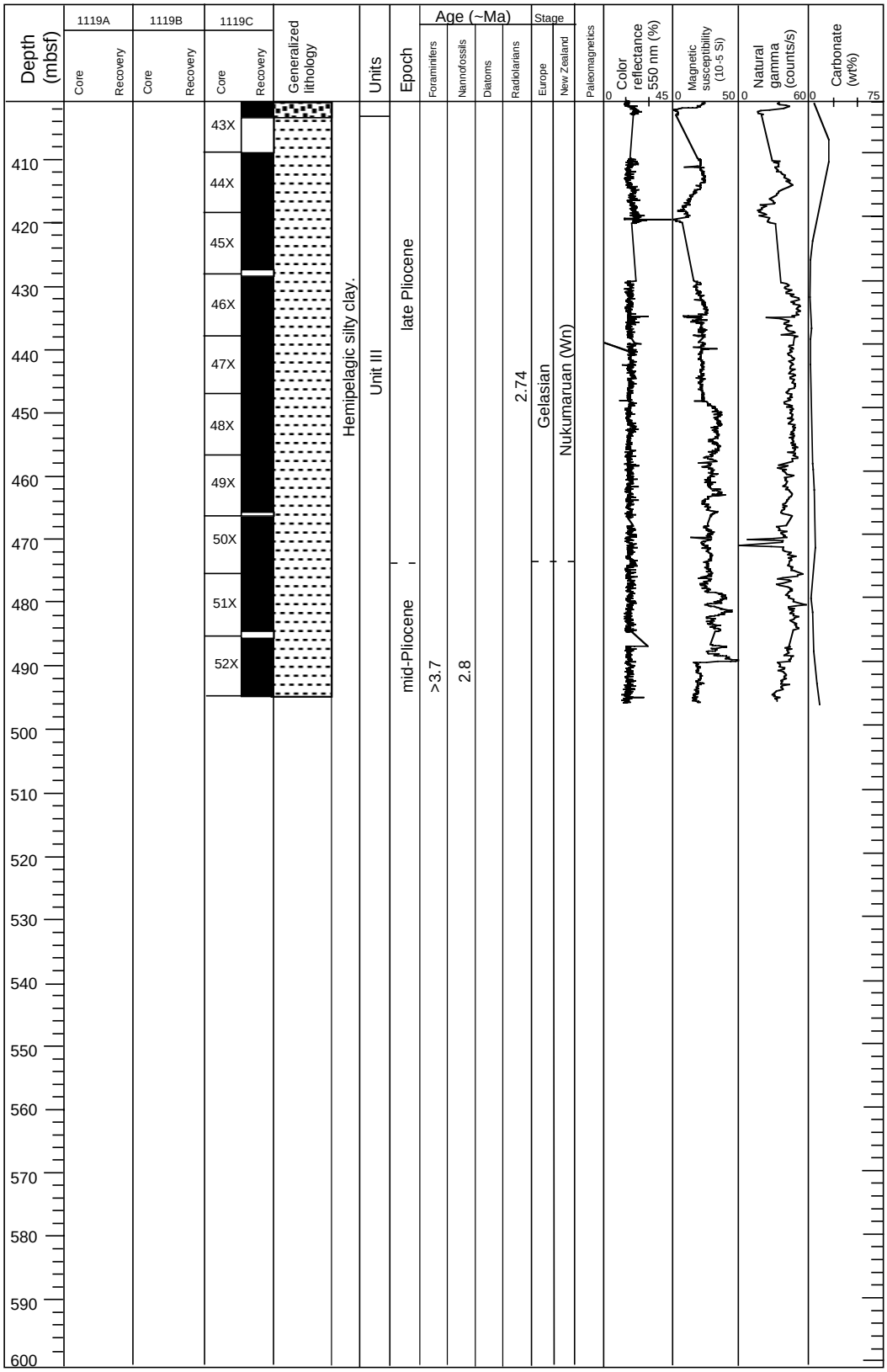

Figure F6. Core depth vs. peak area of major components present on XRD profiles.

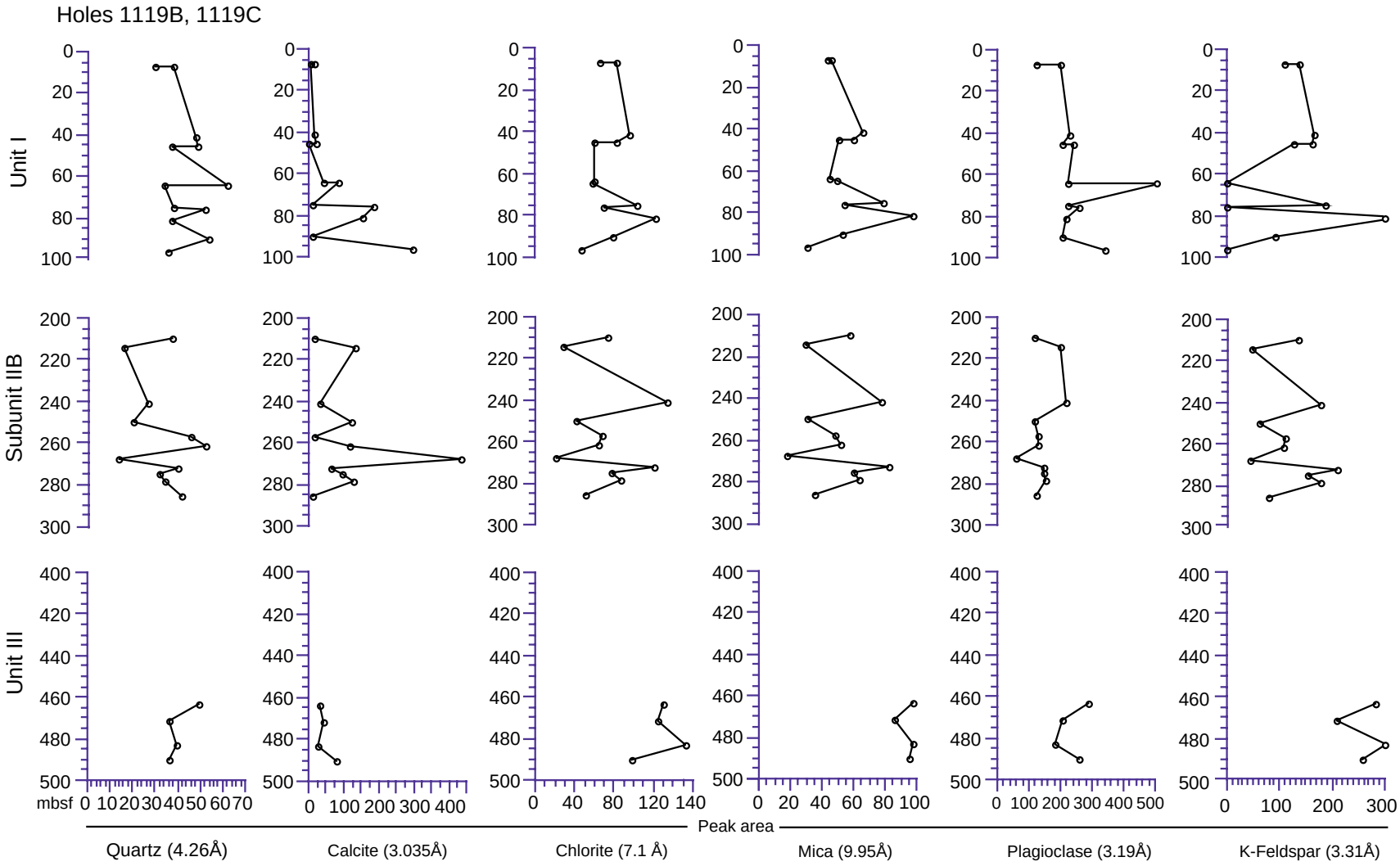

Figure F7. Color banding in upper lithostratigraphic Unit I (~9 mbsf) greenish gray silty clays that may be a reflection of mud turbidites' lighter layers (interval 181-1119C-2H-1, 60–105 cm).

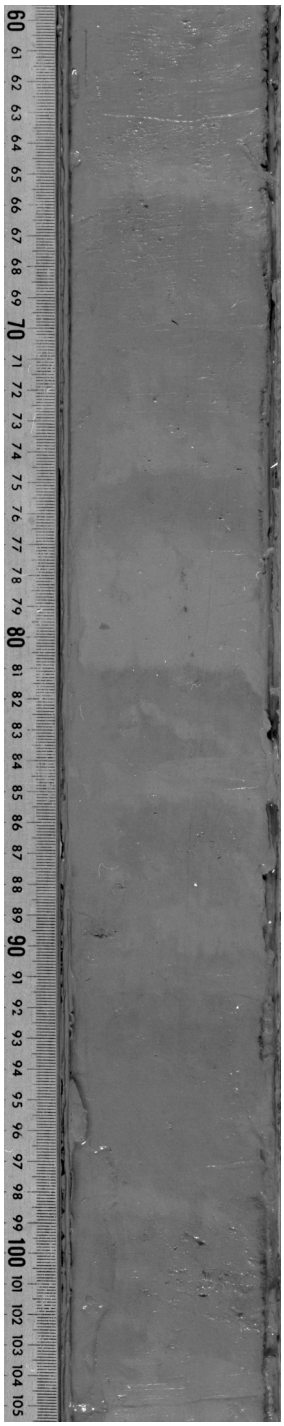

Figure F8. Cored section in upper lithostratigraphic Subunit IIA (~100 mbsf) showing sectioned valves of the cold-water bivalve *Zygochlamys delicatula,* and sand-filled *Thalassinoides* burrows (interval 181-1119C-11H-6, 1–25 cm).

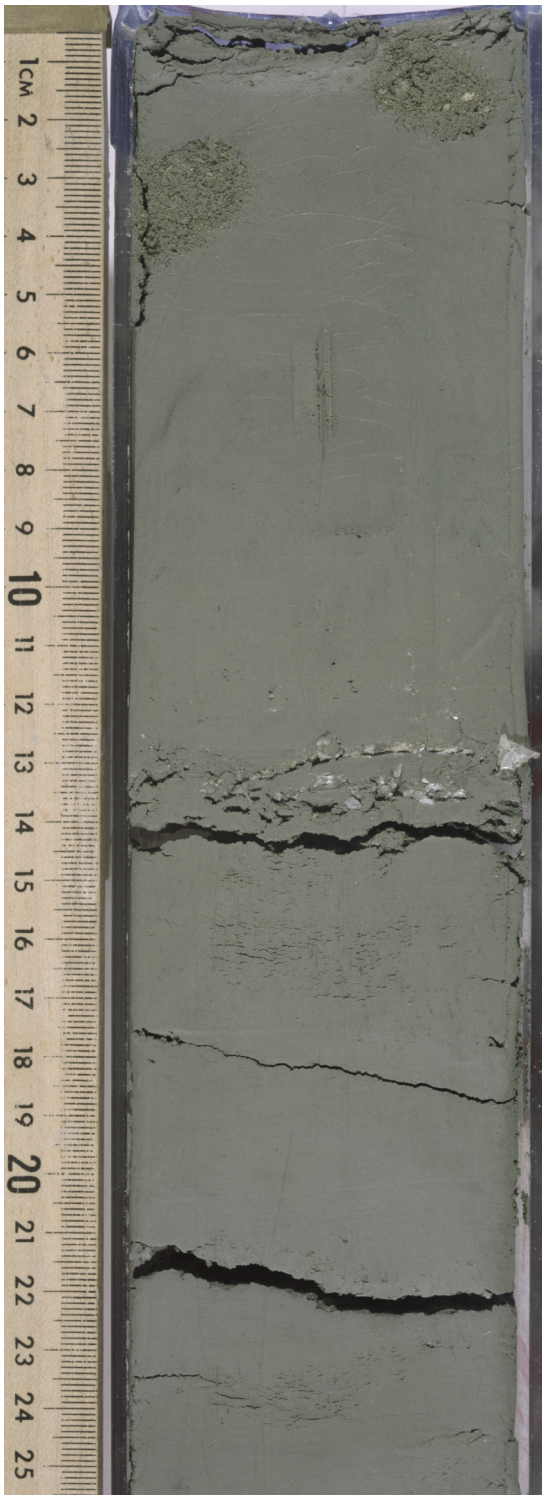

Figure F9. Upper lithostratigraphic Subunit IIA (~97 mbsf) olive-gray silty sand overlying greenish gray silty clay with sand-filled burrows of *Chondrites* (interval 181-1119C-11H-4, 55–80 cm).

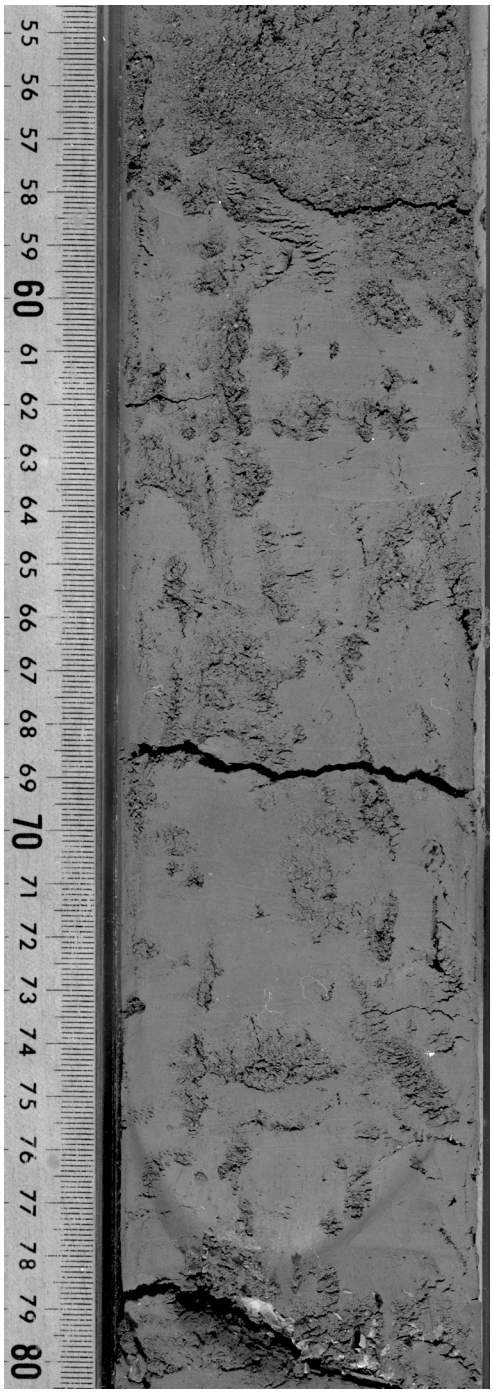

Figure F10. Drift couplet in Subunit IIB (~215 mbsf) of normally graded, shell-bearing, olive-gray sandy silt overlying light-colored silty clay (interval 181-1119C-23X-7, 0–30 cm).

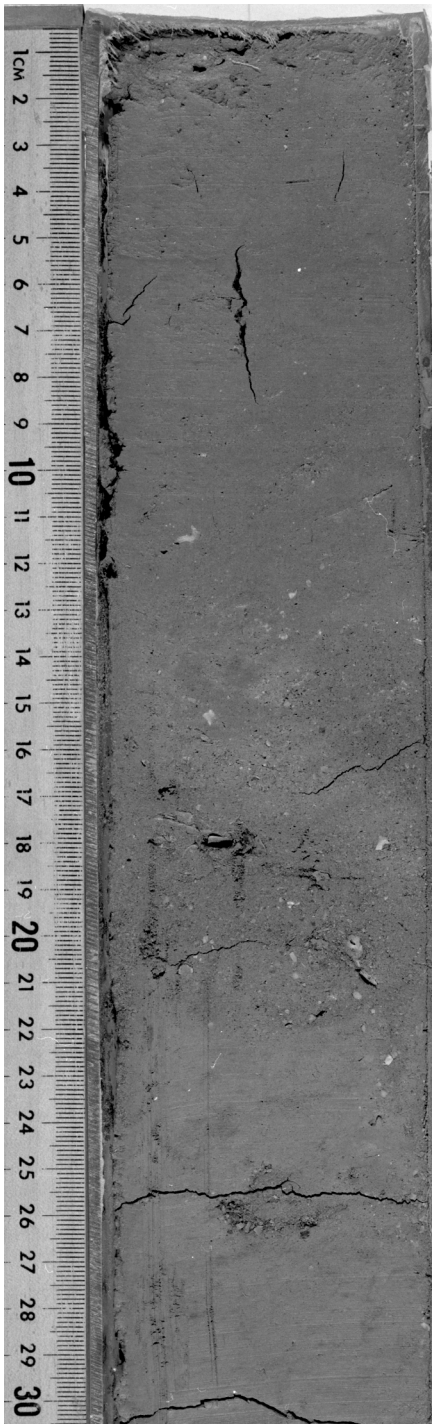

Figure F11. Thin fine-sand turbidite within greenish gray silty clay facies of upper Subunit IIC (~288 mbsf) drift sediments (interval 181-1119C-31X-4, 50–70 cm).

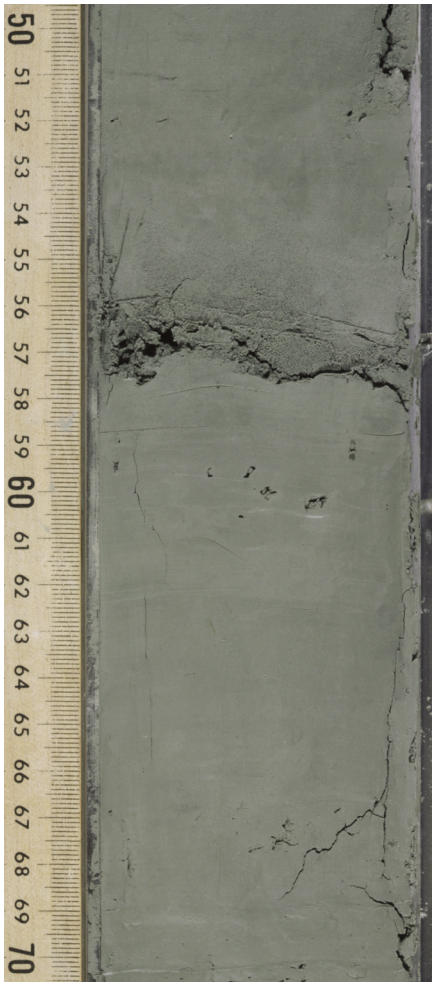

Figure F12. Relative abundance of diatom valves vs. core depth at Hole 1119C. B = barren, T = trace, R = rare, F = few, C = common, D = dominant.

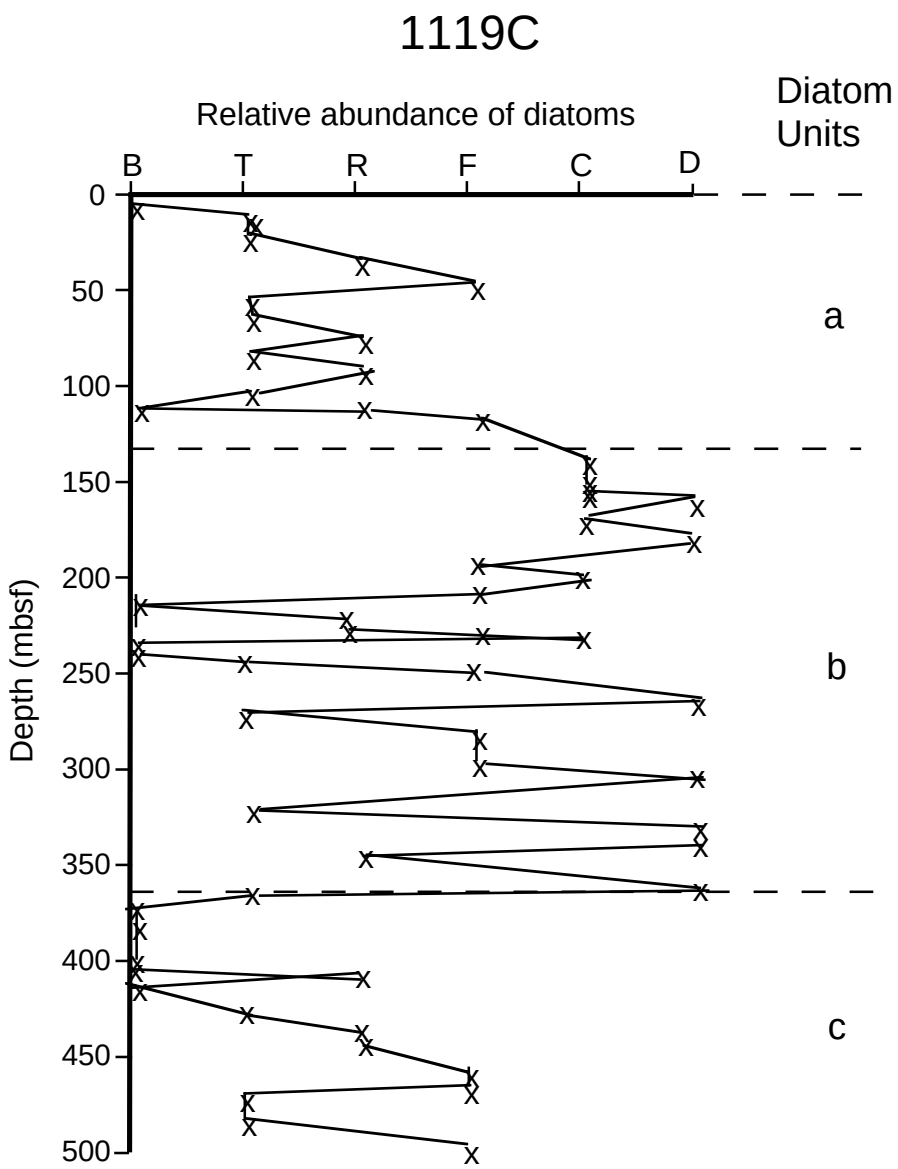

Figure F13. Whole-core magnetic susceptibility from Hole 1119B from the Bartington loop of the shipboard automated multisensor track, archive-half continuous measurements of NRM intensity, and inclination before and after alternating-field demagnetization to 20 mT from the pass-though cryogenic magnetometer. Vertical and subvertical lines between 30–35 mbsf and 134–137 mbsf indicate intervals where measurements were not possible because of nonrecovery or poor core recovery.

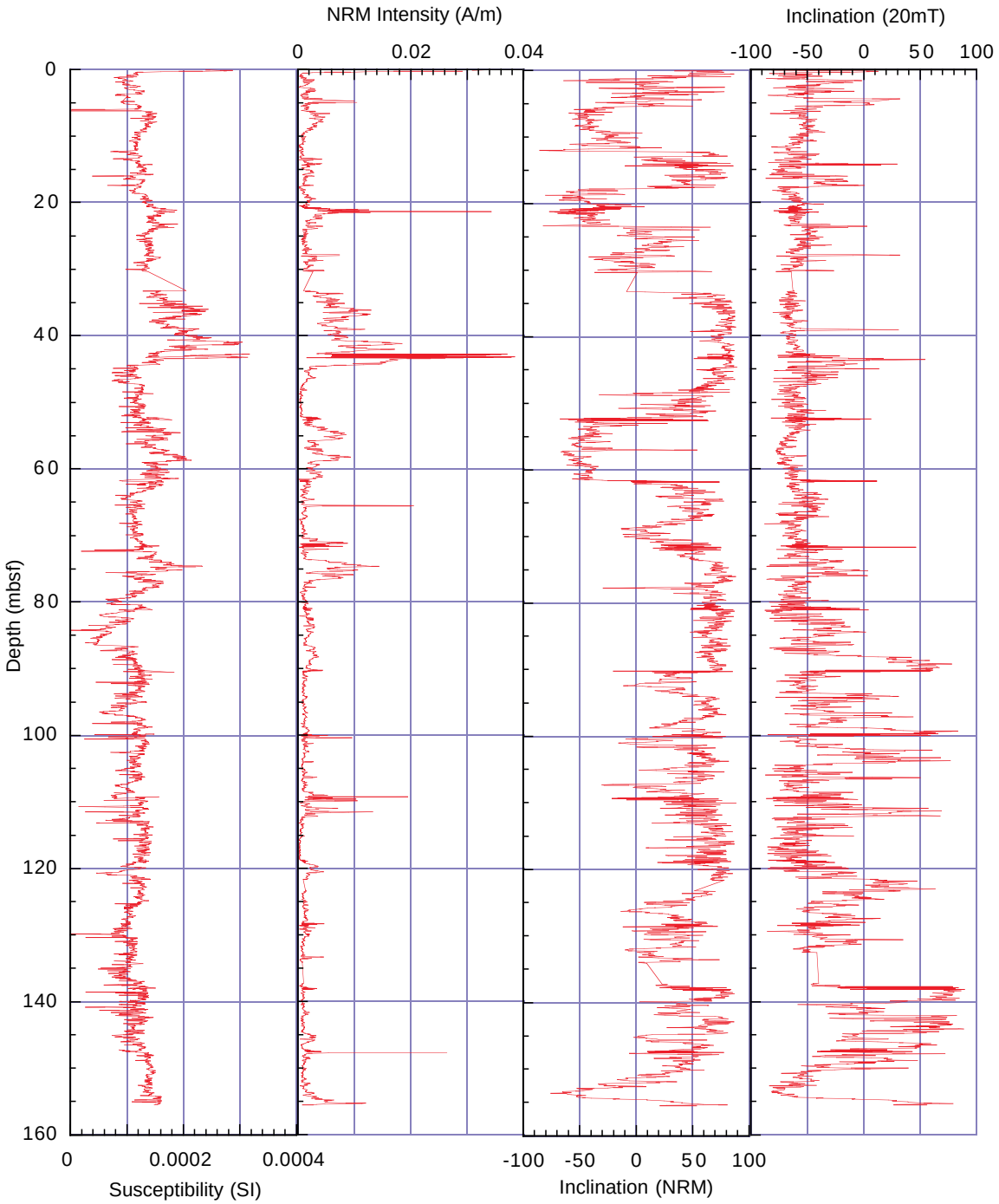

Figure F14. Whole-core magnetic susceptibility for core below 130 mbsf from Hole 1119C from the Bartington loop of the shipboard automated multisensor track, archive-half continuous measurements of NRM intensity, and inclination after alternating-field demagnetization to 20 mT from the pass-through cryogenic magnetometer. Vertical and subvertical lines between 215–225 mbsf and between 342–428 mbsf indicate intervals where measurements were not possible as a result of nonrecovery or poor core recovery.

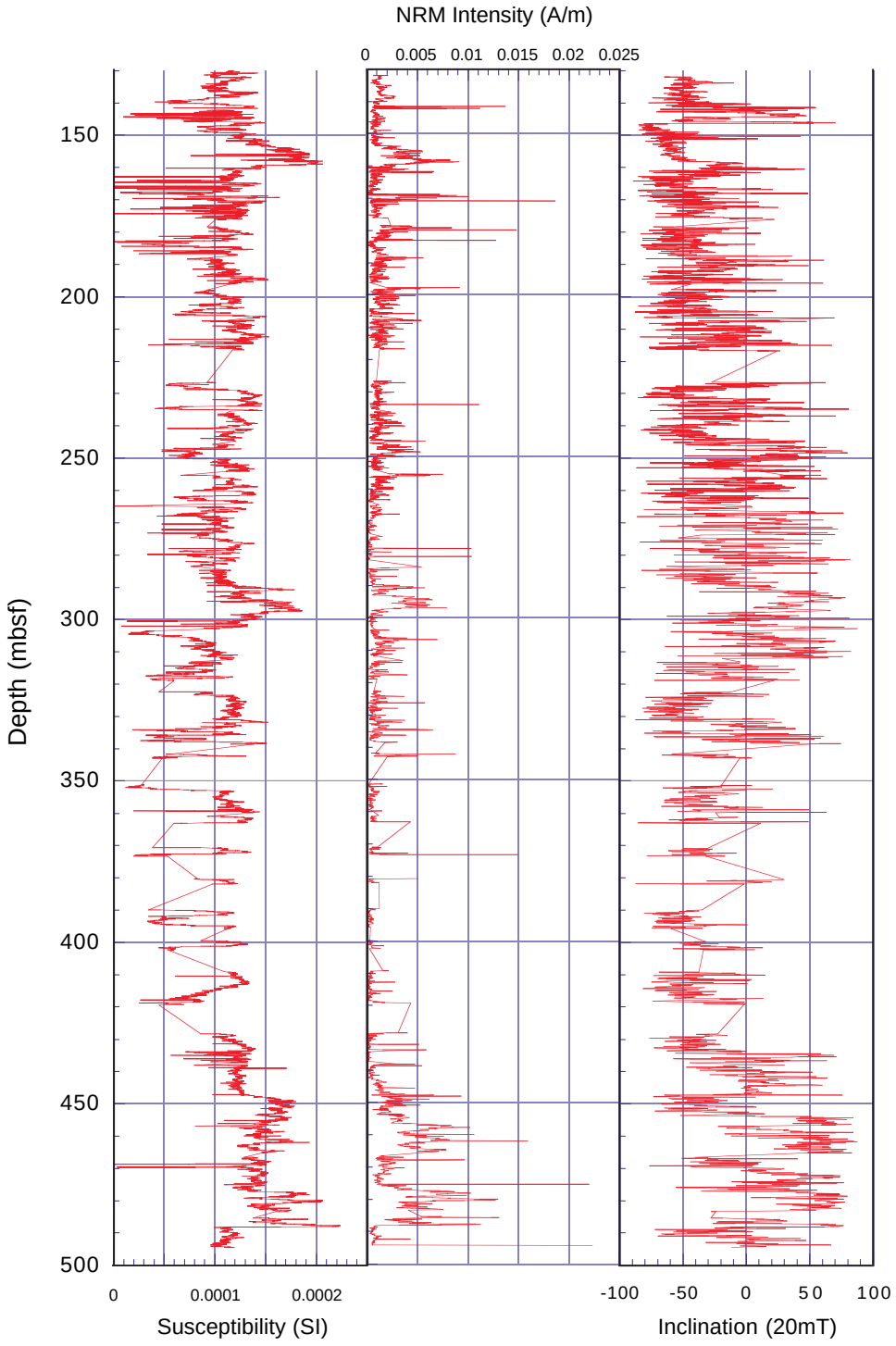

Figure F15. Vector component and equal-area diagrams of demagnetization behavior of representative discrete samples from Site 1119. **A.** AF demagnetization of a sample from 14.10 mbsf. **B.** AF demagnetization of a sample from 36.89 mbsf. **C.** AF demagnetization of a sample from 47.96 mbsf. **D.** AF demagnetization of an SIRM applied to a sample from 151.63 mbsf. **E.** Thermal demagnetization of a sample from 295.64 mbsf. **F.** Thermal demagnetization of a sample from 296.74 mbsf.

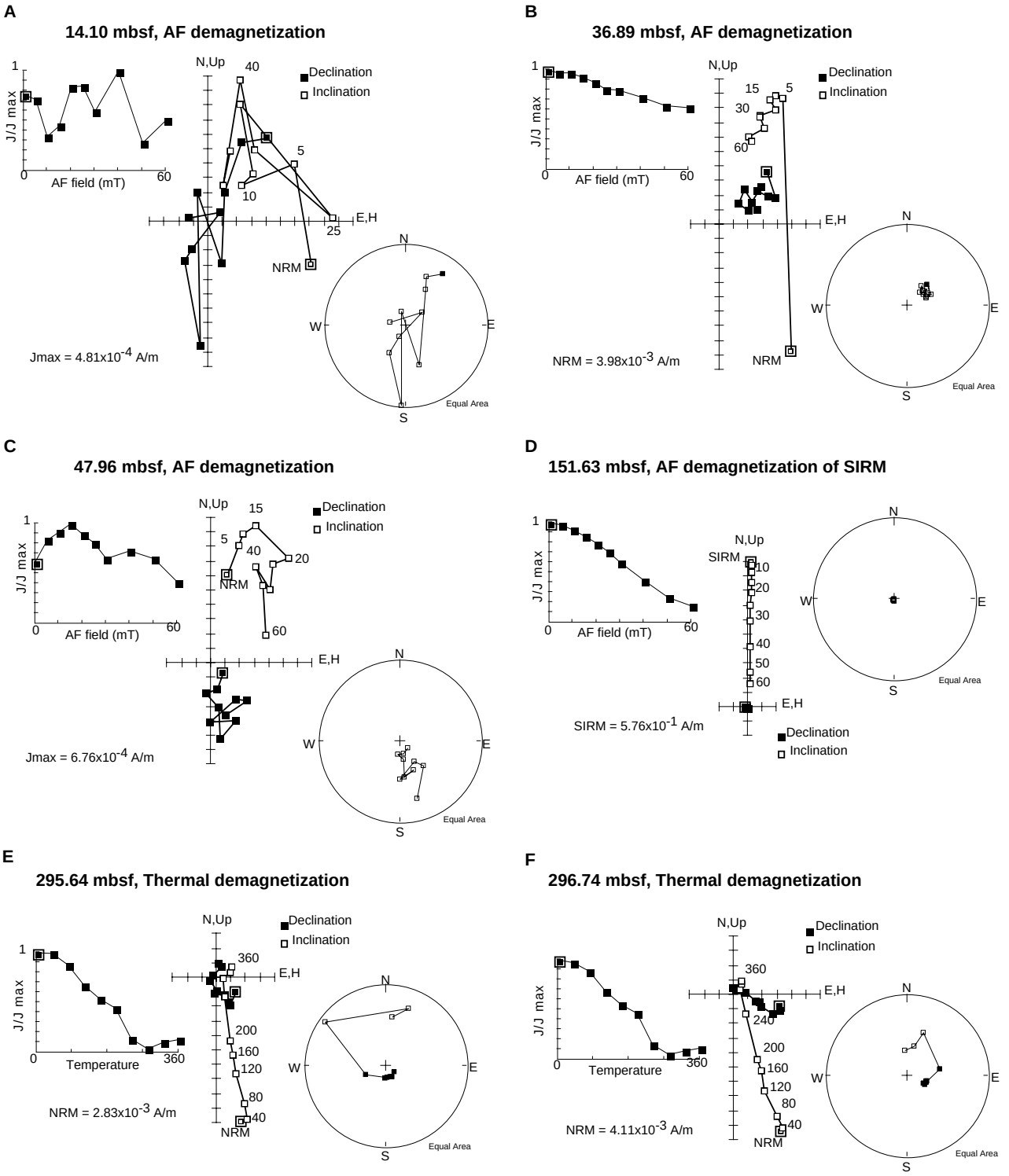

Figure F16. Isothermal remanent magnetization (IRM) and backfield acquisition curves for representative discrete samples from Site 1119. Remanence does not become saturated until 300–500 mT, and B_{cr} is between 50 and 75 mT for all samples.

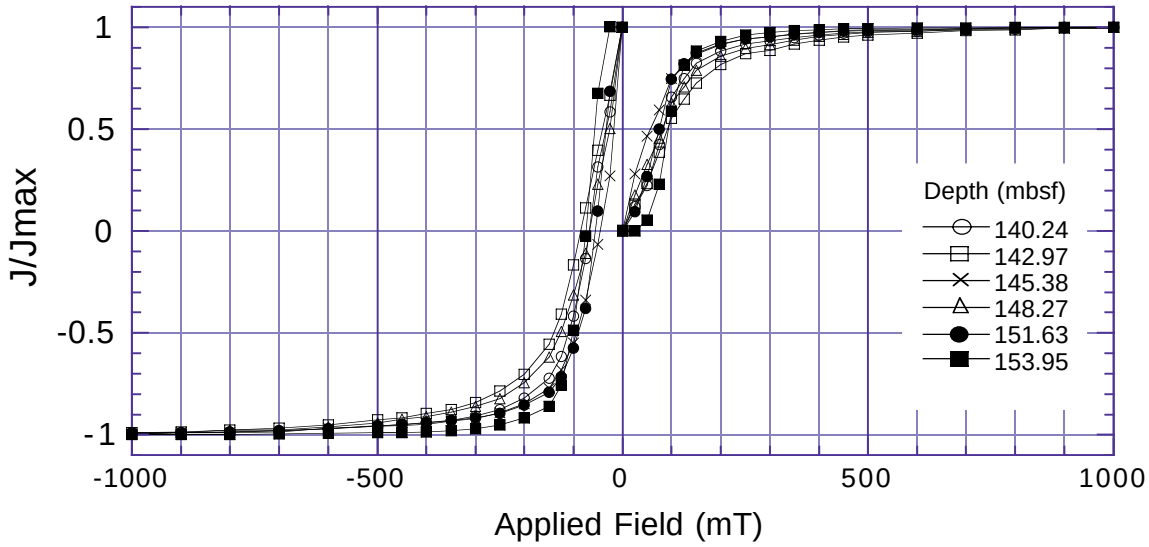

Figure F17. Composite sections for magnetic susceptibility and natural gamma ray. For convenience, MS values from Holes 1119B and 1119C are offset by 10 and 20 × 10^{-5}, respectively, and NGR values from Holes 1119B and 1119C are offset by 15 and 30 counts, respectively. Gaps in the composite section are indicated with triangles. A, B, C = the hole the line represents.

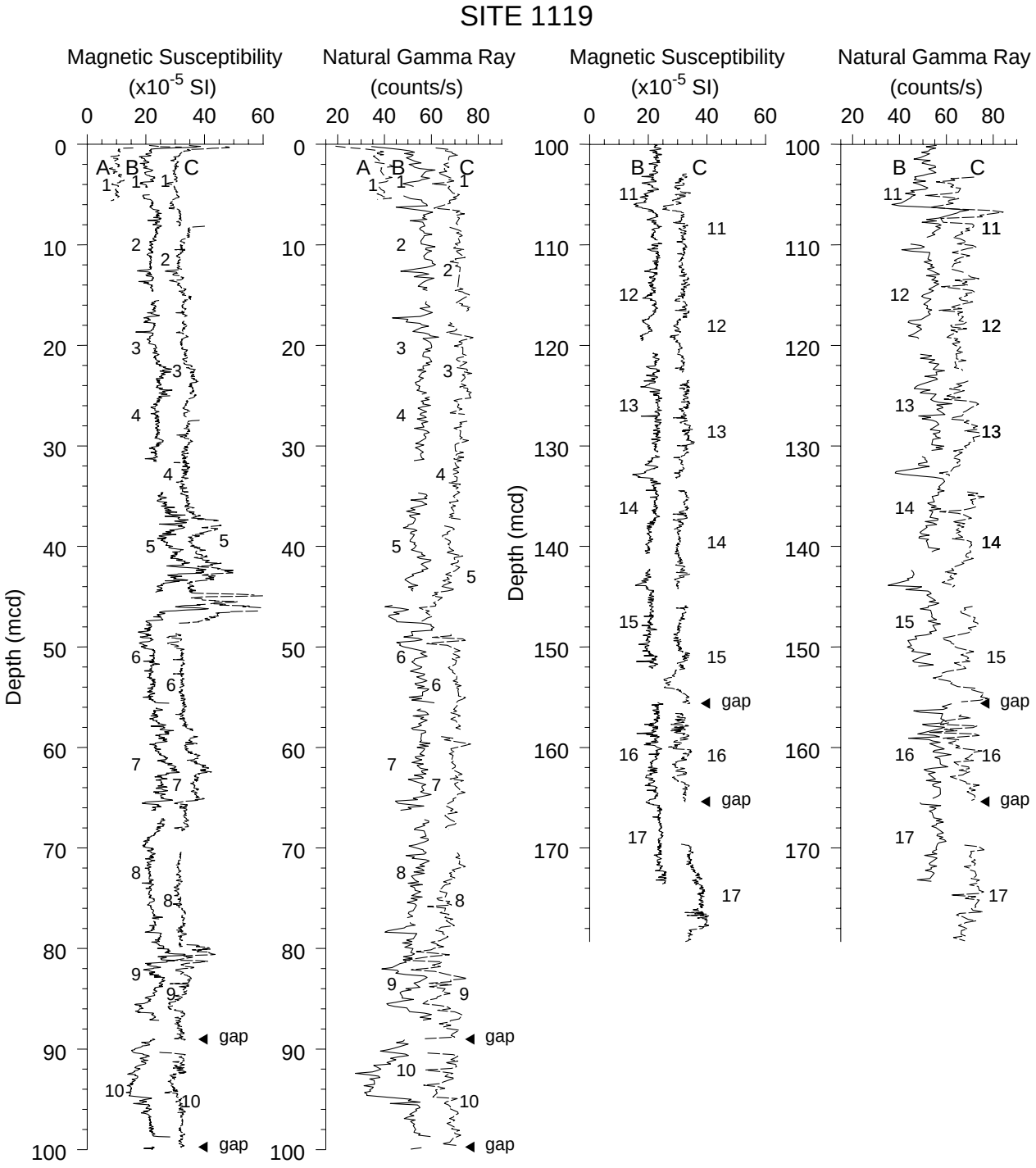

Figure F18. Downhole depth offsets between the mbsf and mcd scales for Site 1119 increase at a rate of ~10%.

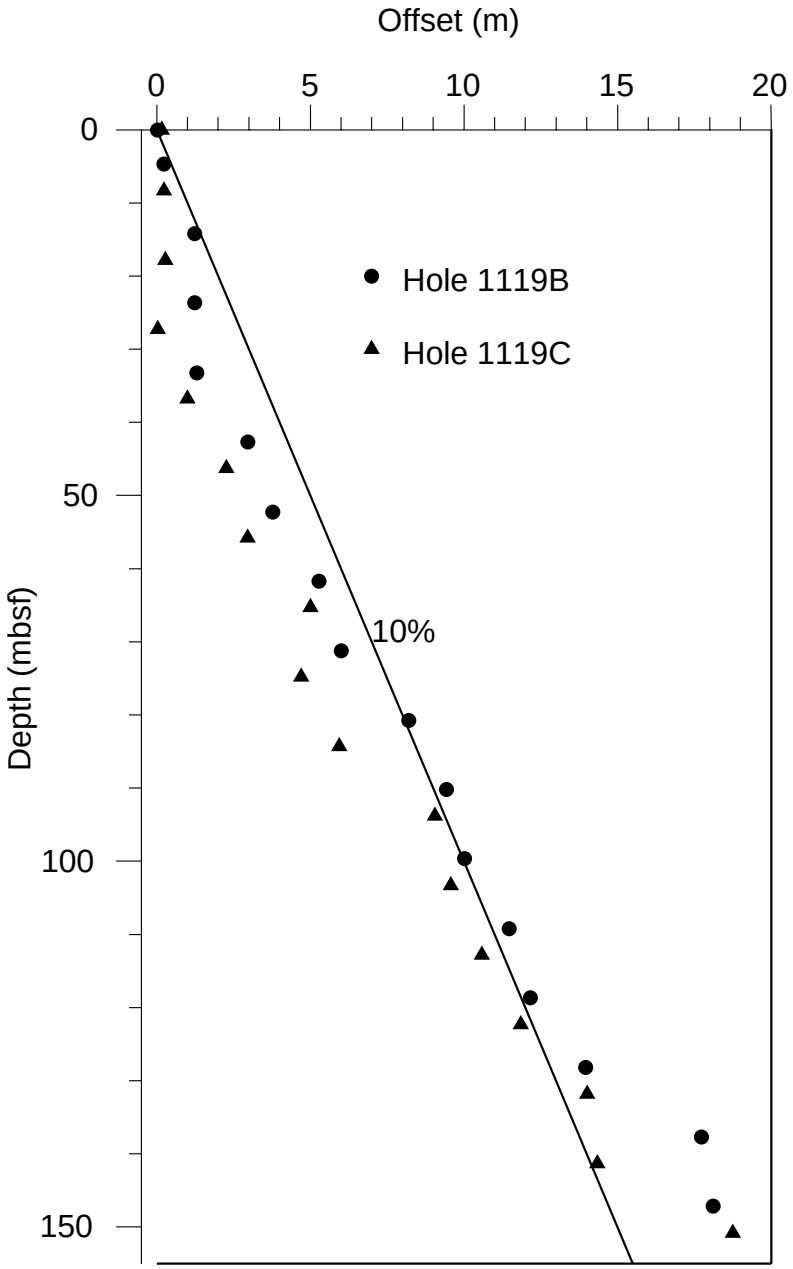

Figure F19. Spliced record for Site 1119. To reduce noise levels, the spliced data illustrated have been smoothed using a Gaussian window. The window width is 25 cm for magnetic susceptibility and 60 cm for natural gamma ray.

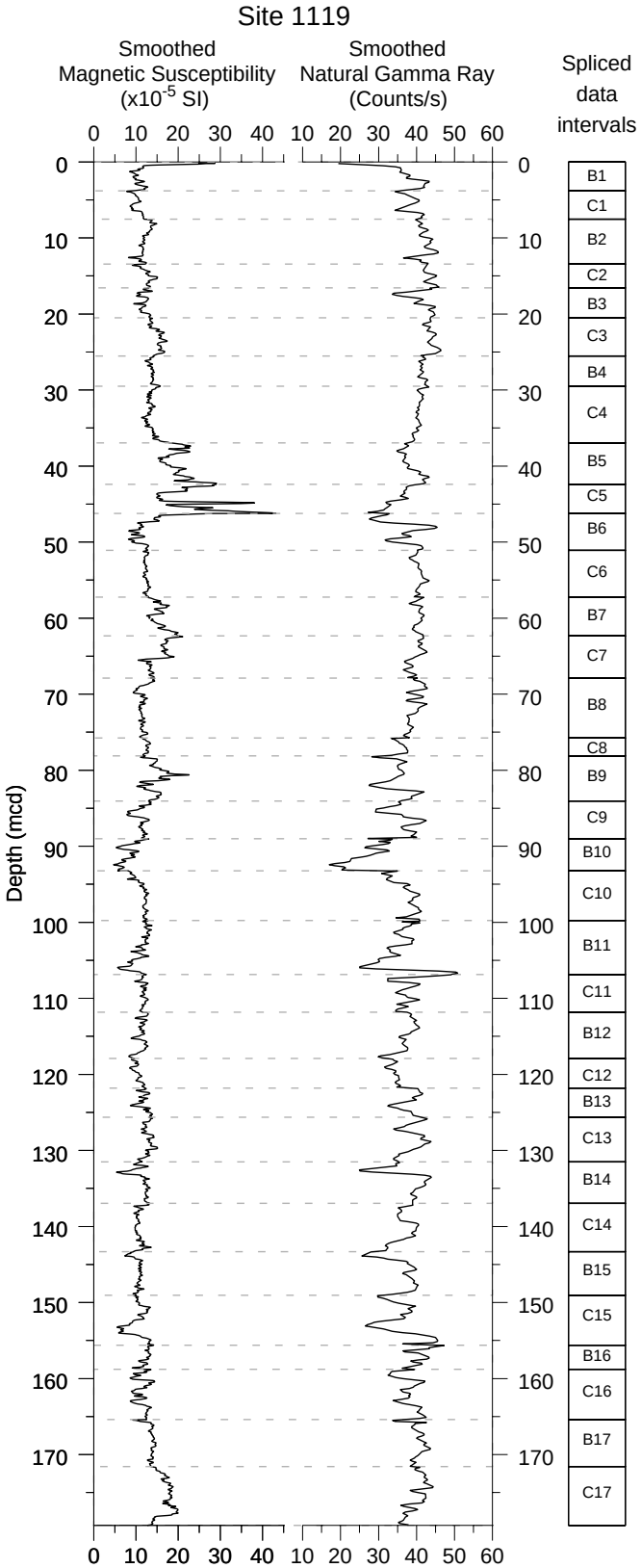

Figure F20. Age-depth curve using multiple microfossil datums for Site 1119. The best fit line is drawn according to subjective weighting of the chronostratigraphic and geochronologic precision of the events shown in Table T3, p. 87, and it shows the preferred average sedimentation rate. Vertical lines on arrows indicate possible errors caused by large sampling intervals (FO errors extend downcore, LO errors extend upcore). Where sampling intervals are decreased, vertical lines are minimized or removed. Larger arrow length indicates uncertainty in age of datum. Question marks indicate additional uncertainties discussed in text.

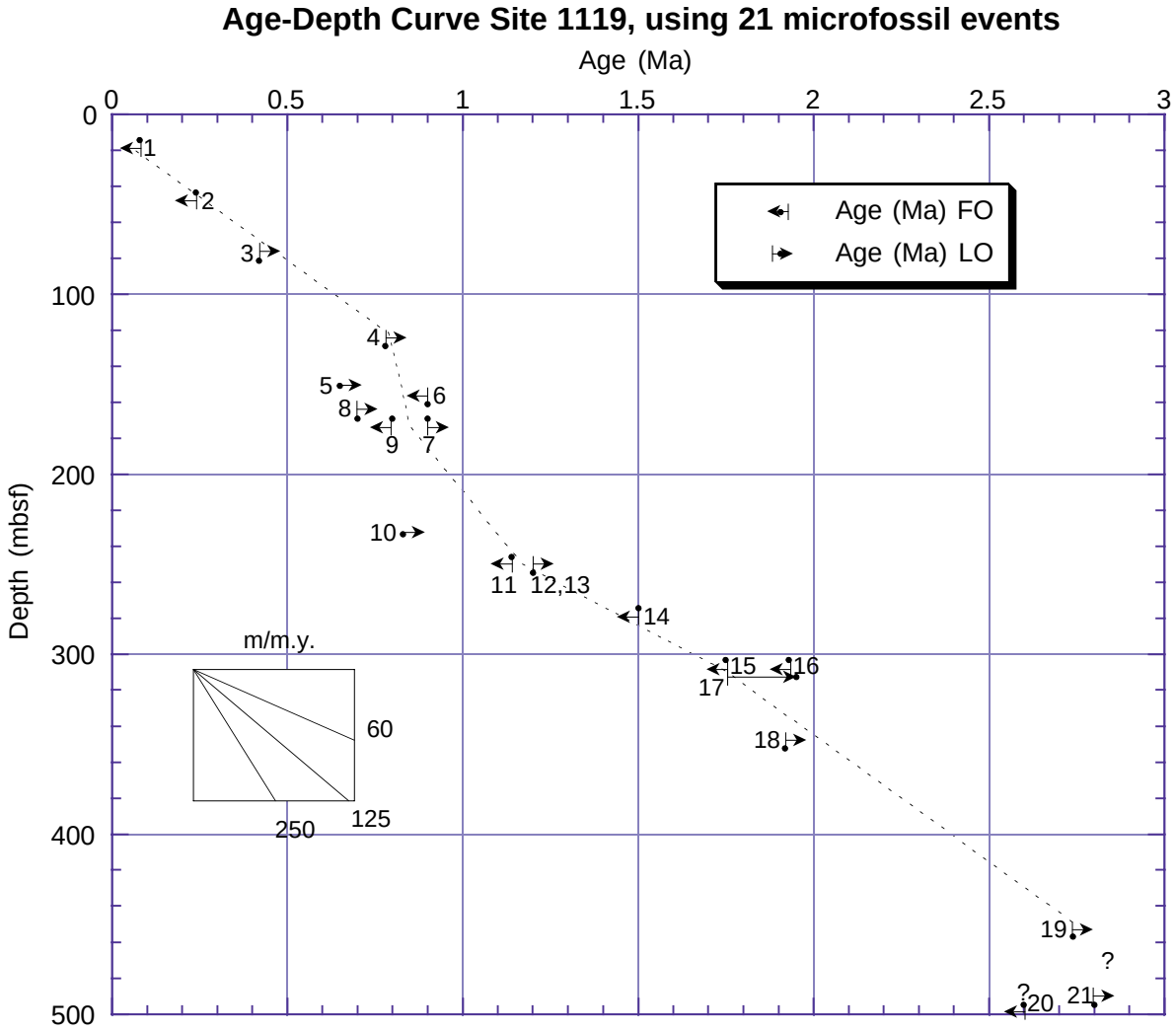

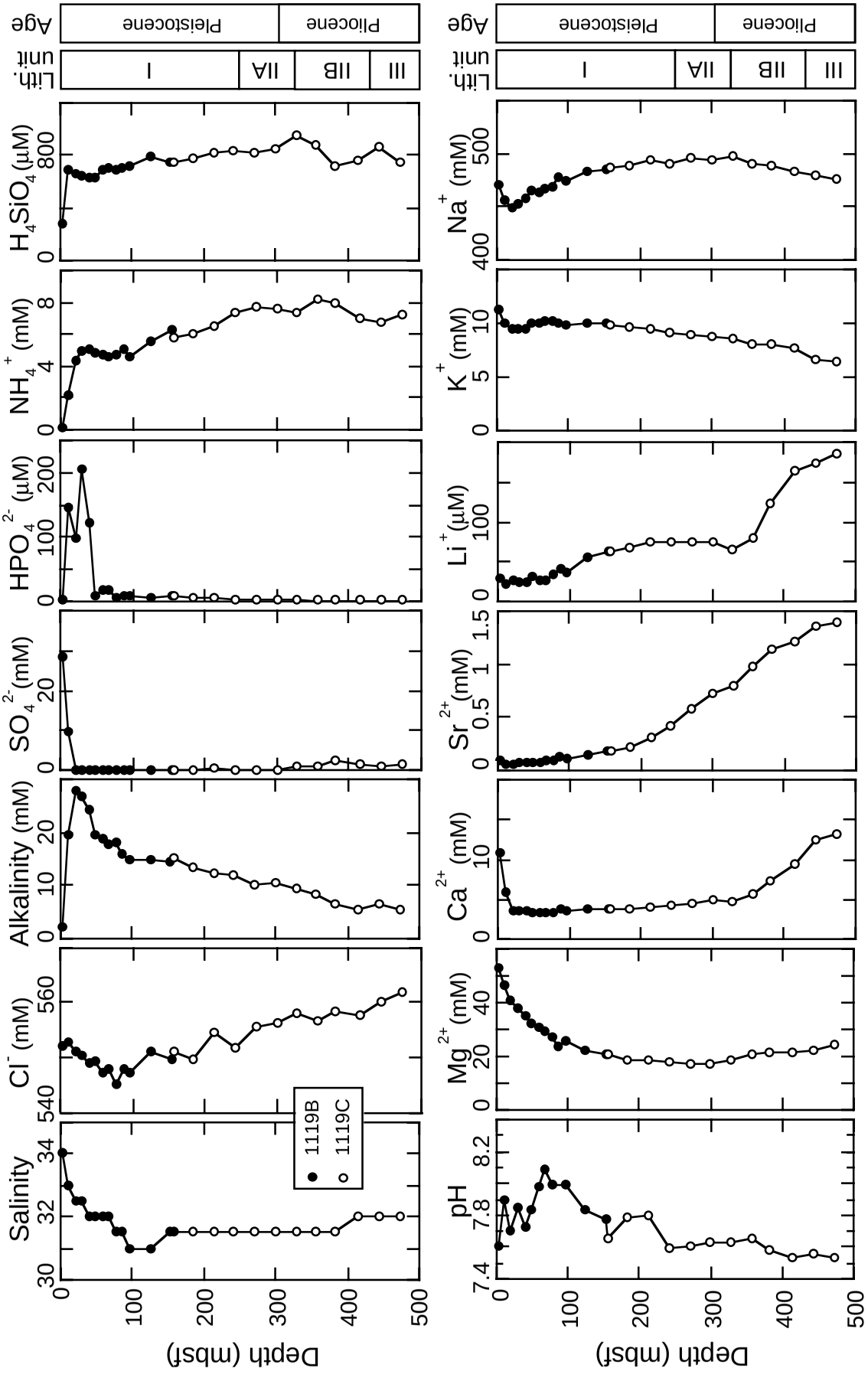

Figure F21. Depth profiles of interstitial-water constituents at Site 1119.

Figure F22. Depth profiles of Sr^{2+}/Ca^{2+} and Mg^{2+}/Ca^{2+}.

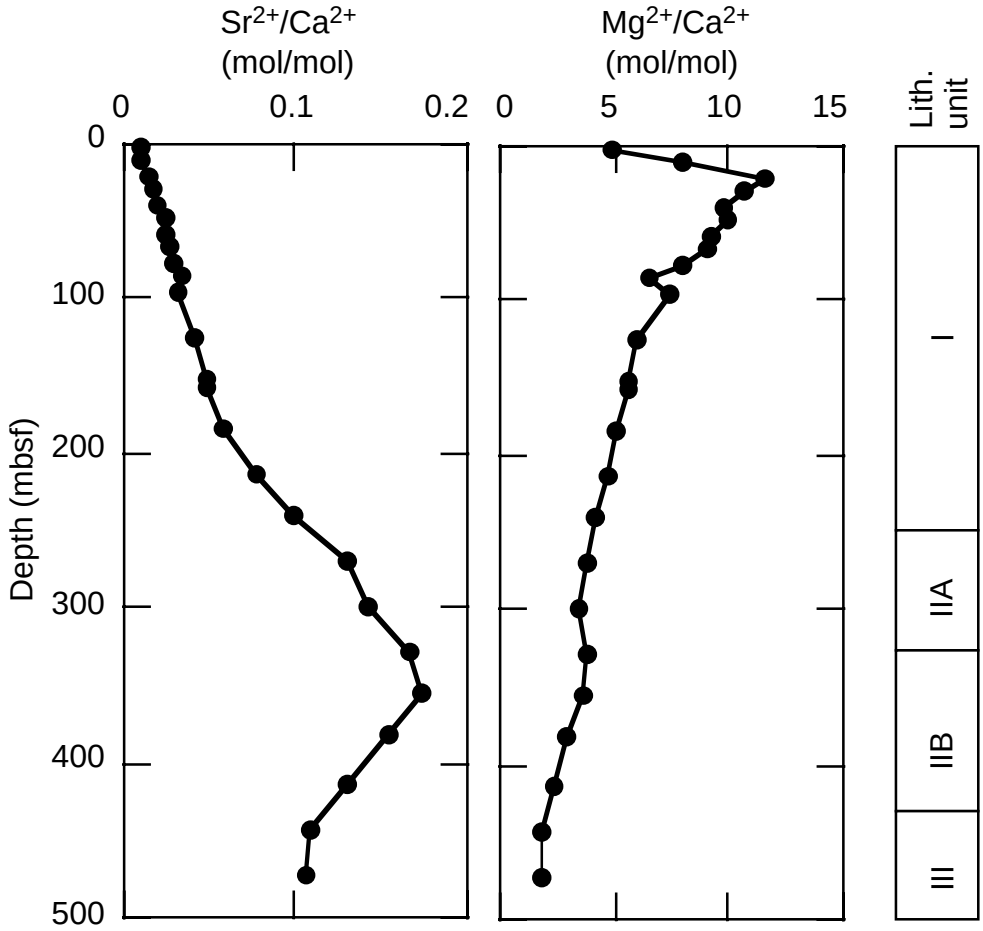

Figure F23. Headspace methane concentrations in sediments from Holes 1119B and 1119C.

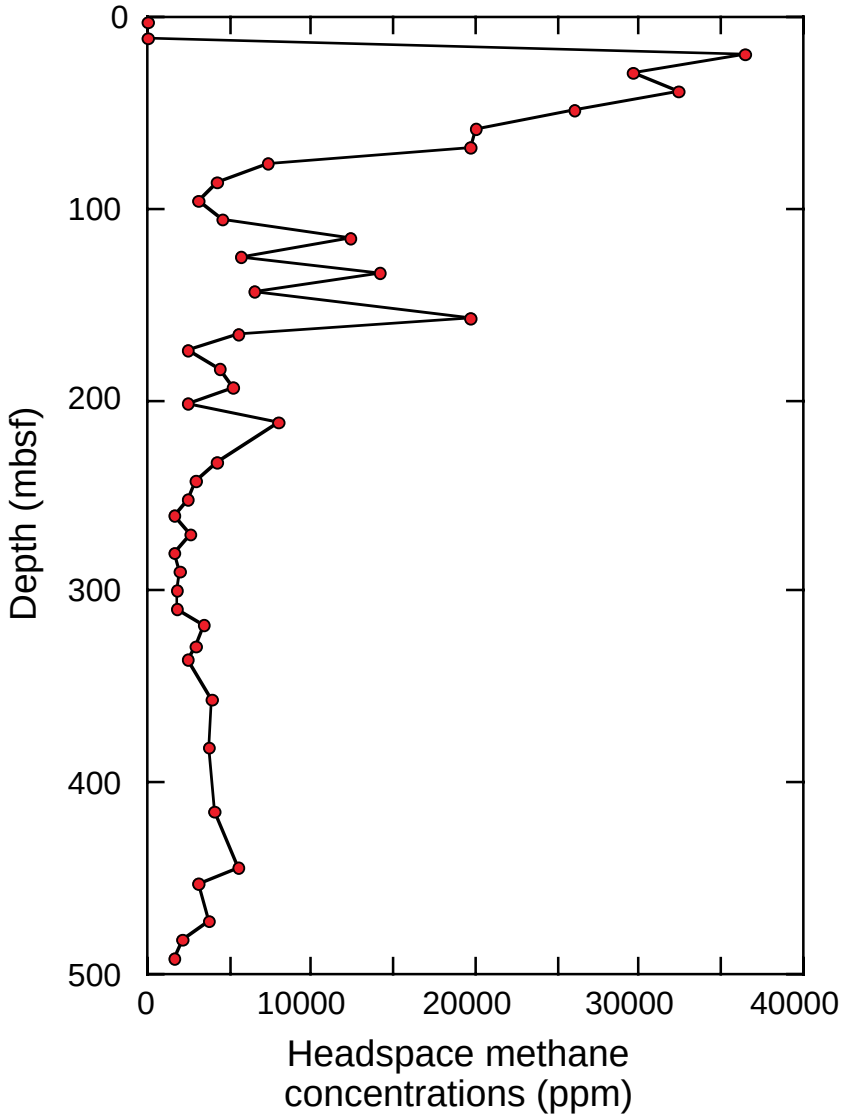

Figure F24. Calcium carbonate contents in sediments from Holes 1119B and 1119C.

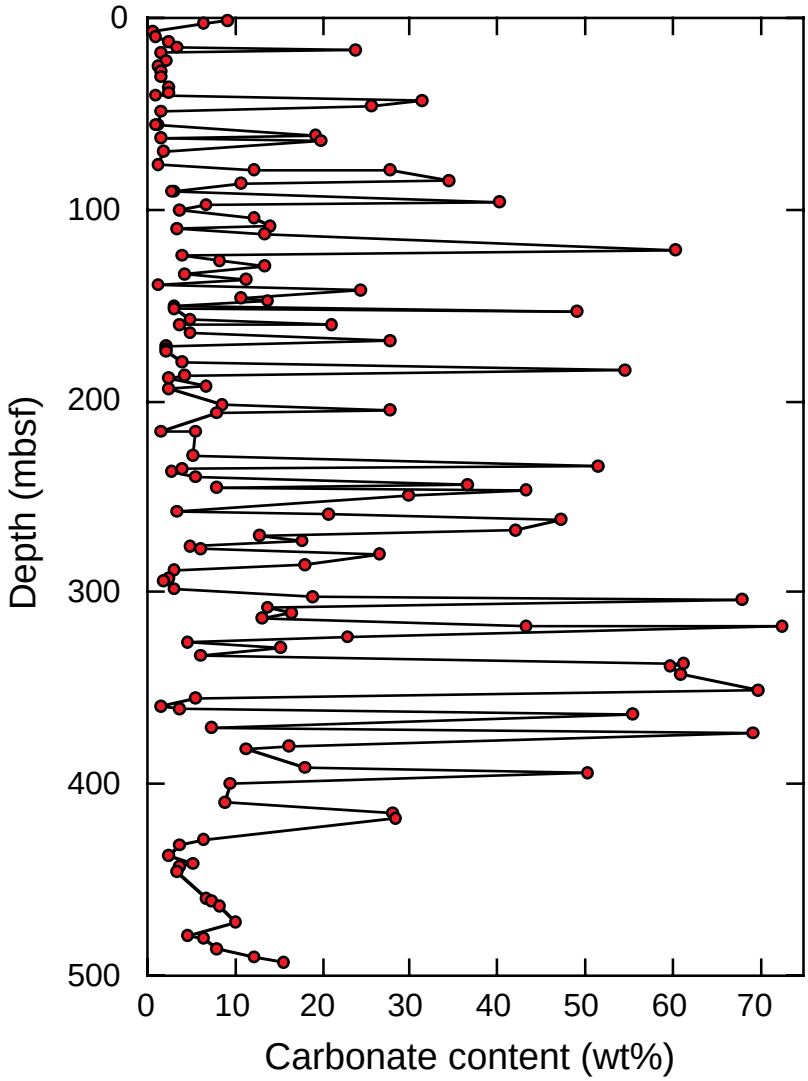

Figure F25. Total organic carbon contents in sediments from Holes 1119B and 1119C.

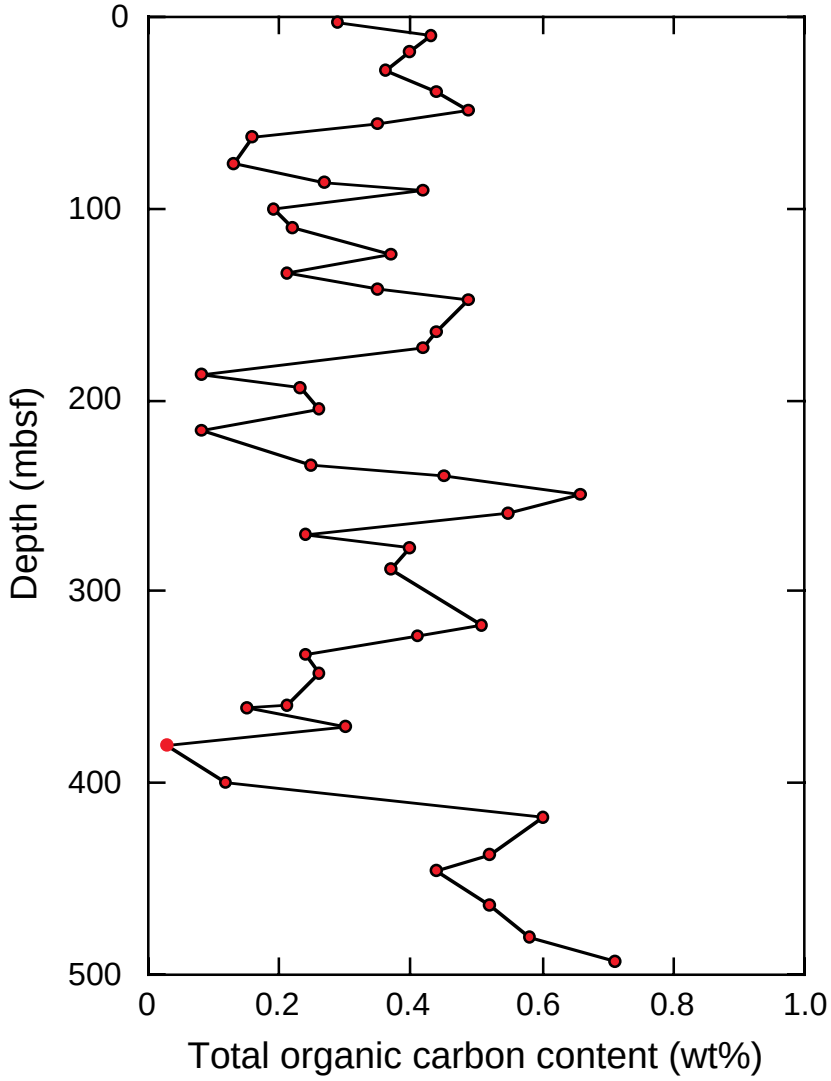

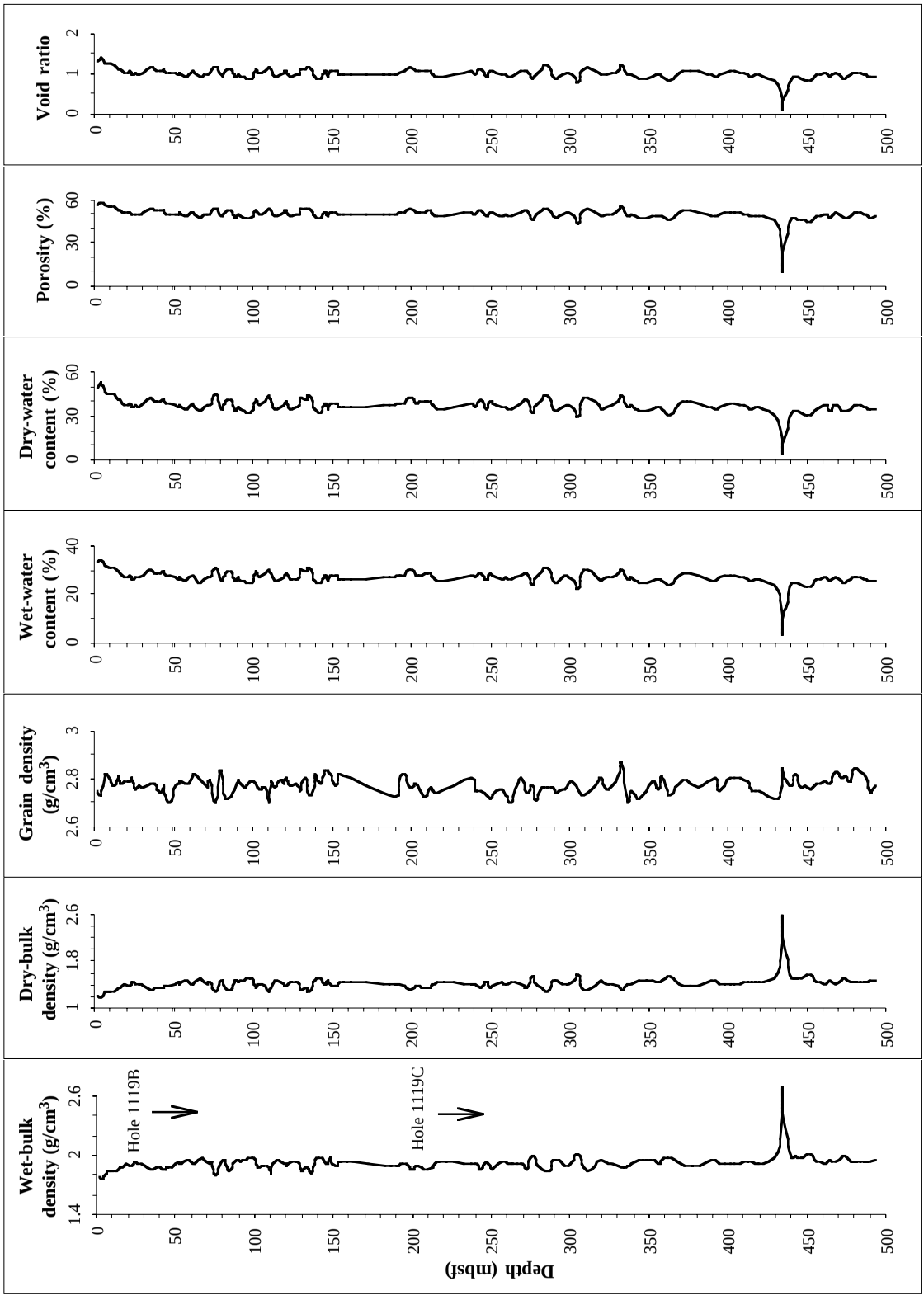

Figure F26. Index properties measured on cores from Holes 1119B and 1119C.

Figure F27. Multisensor track measurements from Hole 1119C including GRAPE density, magnetic susceptibility, and natural gamma-ray intensity.

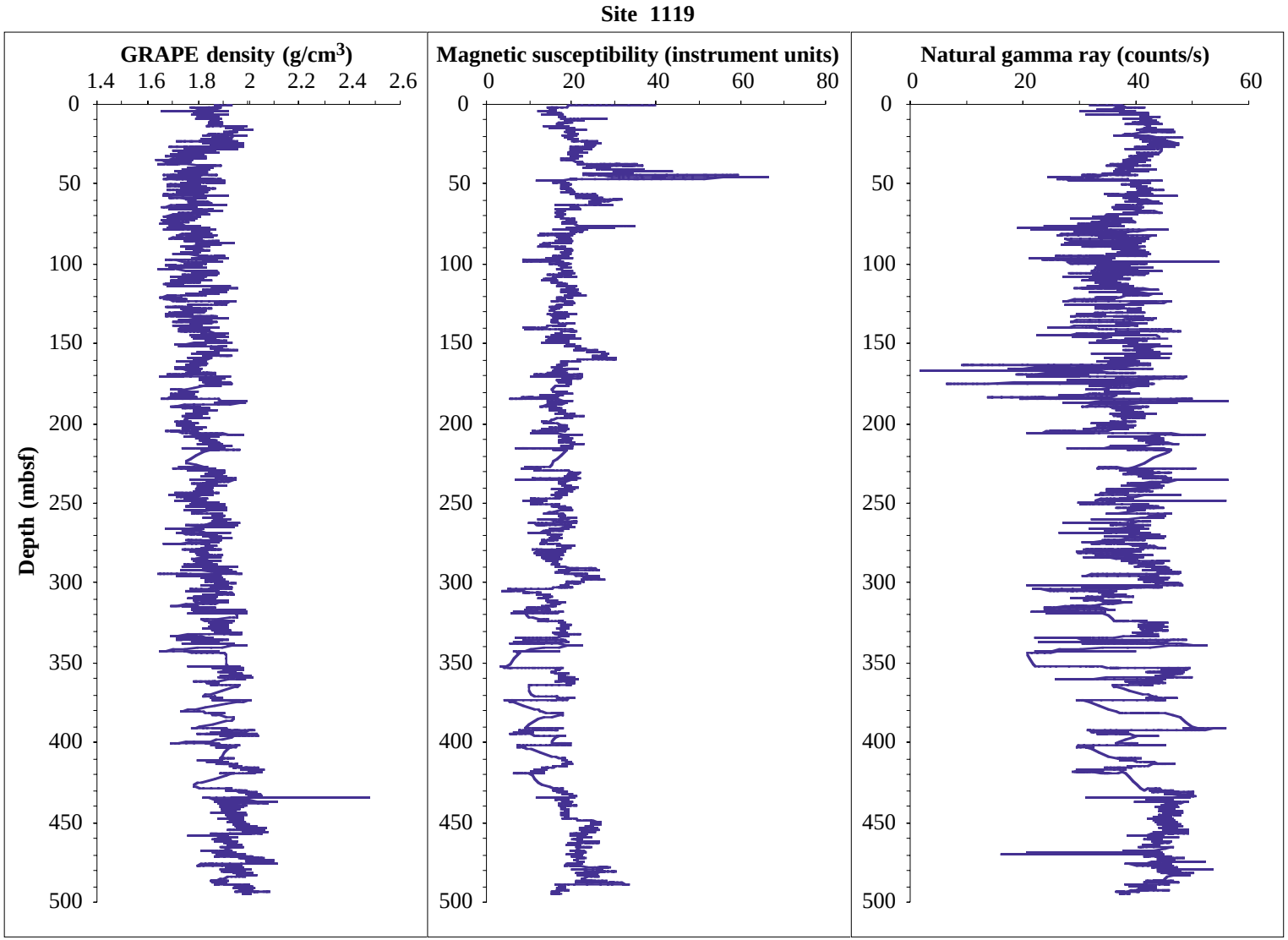

Figure F28. Density measurements using the GRAPE instrument on the MST in comparison with index properties. The circles indicate the distribution of wet-bulk density based on index property measurement.

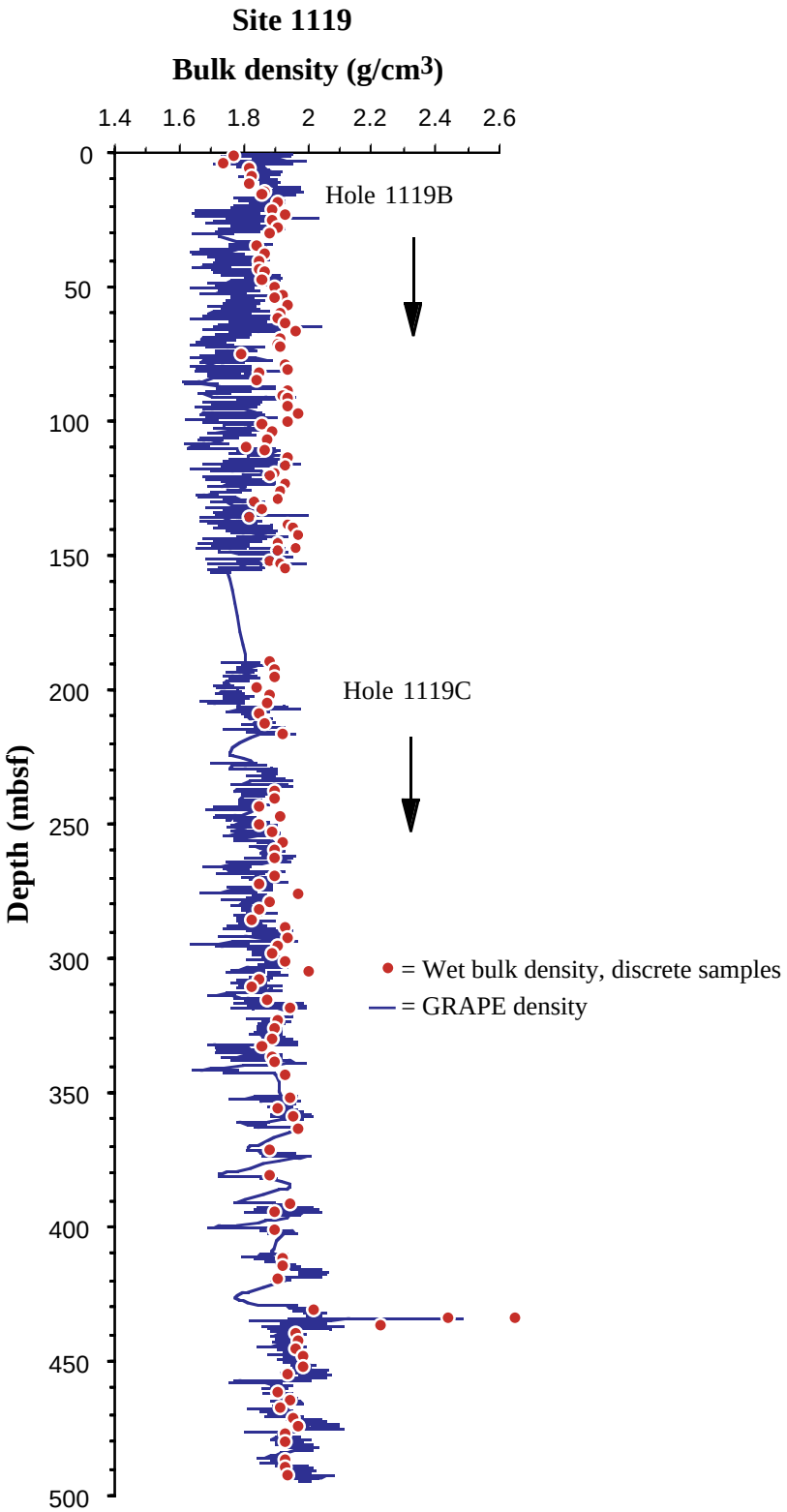

Figure F29. Vane shear strength measured in cores from Hole 1119B and torvane shear strength measured from cores in Hole 1119C.

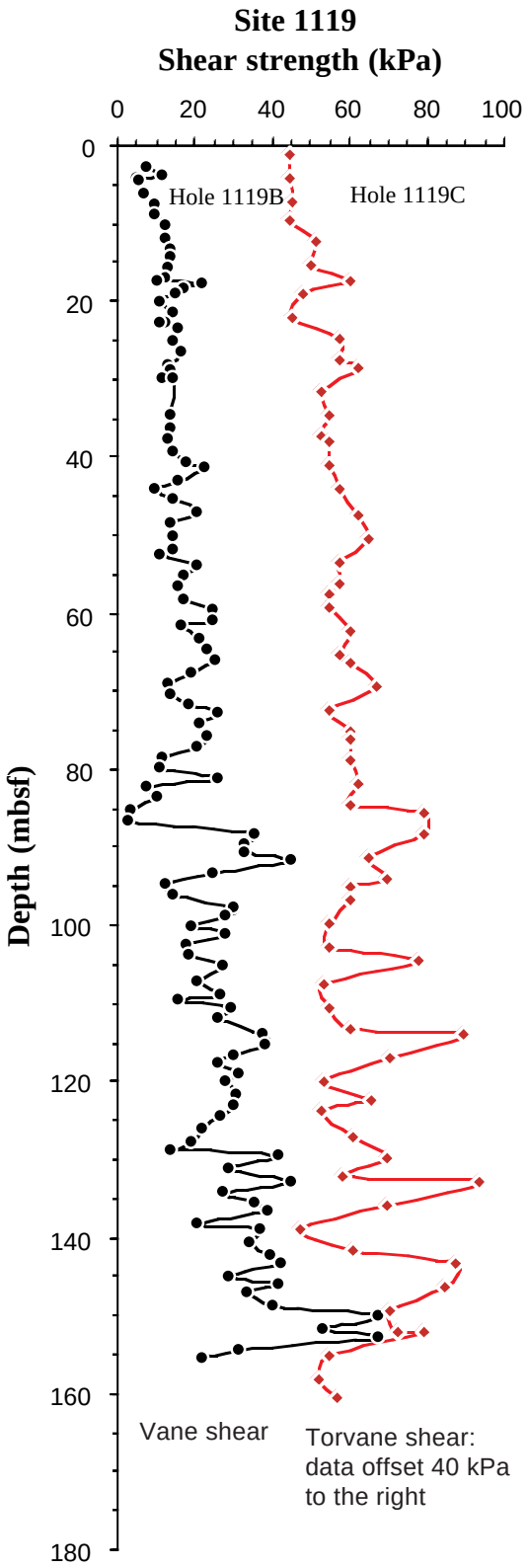

Figure F30. Thermal conductivity measured in cores from Holes 1119B and 1119C.

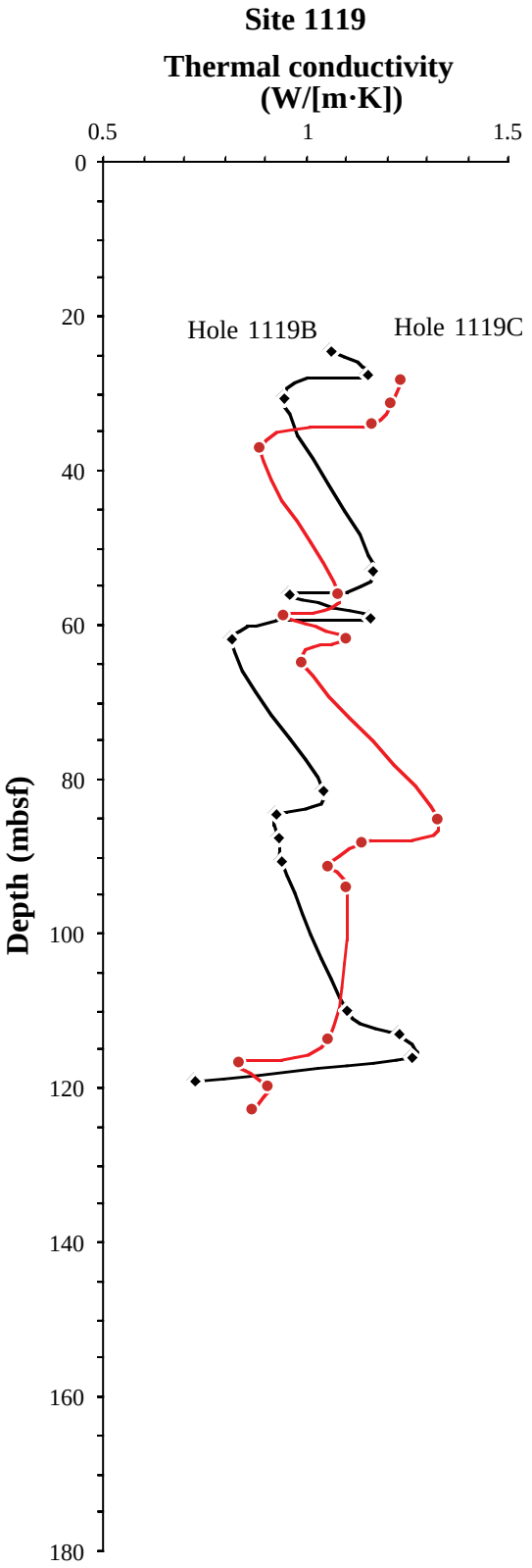

Figure F31. Summary of logging operations at Hole 1119C. The solid lines extending vertically from the pipe show the intervals that were logged. The top of each line shows where logging stopped, while the bottom shows where logging started.

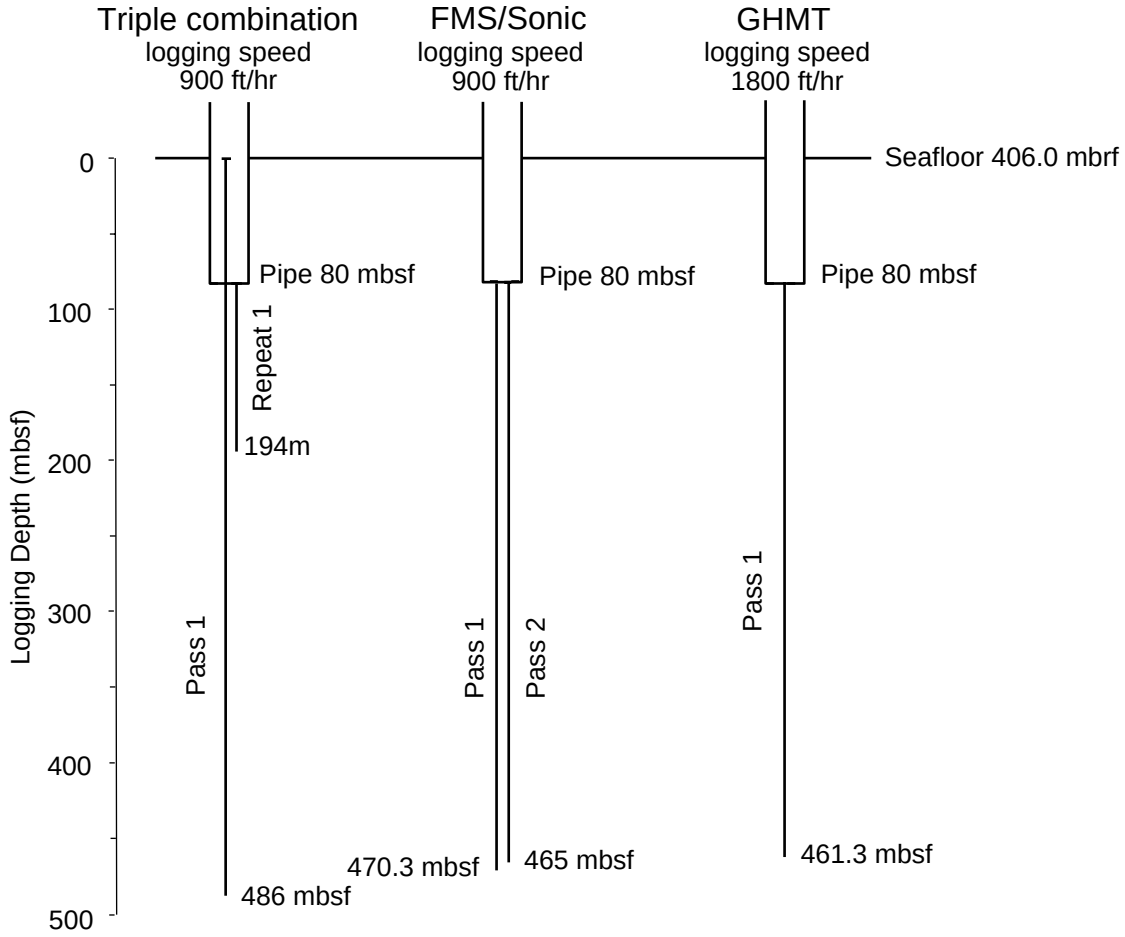

Figure F32. A, B. Results from the downhole logging tools, plotted alongside core recovery. (Continued on next page.)

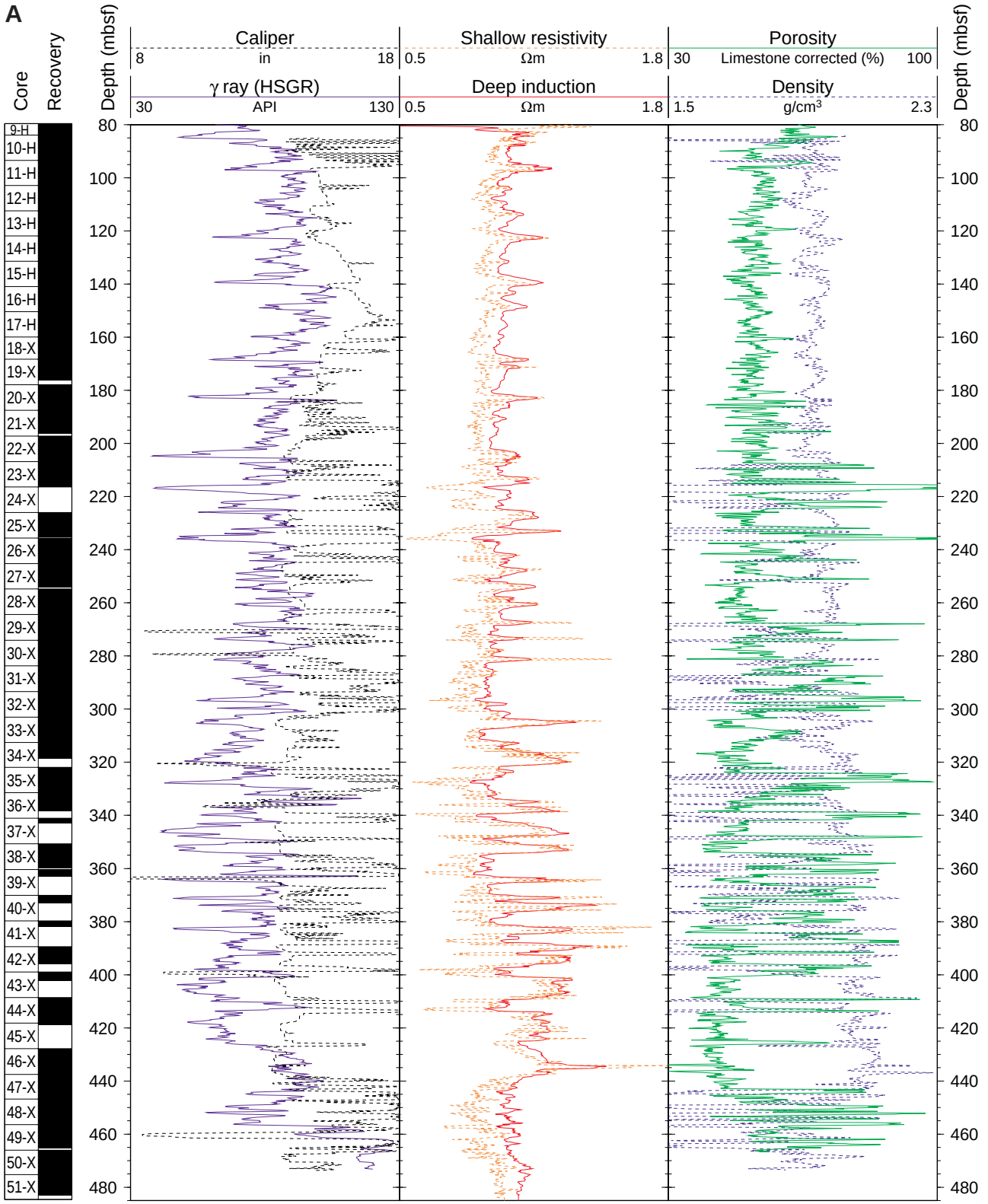

Figure F32 (continued).

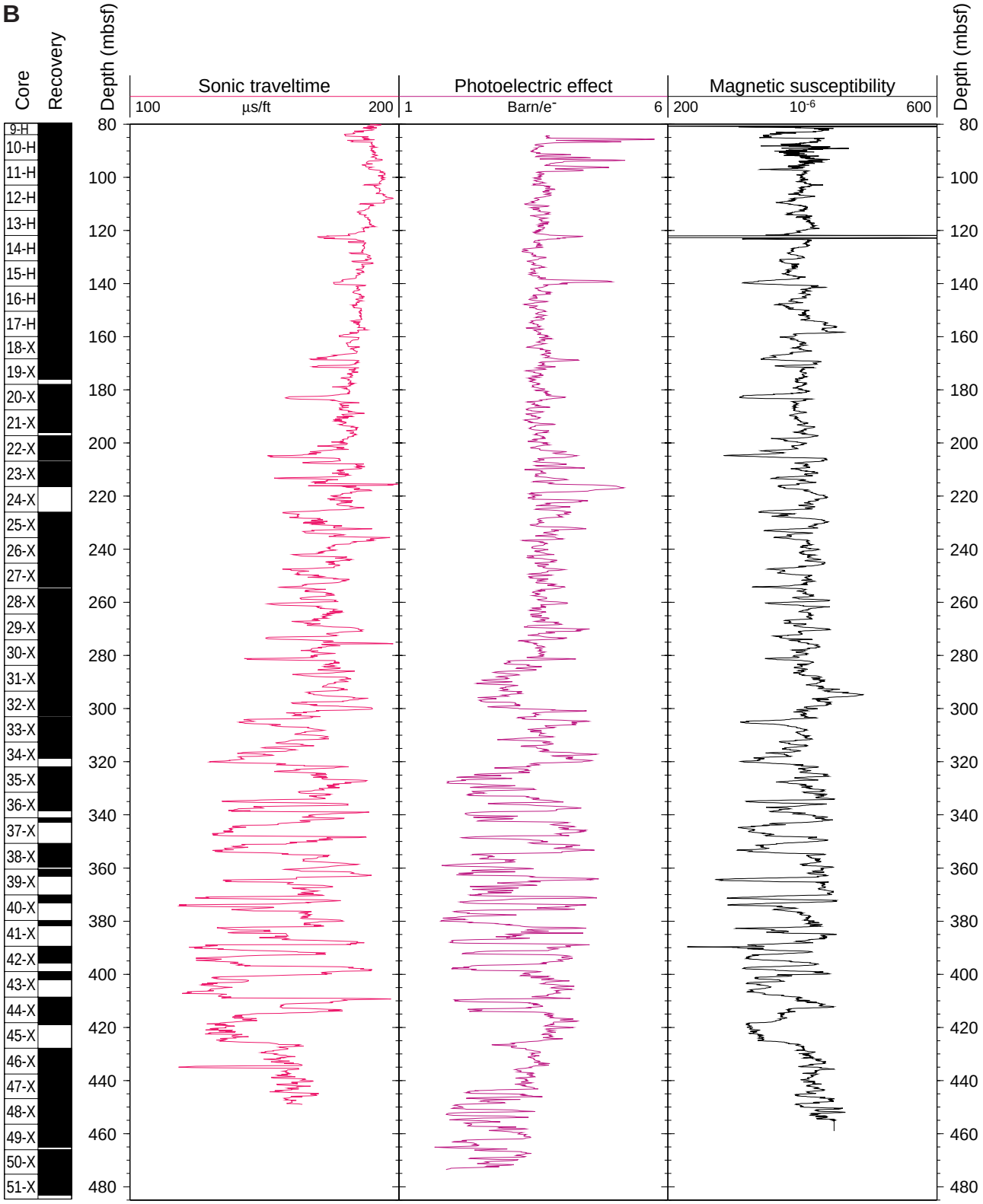

Figure F33. A comparison of edited log-based density measurements from the HLDS, with results from the core.

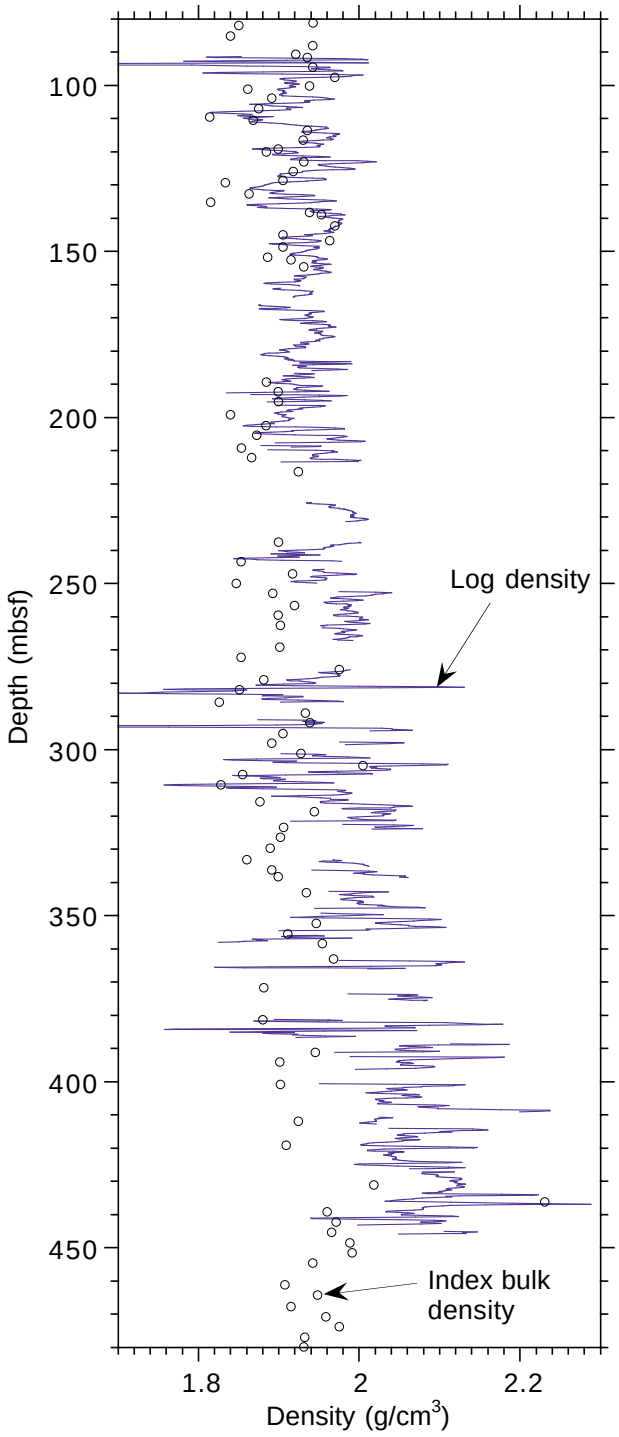

Figure F34. A comparison of log-based magnetic susceptibility measurements from the SUMS, with results from the core.

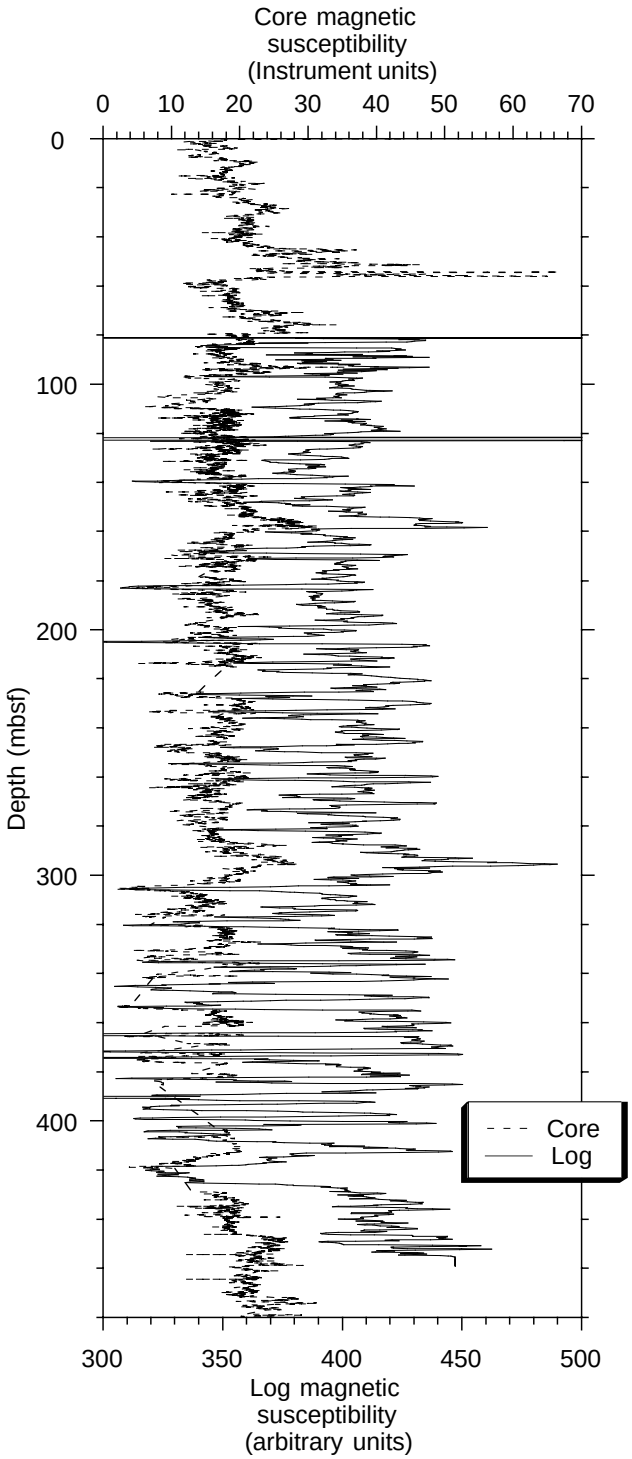

Figure F35. Downhole variations in natural gamma ray, resistivity, and magnetic susceptibility. This figure shows how these data have been used to subdivide the logs into four log units, which are then compared with the results of seismic investigations and lithostratigraphy.

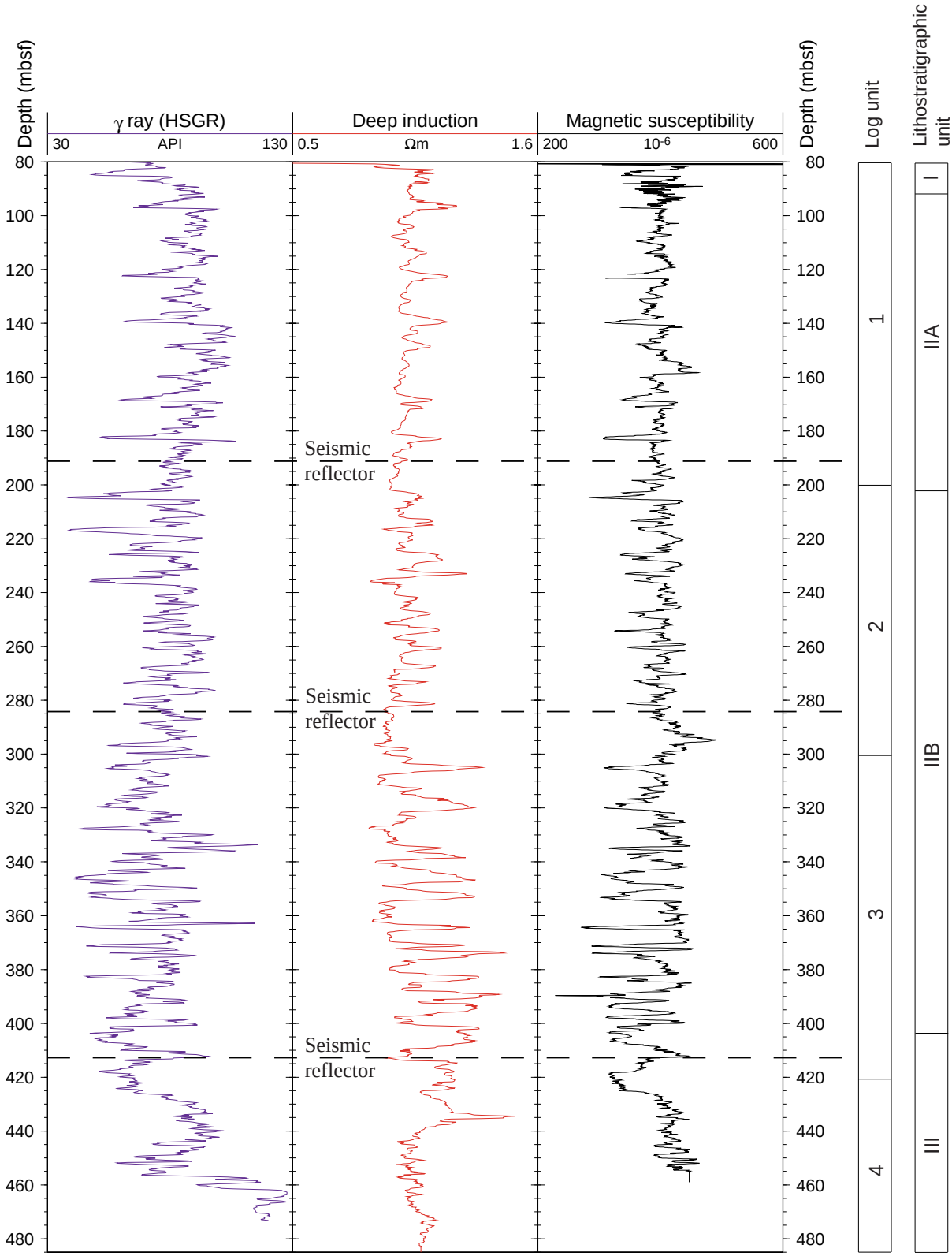

Figure F36. Example of the FMS images from Hole 1119C, taken where the borehole is relatively unaffected by washouts. **A.** Images appear speckled, which is indicative of bioturbation. **B.** Thin (0.1–0.2 m) resistive sand beds, with a spacing of ~2 m.

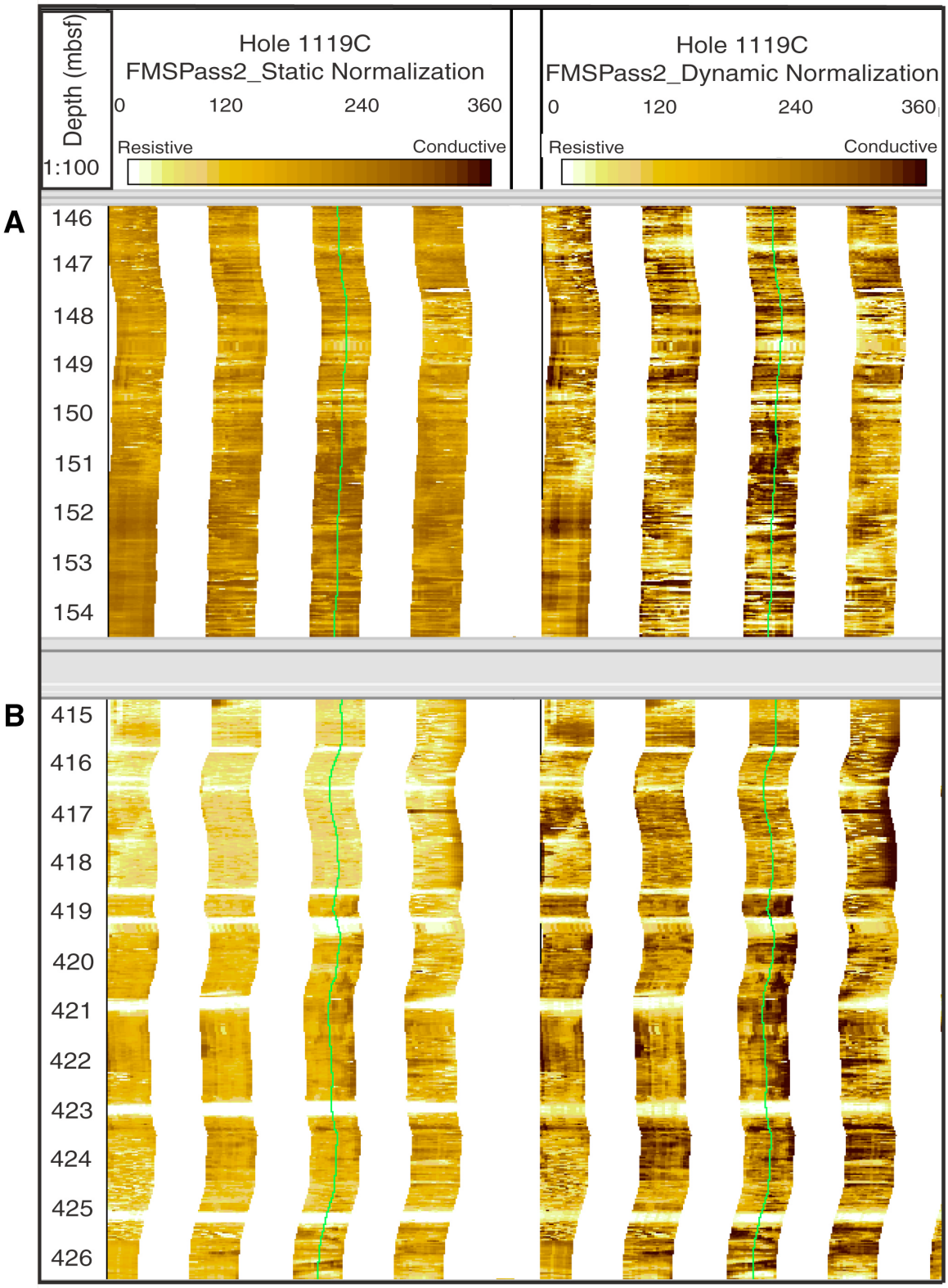

Figure F37. Downhole variations in borehole temperature. Tfast and Tslow refer to fast and slow response thermistors on the tool.

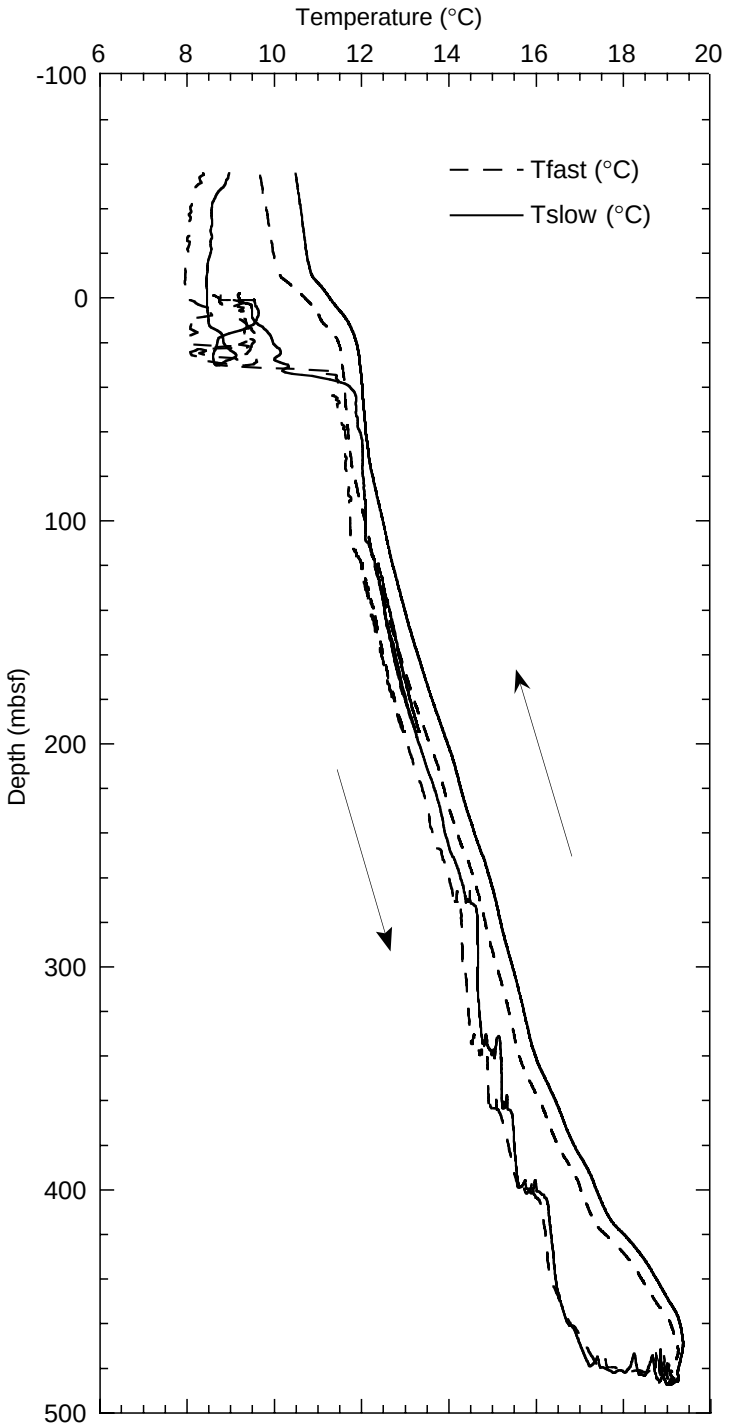

Table T1. Expanded coring summary for Site 1119. (See table note. Continued on next 13 pages.)

Core	Date (August 1998)	Time (UTC)	Core depth (mbsf) Top	Core depth (mbsf) Bottom	Length (m) Cored	Length (m) Recovered	Recovery (%)	Section	Length (m) Liner	Length (m) Curated	Section depth (mbsf) Top	Section depth (mbsf) Bottom	Catwalk samples	Comment
181-1119A-														
1H	22	2225	0.0	6.0	6.0	6.01	100.2							
								1	1.33	1.33	0.00	1.33		
								2	1.50	1.50	1.33	2.83		
								3	1.50	1.50	2.83	4.33		
								4	1.32	1.32	4.33	5.65		
								5	0.13	0.13	5.65	5.78		
								CC	0.23	0.23	5.78	6.01	PAL	
									6.01	6.01				
				Totals:	6.0	6.01	100.20							
181-1119B-														
1H	22	2255	0.0	4.7	4.7	4.73	100.6							
								1	1.5	1.5	0	1.5	PAL	
								2	1.5	1.5	1.5	3	IW	
								3	1.3	1.3	3	4.3	HS	
								4	0.28	0.28	4.3	4.58		
								CC	0.15	0.15	4.58	4.73	PAL	
									4.73	4.73				
2H	22	2345	4.7	14.2	9.5	9.88	104							
								1	1.5	1.5	4.7	6.2		
								2	1.5	1.5	6.2	7.7		
								3	1.5	1.5	7.7	9.2		
								4	1.5	1.5	9.2	10.7	IW	
								5	1.5	1.5	10.7	12.2	HS	
								6	1.5	1.5	12.2	13.7		
								7	0.72	0.72	13.7	14.42		
								CC	0.16	0.16	14.42	14.58	PAL	
									9.88	9.88				
3H	23	0120	14.2	23.7	9.5	10.09	106.2							
								1	1.5	1.5	14.2	15.7		
								2	1.5	1.5	15.7	17.2		
								3	1.5	1.5	17.2	18.7		
								4	1.5	1.5	18.7	20.2	IW	
								5	1.5	1.5	20.2	21.7	HS	
								6	0.8	0.8	21.7	22.5		
								7	0.8	0.8	22.5	23.3		
								8	0.43	0.43	23.3	23.73		
								CC	0.56	0.56	23.73	24.29	PAL	
									10.09	10.09				
4H	23	0217	23.7	33.2	9.5	7.13	75.1							
								1	1.5	1.5	23.7	25.2		
								2	1.5	1.5	25.2	26.7		
								3	1.5	1.5	26.7	28.2		
								4	1.5	1	28.2	29.2		
								5	0	0.56	29.2	29.76	IW	
								6	0.61	0.61	29.76	30.37	HS	

Table T1 (continued).

Core	Date (August 1998)	Time (UTC)	Core depth (mbsf) Top	Core depth (mbsf) Bottom	Length (m) Cored	Length (m) Recovered	Recovery (%)	Section	Length (m) Liner	Length (m) Curated	Section depth (mbsf) Top	Section depth (mbsf) Bottom	Catwalk samples	Comment
								CC	0.52	0.52	30.37	30.89	PAL	
									7.13	7.19				
5H	23	0245	33.2	42.7	9.5	10.27	108.1							
								1	1.5	1.53	33.2	34.73		
								2	1.5	1.5	34.73	36.23		
								3	1.5	1.5	36.23	37.73		
								4	1.4	1.43	37.73	39.16	IW	
								5	1.5	1.55	39.16	40.71	HS	
								6	1.5	1.55	40.71	42.26		
								7	1.07	1.07	42.26	43.33		
								CC	0.3	0.3	43.33	43.63	PAL	
									10.27	10.43				
6H	23	0320	42.7	52.2	9.5	10.35	108.9							
								1	1.5	1.5	42.7	44.2		
								2	1.5	1.5	44.2	45.7		
								3	1.5	1.5	45.7	47.2		
								4	1.5	1.5	47.2	48.7	IW	
								5	1.5	1.5	48.7	50.2	HS	
								6	1.5	1.5	50.2	51.7		
								7	1	0.92	51.7	52.62		
								CC	0.35	0.35	52.62	52.97	PAL	
									10.35	10.27				
7H	23	0400	52.2	61.7	9.5	10.37	109.2							
								1	1.5	1.5	52.2	53.7		
								2	1.5	1.5	53.7	55.2		
								3	1.5	1.5	55.2	56.7		
								4	1.4	1.4	56.7	58.1	IW	
								5	1.5	1.5	58.1	59.6	HS	
								6	1.5	1.5	59.6	61.1		
								7	0.5	0.5	61.1	61.6		
								8	0.27	0.27	61.6	61.87		
								CC	0.7	0.7	61.87	62.57	PAL	
									10.37	10.37				
8H	23	0435	61.7	71.2	9.5	10.44	109.9							
								1	1.5	1.5	61.7	63.2		
								2	1.5	1.5	63.2	64.7		
								3	1.5	1.5	64.7	66.2		
								4	1.55	1.55	66.2	67.75	IW	
								5	1.5	1.5	67.75	69.25	HS	
								6	1.5	1.5	69.25	70.75		
								7	1.07	1.07	70.75	71.82		
								CC	0.32	0.32	71.82	72.14	PAL	
									10.44	10.44				
9H	23	0510	71.2	80.7	9.5	10.35	108.9							
								1	1.5	1.5	71.2	72.7		
								2	1.5	1.5	72.7	74.2		

Table T1 (continued).

Core	Date (August 1998)	Time (UTC)	Core depth (mbsf) Top	Core depth (mbsf) Bottom	Length (m) Cored	Length (m) Recovered	Recovery (%)	Section	Length (m) Liner	Length (m) Curated	Section depth (mbsf) Top	Section depth (mbsf) Bottom	Catwalk samples	Comment
								3	1.5	1.5	74.2	75.7		
								4	1.4	1.4	75.7	77.1	IW	
								5	1.5	1.5	77.1	78.6	HS	
								6	1.5	1.5	78.6	80.1	VAC	
								7	1.07	1.07	80.1	81.17		
								CC	0.38	0.38	81.17	81.55	PAL	
									10.35	10.35				
10H	23	0605	80.7	90.2	9.5	10.22	107.6							
								1	1.42	1.42	80.7	82.12		
								2	1.5	1.5	82.12	83.62		
								3	1.5	1.5	83.62	85.12		
								4	1.5	1.5	85.12	86.62	IW	
								5	1.5	1.5	86.62	88.12	HS	
								6	1.5	1.5	88.12	89.62		
								7	0.94	1	89.62	90.62	VAC	
								CC	0.36	0.36	90.62	90.98	PAL	
									10.22	10.28				
11H	23	0640	90.2	99.7	9.5	10.24	107.8							
								1	1.5	1.5	90.2	91.7		
								2	1.5	1.5	91.7	93.2		
								3	1.5	1.5	93.2	94.7		
								4	1.5	1.5	94.7	96.2	IW	
								5	1.5	1.5	96.2	97.7	HS	
								6	1.5	1.5	97.7	99.2		
								7	0.94	0.94	99.2	100.14		
								CC	0.3	0.3	100.14	100.44	PAL	
									10.24	10.24				
12H	23	0720	99.7	109.2	9.5	10.26	108.0							
								1	1.5	1.5	99.7	101.2	VAC	
								2	1.5	1.5	101.2	102.7		
								3	1.5	1.5	102.7	104.2		
								4	1.5	1.5	104.2	105.7		
								5	1.5	1.5	105.7	107.2	HS	
								6	1.5	1.5	107.2	108.7		
								7	0.92	0.92	108.7	109.62		
								CC	0.34	0.34	109.62	109.96	PAL	
									10.26	10.26				
13H	23	0805	109.2	118.7	9.5	10.51	110.6							
								1	1.5	1.5	109.2	110.7		
								2	1.5	1.5	110.7	112.2		
								3	1.5	1.5	112.2	113.7	VAC	
								4	1.5	1.5	113.7	115.2		
								5	1.5	1.5	115.2	116.7	HS	
								6	1.5	1.5	116.7	118.2		
								7	0.98	0.98	118.2	119.18		
								CC	0.53	0.53	119.18	119.71	PAL	
									10.51	10.51				

Table T1 (continued).

Core	Date (August 1998)	Time (UTC)	Core depth (mbsf) Top	Core depth (mbsf) Bottom	Length (m) Cored	Length (m) Recovered	Recovery (%)	Section	Length (m) Liner	Length (m) Curated	Section depth (mbsf) Top	Section depth (mbsf) Bottom	Catwalk samples	Comment
14H	23	0850	118.7	128.2	9.5	10.33	108.7							
								1	1.5	1.5	118.7	120.2		
								2	1.5	1.5	120.2	121.7		
								3	1.5	1.5	121.7	123.2	VAC	
								4	1.55	1.55	123.2	124.75	IW	
								5	1.5	1.5	124.75	126.25	HS	
								6	1.5	1.5	126.25	127.75		
								7	0.9	0.9	127.75	128.65		
								CC	0.38	0.38	128.65	129.03	PAL	
									10.33	10.33				
15H	23	0920	128.2	137.7	9.5	10.35	108.9							
								1	1.5	1.5	128.2	129.7		
								2	1.5	1.5	129.7	131.2	VAC	
								3	1.5	1.5	131.2	132.7		
								4	1.5	1.5	132.7	134.2		
								5	1.5	1.5	134.2	135.7	HS	
								6	1.5	1.5	135.7	137.2		
								7	1.05	1.05	137.2	138.25		
								CC	0.3	0.3	138.25	138.55	PAL	
									10.35	10.35				
16H	23	1000	137.7	147.2	9.5	10.3	108.4							
								1	1.5	1.5	137.7	139.2	VAC	
								2	1.5	1.5	139.2	140.7		
								3	1.5	1.5	140.7	142.2		
								4	1.5	1.5	142.2	143.7		
								5	1.5	1.5	143.7	145.2	HS	
								6	1.5	1.5	145.2	146.7		
								7	0.89	0.89	146.7	147.59		
								CC	0.41	0.41	147.59	148	PAL	
									10.30	10.30				
17H	23	1045	147.2	155.8	8.6	8.65	100.6							
								1	1.5	1.5	147.2	148.7		
								2	1.5	1.5	148.7	150.2		
								3	1.53	1.53	150.2	151.73		
								4	1.5	1.5	151.73	153.23	IW	
								5	1.5	1.5	153.23	154.73	HS	
								6	0.81	0.81	154.73	155.54		
								CC	0.31	0.31	155.54	155.85	PAL	
									8.65	8.65				
				Totals:	155.8	164.47	105.60							
181-1119C-														
1H	23	1305	0.0	8.3	8.3	8.27	99.6							
								1	1.5	1.5	0	1.5		
								2	1.5	1.5	1.5	3		
								3	1.5	1.5	3	4.5		
								4	1.5	1.5	4.5	6		
								5	1.5	1.5	6	7.5		

Table T1 (continued).

Core	Date (August 1998)	Time (UTC)	Core depth (mbsf) Top	Core depth (mbsf) Bottom	Length (m) Cored	Length (m) Recovered	Recovery (%)	Section	Length (m) Liner	Length (m) Curated	Section depth (mbsf) Top	Section depth (mbsf) Bottom	Catwalk samples	Comment
								6	0.62	0.62	7.5	8.12		
								CC	0.15	0.15	8.12	8.27	PAL	
									8.27	8.27				
2H	23	1335	8.3	17.8	9.5	9.35	98.4							
								1	1.5	1.5	8.3	9.8		
								2	1.5	1.5	9.8	11.3		
								3	1.5	1.5	11.3	12.8		
								4	1.5	1.5	12.8	14.3		
								5	1.5	1.5	14.3	15.8		
								6	1.3	1.3	15.8	17.1		
								7	0.35	0.35	17.1	17.45		
								CC	0.2	0.2	17.45	17.65	PAL	
									9.35	9.35				
3H	23	1415	17.8	27.3	9.5	10.08	106.1							
								1	1.5	1.5	17.8	19.3		
								2	1.5	1.5	19.3	20.8		
								3	1.5	1.5	20.8	22.3		
								4	1.5	1.5	22.3	23.8		
								5	1.5	1.5	23.8	25.3		
								6	1.5	1.5	25.3	26.8		
								7	0.67	0.67	26.8	27.47		
								CC	0.41	0.41	27.47	27.88	PAL	
									10.08	10.08				
4H	23	1445	27.3	36.8	9.5	10.24	107.8							
								1	1.5	1.5	27.3	28.8		
								2	1.5	1.5	28.8	30.3		
								3	1.5	1.5	30.3	31.8		
								4	1.5	1.5	31.8	33.3		
								5	1.5	1.5	33.3	34.8		
								6	1.5	1.5	34.8	36.3		
								7	0.89	1.19	36.3	37.49		
								CC	0.35	0.35	37.49	37.84	PAL	
									10.24	10.54				
5H	23	1515	36.8	46.3	9.5	10.32	108.6							
								1	1.5	1.5	36.8	38.3		
								2	1.5	1.5	38.3	39.8		
								3	1.5	1.5	39.8	41.3		
								4	1.5	1.5	41.3	42.8		
								5	1.5	1.5	42.8	44.3		
								6	1.5	1.5	44.3	45.8		
								7	0.9	0.9	45.8	46.7		
								CC	0.42	0.42	46.7	47.12	PAL	
									10.32	10.32				
6H	23	1545	46.3	55.8	9.5	10.4	109.5							
								1	1.5	1.5	46.3	47.8		
								2	1.5	1.5	47.8	49.3		

Table T1 (continued).

Core	Date (August 1998)	Time (UTC)	Core depth (mbsf) Top	Core depth (mbsf) Bottom	Length (m) Cored	Length (m) Recovered	Recovery (%)	Section	Length (m) Liner	Length (m) Curated	Section depth (mbsf) Top	Section depth (mbsf) Bottom	Catwalk samples	Comment
								3	1.5	1.5	49.3	50.8		
								4	1.5	1.5	50.8	52.3		
								5	1.5	1.5	52.3	53.8		
								6	1.5	1.5	53.8	55.3		
								7	0.9	0.9	55.3	56.2		
								CC	0.5	0.5	56.2	56.7	PAL	
									10.40	10.40				
7H	23	1615	55.8	65.3	9.5	10.67	112.3							
								1	0.74	0.74	55.8	56.54		Crushed Liner
								2	1.5	1.5	56.54	58.04		
								3	1.5	1.5	58.04	59.54		
								4	1.5	1.5	59.54	61.04		
								5	1.5	1.5	61.04	62.54		
								6	1.5	1.5	62.54	64.04		
								7	1.37	1.37	64.04	65.41		
								CC	1.06	1.06	65.41	66.47	PAL	
									10.67	10.67				
8H	23	1650	65.3	74.8	9.5	10.27	108.1							
								1	1.5	1.4	65.3	66.7		
								2	1.5	1.5	66.7	68.2		
								3	1.5	1.5	68.2	69.7		
								4	1.5	1.42	69.7	71.12		
								5	1.5	1.44	71.12	72.56		
								6	1.5	1.5	72.56	74.06		
								7	0.87	0.87	74.06	74.93		
								CC	0.4	0.4	74.93	75.33		
									10.27	10.03				
9H	23	1725	74.8	84.3	9.5	10.48	110.3							
								1	1.5	1.5	74.8	76.3		
								2	1.5	1.5	76.3	77.8	VAC	
								3	1.5	1.34	77.8	79.14		
								4	1.5	1.5	79.14	80.64		
								5	1.5	1.5	80.64	82.14		
								6	1.5	1.5	82.14	83.64		
								7	0.96	0.96	83.64	84.6		
								CC	0.52	0.52	84.6	85.12		
									10.48	10.32				
10H	23	1800	84.3	93.8	9.5	10.15	106.8							
								1	1.5	1.37	84.3	85.67		
								2	1.5	1.5	85.67	87.17		
								3	1.5	1.5	87.17	88.67		
								4	1.5	1.5	88.67	90.17		
								5	1.5	1.5	90.17	91.67		
								6	1.5	1.5	91.67	93.17		
								7	0.79	0.79	93.17	93.96		
								CC	0.36	0.36	93.96	94.32		
									10.15	10.02				

Table T1 (continued).

Core	Date (August 1998)	Time (UTC)	Core depth (mbsf) Top	Core depth (mbsf) Bottom	Length (m) Cored	Length (m) Recovered	Recovery (%)	Section	Length (m) Liner	Length (m) Curated	Section depth (mbsf) Top	Section depth (mbsf) Bottom	Catwalk samples	Comment
11H	23	1830	93.8	103.3	9.5	10.5	110.5							
								1	0.24	0.24	93.8	94.04		
								2	1.5	1.5	94.04	95.54		
								3	1.5	1.5	95.54	97.04	VAC	
								4	1.5	1.5	97.04	98.54		
								5	1.5	1.5	98.54	100.04		
								6	1.5	1.5	100.04	101.54		
								7	1.5	1.5	101.54	103.04		
								8	0.89	0.89	103.04	103.93		
								CC	0.37	0.37	103.93	104.3		
									10.50	10.50				
12H	23	1905	103.3	112.8	9.5	10.19	107.3							
								1	1.5	1.5	103.3	104.8		
								2	1.5	1.5	104.8	106.3		
								3	1.5	1.5	106.3	107.8		
								4	1.5	1.5	107.8	109.3	VAC	
								5	1.5	1.5	109.3	110.8		
								6	1.5	1.5	110.8	112.3		
								7	0.86	0.86	112.3	113.16		
								CC	0.33	0.33	113.16	113.49		
									10.19	10.19				
13H	23	1945	112.8	122.3	9.5	10.31	108.5							
								1	1.5	1.5	112.8	114.3		
								2	1.5	1.5	114.3	115.8	VAC	
								3	1.5	1.5	115.8	117.3		
								4	1.5	1.5	117.3	118.8		
								5	1.5	1.5	118.8	120.3		
								6	1.5	1.5	120.3	121.8		
								7	0.89	0.89	121.8	122.69		
								CC	0.42	0.42	122.69	123.11		
									10.31	10.31				
14H	23	2020	122.3	131.8	9.5	10.53	110.8							
								1	0.26	0.26	122.3	122.56		
								2	1.5	1.5	122.56	124.06		
								3	1.5	1.5	124.06	125.56	VAC	
								4	1.5	1.5	125.56	127.06		
								5	1.5	1.5	127.06	128.56		
								6	1.5	1.5	128.56	130.06		
								7	1.5	1.5	130.06	131.56		
								8	0.89	0.89	131.56	132.45		
								CC	0.38	0.38	132.45	132.83		
									10.53	10.53				
15H	23	2100	131.8	141.3	9.5	10.28	108.2							
								1	1.5	1.5	131.8	133.3		
								2	1.5	1.5	133.3	134.8		
								3	1.5	1.5	134.8	136.3		
								4	1.5	1.5	136.3	137.8		

Table T1 (continued).

Core	Date (August 1998)	Time (UTC)	Core depth (mbsf) Top	Core depth (mbsf) Bottom	Length (m) Cored	Length (m) Recovered	Recovery (%)	Section	Length (m) Liner	Length (m) Curated	Section depth (mbsf) Top	Section depth (mbsf) Bottom	Catwalk samples	Comment
								5	1.5	1.5	137.8	139.3		
								6	1.5	1.5	139.3	140.8		
								7	0.91	0.91	140.8	141.71		
								CC	0.37	0.37	141.71	142.08		
									10.28	10.28				
16H	23	2135	141.3	150.8	9.5	11.12	117.1							
								1	0.93	0.93	141.3	142.23		Disturbed
								2	1.5	1.12	142.23	143.35		
								3	1.5	1.21	143.35	144.56	VAC	
								4	1.5	1.27	144.56	145.83		
								5	1.5	1.44	145.83	147.27		
								6	1.5	1.5	147.27	148.77		
								7	1.5	1.5	148.77	150.27		
								8	0.86	0.86	150.27	151.13	PAL	
								CC	0.33	0.33	151.13	151.46		
									11.12	10.16				
17H	23	2220	150.8	160.3	9.5	10.41	109.6							
								1	1.5	1.5	150.8	152.3		
								2	1.5	1.5	152.3	153.8		
								3	1.5	1.5	153.8	155.3		
								4	1.5	1.5	155.3	156.8	IW	
								5	1.5	1.38	156.8	158.18	HS	
								6	1.5	1.5	158.18	159.68		
								7	0.97	0.89	159.68	160.57		
								CC	0.44	0.44	160.57	161.01	PAL	
									10.41	10.21				
18X	24	0020	160.3	168.7	8.4	9.9	117.9							
								1	1.5	1.5	160.3	161.8		
								2	1.5	1.35	161.8	163.15		
								3	1.5	1.34	163.15	164.49		
								4	1.5	1.4	164.49	165.89		
								5	1.5	1.43	165.89	167.32	HS	
								6	1.5	1.26	167.32	168.58		
								7	0.51	0.46	168.58	169.04		
								CC	0.39	0.39	169.04	169.43	PAL	
									9.9	9.13				
19X	24	0115	168.7	178.3	9.6	7.97	83							
								1	1.5	1.5	168.7	170.2		
								2	1.5	1.45	170.2	171.65		
								3	1.5	1.29	171.65	172.94		
								4	1.5	1.5	172.94	174.44		
								5	1.5	1.37	174.44	175.81	HS	
								CC	0.47	0.47	175.81	176.28	PAL	
									7.97	7.58				
20X	24	0145	178.3	187.9	9.6	9.62	100.2							
								1	1.5	1.5	178.3	179.8		

Table T1 (continued).

Core	Date (August 1998)	Time (UTC)	Core depth (mbsf) Top	Core depth (mbsf) Bottom	Length (m) Cored	Length (m) Recovered	Recovery (%)	Section	Length (m) Liner	Length (m) Curated	Section depth (mbsf) Top	Section depth (mbsf) Bottom	Catwalk samples	Comment
								2	1.5	1.5	179.8	181.3		
								3	1.5	1.43	181.3	182.73	VAC	
								4	1.5	1.5	182.73	184.23	IW	
								5	1.5	1.39	184.23	185.62	HS	
								6	1.5	1.5	185.62	187.12		
								7	0.24	0.24	187.12	187.36		
								CC	0.38	0.38	187.36	187.74	PAL	
									9.62	9.44				
21X	24	0225	187.9	197.6	9.7	8.67	89.4							
								1	1.5	1.5	187.9	189.4		Disturbed
								2	1.5	1.5	189.4	190.9		
								3	1.5	1.5	190.9	192.4	VAC	
								4	1.5	1.5	192.4	193.9		
								5	1.5	1.5	193.9	195.4	HS	
								6	0.67	0.67	195.4	196.07		
								CC	0.5	0.5	196.07	196.57	PAL	
									8.67	8.67				
22X	24	0300	197.6	207.2	9.6	9.28	96.7							
								1	0.29	0.29	197.6	197.89		Disturbed
								2	1.5	1.5	197.89	199.39		
								3	1.5	1.5	199.39	200.89		
								4	1.5	1.5	200.89	202.39		
								5	1.5	1.5	202.39	203.89	HS	
								6	1.5	1.5	203.89	205.39		
								7	1.2	1.2	205.39	206.59		
								CC	0.29	0.29	206.59	206.88	PAL	
									9.28	9.28				
23X	24	0330	207.2	216.8	9.6	10.0	104.2							
								1	0.52	0.52	207.2	207.72		Disturbed
								2	1.5	1.5	207.72	209.22		
								3	1.5	1.5	209.22	210.72		
								4	1.5	1.5	210.72	212.22	IW	
								5	1.5	1.5	212.22	213.72	HS	
								6	1.23	1.23	213.72	214.95	VAC	
								7	1.5	1.5	214.95	216.45		
								8	0.33	0.33	216.45	216.78		
								CC	0.42	0.42	216.78	217.2	PAL	
									10.00	10.00				
24X	24	0405	216.8	226.4	9.6	0.0	0.0							
25X	24	0440	226.4	236	9.6	9.35	97.4							
								1	1.5	1.5	226.4	227.9		Disturbed
								2	1.5	1.5	227.9	229.4	PAL, PAL, PAL, PAL	
								3	1.5	1.5	229.4	230.9		
								4	1.5	1.5	230.9	232.4		
								5	1.5	1.5	232.4	233.9	VAC, HS, PAL, PAL	

Table T1 (continued).

Core	Date (August 1998)	Time (UTC)	Core depth (mbsf) Top	Core depth (mbsf) Bottom	Length (m) Cored	Length (m) Recovered	Recovery (%)	Section	Length (m) Liner	Length (m) Curated	Section depth (mbsf) Top	Section depth (mbsf) Bottom	Catwalk samples	Comment
								6	1.5	1.5	233.9	235.4	PAL, PAL, PAL	
								CC	0.35	0.35	235.4	235.75	PAL	
									9.35	9.35				
26X	24	0525	236	245.6	9.6	9.96	103.8							
								1	1.5	1.5	236	237.5		
								2	1.5	1.5	237.5	239		
								3	1.5	1.5	239	240.5		
								4	1.5	1.5	240.5	242	IW	
								5	1.5	1.5	242	243.5	HS, VAC	
								6	1.18	1.18	243.5	244.68		
								7	0.51	0.51	244.68	245.19		
								CC	0.77	0.77	245.19	245.96	PAL	
									9.96	9.96				
27X	24	0555	245.6	255.2	9.6	9.08	94.6							
								1	1.5	1.5	245.6	247.1		Disturbed
								2	1.5	1.5	247.1	248.6		
								3	1.5	1.5	248.6	250.1		
								4	1.5	1.5	250.1	251.6	VAC	
								5	1.5	1.5	251.6	253.1	HS	
								6	1.03	1.03	253.1	254.13		
								CC	0.55	0.55	254.13	254.68	PAL	
									9.08	9.08				
28X	24	0635	255.2	264.8	9.6	9.72	101.3							
								1	1.5	1.5	255.2	256.7		
								2	1.5	1.5	256.7	258.2		
								3	1.5	1.5	258.2	259.7	VAC	
								4	1.5	1.5	259.7	261.2		
								5	1.5	1.5	261.2	262.7	HS	
								6	1.22	1.22	262.7	263.92		
								CC	1.0	1.0	263.92	264.92	PAL	Disturbed
									9.72	9.72				
29X	24	0715	264.8	274.5	9.7	9.67	99.7							
								1	1.5	1.5	264.8	266.3		Disturbed
								2	1.5	1.5	266.3	267.8		
								3	1.5	1.5	267.8	269.3		
								4	1.5	1.5	269.3	270.8	IW	
								5	1.5	1.5	270.8	272.3	HS, VAC	
								6	1.5	1.5	272.3	273.8		
								7	0.15	0.15	273.8	273.95		
								CC	0.52	0.52	273.95	274.47	PAL	
									9.67	9.67				
30X	24	0750	274.5	284.1	9.6	9.55	99.5							
								1	1.5	1.5	274.5	276		
								2	1.5	1.5	276	277.5		
								3	1.5	1.5	277.5	279		
								4	1.5	1.5	279	280.5		

Table T1 (continued).

Core	Date (August 1998)	Time (UTC)	Core depth (mbsf) Top	Core depth (mbsf) Bottom	Length (m) Cored	Length (m) Recovered	Recovery (%)	Section	Length (m) Liner	Length (m) Curated	Section depth (mbsf) Top	Section depth (mbsf) Bottom	Catwalk samples	Comment
								5	1.5	1.5	280.5	282	HS	
								6	1.5	1.5	282	283.5		
								CC	0.55	0.55	283.5	284.05	PAL	
									9.55	9.55				
31X	24	0835	284.1	293.8	9.7	9.68	99.8							
								1	0.47	0.47	284.1	284.57		Disturbed
								2	1.5	1.5	284.57	286.07		
								3	1.5	1.5	286.07	287.57		
								4	1.5	1.5	287.57	289.07		
								5	1.5	1.5	289.07	290.57	HS, VAC	
								6	1.5	1.5	290.57	292.07		
								7	1.37	1.37	292.07	293.44		
								CC	0.34	0.34	293.44	293.78	PAL	
									9.68	9.68				
32X	24	0910	293.8	303.4	9.6	9.44	98.3							
								1	1.5	1.5	293.8	295.3		Disturbed
								2	1.5	1.5	295.3	296.8		
								3	1.5	1.5	296.8	298.3	VAC	
								4	1.5	1.5	298.3	299.8	IW	
								5	1.5	1.5	299.8	301.3	HS	
								6	1.5	1.5	301.3	302.8		
								CC	0.44	0.44	302.8	303.24	PAL	
									9.44	9.44				
33X	24	0945	303.4	313	9.6	9.48	98.8							
								1	1.5	1.5	303.4	304.9		
								2	1.5	1.5	304.9	306.4		
								3	1.24	1.24	306.4	307.64	VAC	
								4	1.5	1.5	307.64	309.14		
								5	1.5	1.5	309.14	310.64	HS	
								6	1.5	1.5	310.64	312.14		
								7	0.2	0.2	312.14	312.34		
								CC	0.54	0.54	312.34	312.88	PAL	
									9.48	9.48				
34X	24	1025	313	322.3	9.3	6.22	66.9							
								1	1.5	1.5	313	314.5	PAL, PAL	
								2	1.39	1.39	314.5	315.89	VAC	
								3	1.5	1.5	315.89	317.39		
								4	1.52	1.52	317.39	318.91	HS	
								CC	0.31	0.31	318.91	319.22	PAL	
									6.22	6.22				
35X	24	1055	322.3	331.9	9.6	9.71	101.1							
								1	1.5	1.5	322.3	323.8		
								2	1.5	1.5	323.8	325.3		
								3	1.5	1.5	325.3	326.8		
								4	1.5	1.5	326.8	328.3	IW	
								5	1.5	1.5	328.3	329.8	HS	

Table T1 (continued).

Core	Date (August 1998)	Time (UTC)	Core depth (mbsf) Top	Core depth (mbsf) Bottom	Length (m) Cored	Length (m) Recovered	Recovery (%)	Section	Length (m) Liner	Length (m) Curated	Section depth (mbsf) Top	Section depth (mbsf) Bottom	Catwalk samples	Comment
								6	1.5	1.5	329.8	331.3		
								7	0.42	0.42	331.3	331.72		
								CC	0.29	0.29	331.72	332.01	PAL	
									9.71	9.71				
36X	24	1135	331.9	341.5	9.6	6.98	72.7							
								1	1.5	1.5	331.9	333.4		
								2	1.5	1.5	333.4	334.9	VAC	
								3	1.5	1.5	334.9	336.4		
								4	1.5	1.5	336.4	337.9	HS	
								5	0.65	0.65	337.9	338.55		
								CC	0.33	0.33	338.55	338.88	PAL	
									6.98	6.98				
37X	24	1230	341.5	351.1	9.6	1.76	18.3							
								1	1.5	1.5	341.5	343		
								CC	0.26	0.26	343	343.26	PAL	
									1.76	1.76				
38X	24	1310	351.1	360.8	9.7	9.12	94							
								1	1.5	1.5	351.1	352.6	PAL, PAL	
								2	1.5	1.5	352.6	354.1	PAL, PAL	
								3	1.5	1.5	354.1	355.6		
								4	1.5	1.5	355.6	357.1	IW	
								5	1.5	1.5	357.1	358.6	HS	
								6	1.24	1.24	358.6	359.84		
								CC	0.38	0.38	359.84	360.22	PAL	
									9.12	9.12				
39X	24	1355	360.8	370.5	9.7	2.69	27.7							
								1	1.5	1.5	360.8	362.3		
								2	0.87	0.87	362.3	363.17		
								CC	0.32	0.32	363.17	363.49	PAL	
									2.69	2.69				
40X	24	1440	370.5	380.1	9.6	3.06	31.9							
								1	1.5	1.5	370.5	372		
								2	1.26	1.26	372	373.26		
								CC	0.3	0.3	373.26	373.56	PAL	
									3.06	3.06				
41X	24	1600	380.1	389.8	9.7	2.19	22.6							
								1	1.5	1.5	380.1	381.6	IW	
								2	0.35	0.35	381.6	381.95	HS	
								CC	0.34	0.34	381.95	382.29	PAL	
									2.19	2.19				
42X	24	1730	389.8	399.4	9.6	6.54	68.1							
								1	1.5	1.5	389.8	391.3		
								2	1.5	1.5	391.3	392.8		
								3	1.5	1.5	392.8	394.3		
								4	1.5	1.5	394.3	395.8		

Table T1 (continued).

Core	Date (August 1998)	Time (UTC)	Core depth (mbsf) Top	Core depth (mbsf) Bottom	Length (m) Cored	Length (m) Recovered	Recovery (%)	Section	Length (m) Liner	Length (m) Curated	Section depth (mbsf) Top	Section depth (mbsf) Bottom	Catwalk samples	Comment
								5	0.25	0.25	395.8	396.05		
								CC	0.29	0.29	396.05	396.34	PAL	
									6.54	6.54				
43X	24	1830	399.4	409	9.6	3.24	33.8							
								1	1.5	1.5	399.4	400.9		
								2	1.4	1.4	400.9	402.3		
								CC	0.34	0.34	402.3	402.64	PAL	
									3.24	3.24				
44X	24	1940	409.0	418.6	9.6	9.9	103.1							
								1	1.5	1.5	409	410.5		
								2	1.5	1.5	410.5	412		
								3	1.5	1.5	412	413.5		
								4	1.5	1.5	413.5	415	IW	
								5	1.5	1.5	415	416.5	HS	
								6	1.5	1.5	416.5	418	VAC	
								7	0.47	0.47	418	418.47		
								CC	0.43	0.43	418.47	418.9	PAL	
									9.90	9.90				
45X	24	2100	418.6	428.2	9.6	0.82	8.5							
								1	0.64	0.64	418.6	419.24		
								CC	0.18	0.18	419.24	419.42	PAL	
									0.82	0.82				
46X	24	2245	428.2	437.9	9.7	9.62	99.2							
								1	1.5	1.5	428.2	429.7		
								2	1.5	1.5	429.7	431.2		
								3	1.5	1.5	431.2	432.7		
								4	1.5	1.5	432.7	434.2	PAL	
								5	1.5	1.5	434.2	435.7		
								6	1.5	1.5	435.7	437.2	VAC	
								CC	0.62	0.62	437.2	437.82	PAL	
									9.62	9.62				
47X	25	0005	437.9	447.2	9.3	9.62	103.4							
								1	1.5	1.5	437.9	439.4		
								2	1.5	1.5	439.4	440.9		
								3	1.5	1.5	440.9	442.4		
								4	1.5	1.5	442.4	443.9	IW	
								5	1.5	1.5	443.9	445.4	HS	
								6	1.5	1.5	445.4	446.9		
								7	0.43	0.43	446.9	447.33		
								CC	0.19	0.19	447.33	447.52	PAL	
									9.62	9.62				
48X	25	0130	447.2	456.8	9.6	9.8	102.1							
								1	1.5	1.5	447.2	448.7		
								2	1.5	1.5	448.7	450.2		
								3	1.5	1.5	450.2	451.7		
								4	1.5	1.5	451.7	453.2		

Table T1 (continued).

Core	Date (August 1998)	Time (UTC)	Core depth (mbsf) Top	Core depth (mbsf) Bottom	Length (m) Cored	Length (m) Recovered	Recovery (%)	Section	Length (m) Liner	Length (m) Curated	Section depth (mbsf) Top	Section depth (mbsf) Bottom	Catwalk samples	Comment
								5	1.5	1.5	453.2	454.7	HS	
								6	1.5	1.5	454.7	456.2	VAC	
								7	0.36	0.36	456.2	456.56		
								CC	0.44	0.44	456.56	457	PAL	
									9.80	9.80				
49X	25	0300	456.8	466.4	9.6	8.77	91.4							
								1	1.5	1.5	456.8	458.3		
								2	1.5	1.5	458.3	459.8		
								3	1.5	1.5	459.8	461.3		
								4	1.5	1.5	461.3	462.8		
								5	1.5	1.5	462.8	464.3	HS	
								6	0.95	0.95	464.3	465.25		
								CC	0.32	0.32	465.25	465.57	PAL	
									8.77	8.77				
50X	25	0440	466.4	475.6	9.2	9.67	105.1							
								1	1.5	1.5	466.4	467.9		
								2	1.5	1.5	467.9	469.4		
								3	1.5	1.5	469.4	470.9	VAC	
								4	1.5	1.5	470.9	472.4	IW, IW	
								5	1.5	1.5	472.4	473.9	HS, HS	
								6	1.5	1.5	473.9	475.4		
								7	0.35	0.35	475.4	475.75		
								CC	0.32	0.32	475.75	476.07	PAL	
									9.67	9.67				
51X	25	0600	475.6	485.2	9.6	8.06	84							
								1	1.5	1.5	475.6	477.1		
								2	1.5	1.5	477.1	478.6		
								3	1.5	1.5	478.6	480.1		
								4	1.5	1.5	480.1	481.6		
								5	1.5	1.5	481.6	483.1	HS	
								6	0.23	0.23	483.1	483.33		
								CC	0.33	0.33	483.33	483.66	PAL	
									8.06	8.06				
52X	25	0745	485.2	494.8	9.6	9.52	99.2							
								1	1.5	1.5	485.2	486.7		
								2	1.5	1.5	486.7	488.2		
								3	1.5	1.5	488.2	489.7		
								4	1.5	1.5	489.7	491.2		
								5	1.5	1.5	491.2	492.7	HS	
								6	1.5	1.5	492.7	494.2		
								7	0.24	0.24	494.2	494.44		
								CC	0.28	0.28	494.44	494.72	PAL	
									9.52	9.52				
				Totals:	494.8	442.23	89.40							

Note: PAL = paleontology, IW = interstitial water, HS = headspace, VAC = vacutainer. This table is also available in **ASCII format.**

Table T2. Depths to seismic reflectors, Site 1119.

Seafloor feature	Seismic unit	Paleoshelf edge (pse)	Site distance from pse (km)	Reflector	Distance to reflector (ms)	Average velocity	Velocity increase (m/s)	Downhole depth (mbsf)	Age (Ma)	Sed. rate (cm/k.y.)
Modern shelf edge		10	5	Seabed	501	0	—	0	0.00	0.0
Slope toe (downlap)	A1	9	5	1	50	1375	—	34	0.13	26.4
Slope toe (grades)	A2	8	9.5	2	80	1381	6	55	0.26	21.2
		7	12.5	3	100	1385	4	69	0.37	18.7
		7	12.5	4	124	1389	4	86	0.51	16.9
Midslope drift (upper)	B1	6	13.5	5	160	1375	–14	110	0.68	16.2
		5	13	6	182	1378	3	125	0.78	16.1
		5	13	7	224	1380	2	155	0.88	17.6
		5	13	8	260	1384	4	180	0.95	18.9
		5	13	9	278	1382	–2	192	1.00	19.2
Midslope drift (lower)	B2	4	12.5	10	300	1389	7	208	1.08	19.4
		4	12.5	11	340	1394	5	237	1.17	20.3
		4	12.5	12	380	1421	27	270	1.27	21.3
		4	12.5	13	392	1445	24	283	1.32	21.5
Midslope drift (gutter)	B3	3	11	14	410	1441	–4	295	1.68	17.6
		3	11	15	450	1454	13	327	1.92	17.0
		3	11	16	460	1461	7	336	1.95	17.2
		2	14	17	500	1475	14	369	2.16	17.1
Drape of large slope drift	C	2	14	18	545	1515	40	413	2.39	17.2
		2	14	19	578	1559	44	451	2.59	17.4
		2	14	20	600	1565	6	470	2.68	17.5
		1	15	21	625	1557	–8	487	2.78	17.5
		1	15	22	655	1558	1	510 (not drilled)	2.8	0.0
Top of large slope drift	D							(not drilled)		

Notes: Solid lines separate major stratigraphic units; dashed lines separate individual drift components within drift-complex B. Sed. = sedimentation.

Table T3. Biostratigraphic events, correlated with zones, epochs, and New Zealand stages, identified at Site 1119.

Event	Group	NZ stage	Zone (base)	Epoch	Age (Ma)	Sample	Depth (mbsf)
FO *Globorotalia hirsuta*	F				<0.45	1119B-1H-CC	
FO Acme *Emiliania huxleyi*	N	Wq		latest Pleistocene	0.08	1119B-2H-CC	19
FO *Emiliania huxleyi*	N	Wq	NN21	middle Pleistocene	0.24	1119B-5H-CC	48.5
LO *Pseudoemiliania lacunosa*	N	Wc/Wq	NN20	middle Pleistocene	0.42	1119B-9H-CC	77
LO Plectofrondicularia advera	F			middle Pleistocene	~0.62	1119B-10H-CC	
LO *Plectofrondicularia pellucida*	F	?Wn/Wc			~0.62	1119B-13H-CC	
LO Acme *Gephyrocapsa parallela* (small)	N			middle Pleistocene	0.78	1119B-14H-CC	123
LO *Bolivina affiliata*	F	?Wn/Wc				1119B-15H-CC	
LO *Actinocyclus ingens* f. *planus*	D	Wc			>0.62-0.65	1119C-16-8, 60 cm	144
FO *Gephyrocapsa parallela*	N			early Pleistocene	0.9	1119C-17H-CC	155
LO Dominant *Gephyrocapsa* (small)	N				0.9	1119C-18X-CC	164
LO *Anomalinoides parvumbilicus*	F	?Wn/Wc				1119C-18X-CC	164
LO *Globorotalia puncticuloides*	F	e Wc		early Pleistocene	~0.7	1119C-18X-CC	173
FO *Globorotalia truncatulinoides*	F				~0.8	1119C-18X-CC	173
LO *Pterocanium trilobum*	R	e Wc		early Pleistocene	>0.83	1119C-25-5,111	233
FO Dominant *Gephyrocapsa* (small)	N			early Pleistocene	1.14	1119C-26X-CC	240
LO *Helicosphaera sellii*	N	Wn		early Pleistocene	1.2	1119C-27X-CC	250
LO *Gephyrocapsa oceanica* (small)	N	Wn		early Pleistocene	~1.2	1119C-27X-CC	250
FO *Gephyrocapsa* (large)	N			early Pleistocene	~1.5	1119C-29X-CC	
FO *Gephyrocapsa* (medium)	N			early Pleistocene	1.75	1119C-32X-CC	298
FO *Lithelius nautiloides*	R	Wn		late Pliocene	<1.93	1119C-31X-CC	298
FO *Gephyrocapsa oceanica*	N	Wn	NN19	late Pliocene	1.75-1.95	1119C-33X-CC	308
LO *Haeuslerella plioceneenica*	F	Wn		late Pliocene	>1.1	1119C-36X-CC	336
LO *Eucyrtidium calvertense*	R				>1.92	1119C-38-1, 110 cm	353
LO *Karreriella cylindrica*	F	Wn/Wc		late Pliocene	>1.1	1119C-38-1,64	353
FO *Globorotalia crassula*	F	Wm/Wn		late Pliocene	2.6	1119C-41X-CC	382
FO–LO *Globorotalia crassaformis* (dextral)	F	Wm/Wn		late Pliocene	2.1-3.0	1119C-41X-CC	
LO *Nitzschia weaveri*	D			late Pliocene	~2.74	1119C-48X-CC	452
LO *Discoaster asymmetricus*	N	Wm/Wn		mid-Pliocene	~2.8	1119C-52X-CC	489
LCO *Globorotalia puncticulata*	F	Wo/Wp		Pliocene	3.7	1119C-52X-CC	

Notes: F = foraminifer, N = calcareous nannofossil, D = diatom, R = radiolarian. Wq = Haweran, Wc = Castlecliffian, Wn = Nukumaruan, Wm = Mangapanian, Wo = Opoitian, Wp = Waipipian. See also Figure **F7,** p. 46, in the "Explanatory Notes" chapter.

Table T4. Identification and abundance of nannofossils observed at Site 1119.

Core, section, interval (cm)	Depth (mbsf)	Preservation	Group abundance	*Braarudosphaera bigelowii*	*Calcidiscus leptoporus*	*Calcidiscus macintyrei*	*Coccolithus pelagicus*	*Coronocyclus nitescens*	*Crenalithus* sp.	*Cyclicargolithus abisectus*	*Cyclicargolithus floridanus*	*Dictyococcites bisectus*	*Dictyococcites productus*	*Discoaster asymmetricus*	*Discoaster deflandrei*	*Emiliania huxleyi*	*Gephyrocapsa* (large)	*Gephyrocapsa* (medium)	*Gephyrocapsa parallela*	*Gephyrocapsa* (small)	*Helicosphaera ampliaperta*	*Helicosphaera carteri*	*Helicosphaera intermedia*	*Helicosphaera sellii*	*Pontosphaera* spp.	*Pseudoemiliania lacunosa*	*Reticulofenestra pseudoumbilicus*	*Reticulofenestra* (small)	*Reticulofenestra umbilicus*	*Sphenolithus heteromorphus*	*Sphenolithus moriformis*	*Syracosphaera pulchra*	*Thoracosphaera* spp.	*Triquetrorhabdulus rugosus*	*Umbilicosphaera angustiforamen*	*Umbilicosphaera sibogae*	*Watznaueria barnesae*
181-1119A-																																				
1H-CC, 18-23	5.96	G	C		F		C									A		A				F						C								
181-1119B-																																				
1H-CC, 10-15	4.68	G	C		F		C				R				R	D		A										C			F		R		C	
2H-CC, 11-16	14.53	G	C		R		C	R			R	R				D		A															R			
3H-CC, 51-56	24.24	G	C				C									C		C	F									C								
4H-CC, 47-52	30.84	G	C								R	R				F		C	F						R			F								
5H-CC, 25-30	43.58	G	A				C				R					F		C										C								
6H-CC, 30-35	52.92	G	F				F								R			C										C								
7H-CC, 65-70	62.52	G	C				C											A	F			F						C								
8H-CC, 27-32	72.09	G	C		F		A				R	R										F		R			R	F								
9H-CC, 33-38	81.50	G	C		F		A				R	R						A				F	R			R		C								
10H-CC, 31-36	90.93	G	C		C		C				R	R						C	F			F					F	C								
11H-CC, 25-30	100.39	M	F		C																							C								
12H-CC, 29-34	109.91	VG	A		R		C											A										A						R		
13H-CC, 48-53	119.66	G	A				C				R							A										C								
14H-CC, 33-38	128.98	G	A				C											A	A								R	A								
15H-CC, 25-30	138.50	VG	A				F											A	A									A					R			
16H-CC, 36-41	147.95	G	A	R	R		C				R	R			R			A	C								R	C								
17H-CC, 26-31	155.80	G	A		R		C				R							A	C			R				R	R	A					R			
181-1119C-																																				
17H-CC, 39-44	160.96	G	A		R		C				R							A	C	C		R				R		A								
18X-CC, 34-39	169.38	G	A		F		C				R									A		C			R	F	R	C								
19X-CC, 42-47	176.57	G	A				A			R	R	R								D		C						C								
20X-CC, 33-38	187.69	G	A				R		C			R								D		R						C								
21X-CC, 45-50	196.52	G	A				C					R	F		R					D		F				R		C					R	R		
22X-CC, 24-29	206.83	G	R		F								F							D							F	F								
23X-CC, 37-42	217.15	M	F				C			R	R		C							A		F						C	R	R			R			
25X-CC, 30-35	235.70	G	F		F		C						C							A													R			R
26X-CC, 72-77	245.91	VG	A		C		C					R								D					R	F		C				R				
27X-CC, 50-55	254.63	G	C	R	C		F						C				A			F		C		C	F	C		C								
28X-CC, 50-55	264.87	G	A		F		C					R	C				C		R	F				F		F		F				R				
29X-CC, 47-52	274.42	G	A		F		C						C				F	C		F		F		C	R	F		F								
30X-CC, 50-55	284.00	P	F		R		R				R		A					C		F					R	R		F								
31X-CC, 29-34	293.73	G	C		F		C						A		R					C								C								
32X-CC, 39-44	303.19	G	A									R	C					A		C		R		R				R								
33X-CC, 49-54	312.83	G	R		F		C						A					R		C		R		C				C								
34X-CC, 26-31	319.17	P	F		F		F						C							F																
35X-CC, 24-29	331.96	M	C		R		D						C							C				C		F		C								
36X-CC, 23-33	338.78	M	C				A					R	C											R				F								
37X-CC, 16-26	343.16	P	A		F		C						D							F				F				C			R				R
38X-CC, 28-38	360.12	M	C		R		D																	R				F			R				
39X-CC, 22-32	363.39	P	F				D				F		F																							
40X-CC, 20-30	373.46		B																																	
41X-CC, 29-34	382.24		T				F						F															R								
42X-CC, 19-29	396.24	M	A				F						D							F								F								
43X-CC, 29-34	402.59	M	A		C		F						D							C					R											
44X-CC, 38-43	418.85	M	A				C						D							F				R				F								
45X-CC, 13-18	419.37	M	A				C						D							A								C				R				
46X-CC, 57-62	437.77	G	A				F				R		A											F		R	R						R			
47X-CC, 14-19	447.47	G	C		F		C						C							C				F		F						R				
48X-CC, 39-44	456.95	G	A		C		C				R		D									R		R		F		C				R	R			
49X-CC, 27-32	465.52	G	A		C		A				R		A											R		R										
50X-CC, 27-32	476.02	G	F				C						D								R			R												
51X-CC, 23-33	483.56	G	A		F		C						A									C		C	R	F										
52X-CC, 18-28	494.62	G	A		R		C						A	R								C		C	R		R									

Note: Preservation: VG = very good, G = good, M = moderate, and P = poor; total (group) and relative abundance of calcareous nannofossils: D = dominant, A = abundant, C = common, F = few, R = rare, T = trace, and B = barren.

Table T5. Identification and abundance of planktonic foraminifers observed at Site 1119.

Core, section, interval (cm)	Depth (mbsf)	Preservation	Group abundance	*Globigerina bulloides*	*Globigerina falconensis*	*Globigerina quinqueloba*	*Globigerina* spp.	*Globigerina umbilicata*	*Globigerinella aequilateralis*	*Globigerinita glutinata*	*Globorotalia crassacarina*	*Globorotalia crassaformis* (dextral)	*Globorotalia crassaformis* (sinistral)	*Globorotalia crassula*	*Globorotalia hirsuta*	*Globorotalia inflata*	*Globorotalia puncticulata*	*Globorotalia puncticuloides*	*Globorotalia scitula*	*Globorotalia truncatulinoides*	*Neogloboquadrina pachyderma*	*Orbulina universa*
181-1119B-																						
1H-1, 0-1	0	VG	A	A		A		F	R	R						F				R	F	R
181-1119A-																						
1H-CC, 18-23	5.96	VG	A	F	R	F		F		R						F				R	F	
181-1119B-																						
1H-CC, 10-15	4.68	VG	A	F		F		F							P	F				R	F	P
3H-CC, 51-56	24.24	VG	C	A		F										R				P	F	
4H-CC, 47--52	30.84	VG	A	A				A		A				F		F			P	R	A	
5H-CC, 25-30	43.58	VG	C	A	F	F		F								F				P	F	
6H-CC, 30-35	52.92	VG	A	A	R	F		A		R				R		F				R	A	
7H-CC, 65-70	62.52	VG	C	A		F										F				P	F	
9H-CC, 33-38	81.50	VG	C	A		F										F					F	
11H-CC, 25-30	100.39	VG	C	D		F								P		F			P	P	F	
13H-CC, 48-53	119.66	VG	C	D		F								P		R			P	P	F	
15H-CC, 25-30	138.50	VG	C	D		F								P		P			P		F	
16H-CC, 36-41	147.95	VG	C	D		F			P					R		R				P	F	
17H-CC, 26-31	155.80	VG	R			D															A	
181-1119C-																						
17H-CC, 39-44	160.96	VG	A	R			D	R		R									P		R	
18X-CC, 34-39	169.38	VG	C	F		F		R		P				R		F		P	P	P	F	P
19X-CC, 42-47	176.57	VG	C	D		F								P			R	P	R		F	
25X-2, 33-37	228.23	VG	A	R	F	F	A							R		R		F	R		F	
25X-2, 123-126	229.13	VG	A								P			P		R	R				P	
25X-2, 140-146	229.30	VG	F	P		A										R		R	R		F	
25X-5, 113-119	233.53	G	R	R		F	A	F									R		R		R	
25X-6, 56-58	234.46	G	C	R		R	D	R		R				P		P	P				R	
25X-6, 70-75	234.60	VG	A	F	R	F	F			R				F		R		F			F	
25X-CC, 30-35	235.70	G	C	A		F					P			P		P	R	R	P		F	
28X-CC, 95-100	264.87	VG	C	A		F										P		R			F	
29X-CC, 47-52	274.42	G	A	A			D	R						P			R		P		F	
31X-CC, 29-34	293.73	G	F	A		F	D	P		P	P					R	R	R			F	
35X-CC, 24-29	331.96	M	A	F			D	R					P	P			R		P			
36X-CC, 23-33	338.78	VG	A	F		F	A	R						P		R		F			F	
37X-CC, 16-26	343.16	M	A				D	R						P		P	R					
38X-1, 64-68	351.74	M	A	R			D	F								P		F	P		R	
38X-2, 100-107	353.60	G	F	P		F	A	R										R	R		R	
41X-CC, 29-34	382.24	VG	A	F		F	A					P		P		R	R		P		R	
44X-CC, 38-43	418.85	G	A	R			D										R					
45X-CC, 13-18	419.37	M	A	R			D						P				R	P	P			
46X-CC, 57-62	437.77	G	F	P									P			P	P	R				
47X-CC, 14-19	447.47	G	F	A		F										P	R	R	R		F	
49X-CC, 27-32	465.52	VG	F	A		F				P						P	R	F	P			
50X-CC, 27-32	476.02	VG	F	A		F										P	R	A	R			P
52X-CC, 18-28	494.62	VG	F	A		F	D	R								P	A	R	R		F	P

Note: Preservation: VG = very good, G = good, and M = moderate; total (group) and relative abundance of planktonic foraminifers: D = dominant, A = abundant, C = common, F = few/frequent, R = rare, and P = present.

Table T6. Identification and abundance of benthic foraminifers observed at Site 1119. (**See table note.** Continued on next page.)

Core, section, interval (cm)	Depth (mbsf)	Preservation	Group abundance	*Anomalinoides parvumbilius*	*Anomalinoides sphericus*	*Astrononion novozealandicum*	*Bolivina affiliata*	*Bolivina barbata*	*Bolivina* spp.	*Bolivinita pliozea*	*Bolivinita quadrilatera*	*Bulimina exilis*	*Bulimina marginata*	*Buliminella elegantissima*	*Cassidulina carinata*	*Cassidulina norcrossi*	*Cassidulina* spp.	*Cibicidoides* aff. *pachyderma*	*Cibicidoides* spp.	*Cornuspira involvens*	*Dentalina* spp.	*Discanomalina semipunctata*	*Discorbinella bertheloti*	*Discorbinella complanata*	*Eggerella bradyi*	*Ehrenbergina mestayeri*	*Elphidium excavatum* f. *clavatum*	*Epistominella exigua*	*Evolvocassidulina orientalis*	*Fissurina* spp.	*Gavelinopsis praegeri*	*Globobulimina turgida*	*Globocassidulina* spp.	*Globocassidulina subglobosa*	*Haeuslerella pliocenica*	*Heronallenia lingulata*	*Hoeglundina elegans*	*Karreriella cylindrica*	*Karreriella* spp.	*Lagena* spp.	*Laticarinina altocamerata*	*Lenticulina calcar*	*Lenticulina* spp.
181-1119B-																																										
1H-CC, 10-15	4.68	VG	C		R	R		F	T								F		F	T		T						T		T	T			R				T			
3H-CC, 51-56	24.24	VG	C			R		R											R	T													R									
5H-CC, 25-30	43.58	VG	C			R		R	R	R		T																										T			T	
7H-CC, 65-70	62.52	VG	C		R				R																								R					T				
9H-CC, 33-38	81.50	VG	C						F								R									T																
11H-CC, 25-30	100.39	VG	C		T	R			R				T				R									T																
13H-CC, 48-53	119.66	VG	C							R			T															T														
15H-CC, 25-30	138.50	VG	C		T	R				R	R	R		T									T																		T	
17H-CC, 26-31	155.80	VG	R			F			F			T					F					F				R	T			R											R
181-1119C-																																										
16H-8, 60-61	150.87	G	C				T			R							F		F										R												
17H-CC, 39-44	160.96	G	R												T				T																						
18X-CC, 34-39	169.38	VG	C	T	T	F				F	F				F							T					T	F			F				T						
19X-CC, 42-47	176.57	VG	C			F			T	R	T		T		R								T				T		T			F									
25X-2, 33-37	228.23	VG	A			T				R		T	R		R				R			T	R									R									
25X-2, 123-126	229.13	VG	A						T	R			T						T								T													T	
25X-2, 140-146	229.30	VG	R																																						
25X-5, 31-33	232.71	VG	C			R				T			R						R	T							R		R					R							
25X-5, 34-38	232.74	G	R							R			T						R				F				F														
25X-5, 113-119	233.53	G	F			R				R		T			R				R	T			R				T		T					R							
25X-6, 56-58	234.46	G	C						T										T		R																				
25X-6, 70-75	234.60	VG	C		F	T				F					R				R	T		T	R				T		T	T			R		T						
25X-CC, 30-35	235.70	VG	C		T	F				R		R			R				R																						
28X-CC, 95-100	264.87	VG	C			R				R		R			R					T											T										T
31X-CC, 29-34	293.73	VG	C			F						T					F										F				T	R								R
35X-CC, 24-29	331.96	G	F							T								T																						
36X-CC, 23-33	338.78	G	C			F				F							R		R				R				T								T						
38X-1, 64-68	351.74	M	A	F	T	R			T	T									R		T	T	R						T				R		T		T				
38X-2, 100-107	353.60	G	F			R				R			T		R		R																	R							
39X-CC, 22-32	363.39	G	F																																T	T					
41X-CC, 29-34	382.24	G	F			R							R						R				R												T	T					T
45X-CC, 13-18	419.37	G	C						T																										T	T					
47X-CC, 14-19	447.47	VG	F						R	R		T			F												F								R						
48X-CC, 39-44	456.95	VG	F			R				R		T			F								R				R			R					T	T					T
50X-CC, 27-32	476.02	VG	F	T	T	R				R		R			R				R								R			R					T						
52X-CC, 18-28	494.62	VG	F	T	R	R			R	F		T			R				R				R			T							R		T						T

Note: Preservation: VG = very good, G = good, and M = moderate; total (group) and relative abundance of benthic foraminifers: A = abundant, C = common, F = few/frequent, R = rare, and T = trace.

Table T6 (continued).

Core, section, interval (cm)	Depth (mbsf)	Preservation	Group abundance	*Martinottiella communis*	*Melonis affinis*	*Melonis barleeanus*	*Nonionella labradorica*	*Nonionella magnalingua*	*Nonionella* sp.	*Nonionellina flemingi*	*Notorotalia finlayi*	*Notorotalia* spp.	*Notorotalia zelandica*	*Oolina hexagona*	*Oolina* spp.	*Oridorsalis umbonatus*	*Patellina corrugata*	*Pileolina patelliformis*	*Planulina ariminensis*	*Planulina wuellerstorfi*	*Plectofrondicularia advena*	*Plectofrondicularia pellucida*	*Pleurostomella* spp.	*Pullenia bulloides*	*Pullenia quinqueloba*	*Pyrgo anomala*	*Pyrgo* spp.	*Pyrulina* sp.	*Quinqueloculina* spp.	*Rectobolivina striatula*	*Rosalina* spp.	*Sigmoilopsis* crs. sp.	*Sigmoilopsis schlumbergeri*	*Siphotextularia wairoana*	*Sphaeroidina bulloides*	*Textularia* spp.	*Trifarina angulosa*	*Uvigerina peregrina*	*Uvigerina* spp.	*Vaginulina* sp.
181-1119B-																																							
1H-CC, 10-15	4.68	VG	C					T	T	F		F								R				R	T		T				T		R		T		T
3H-CC, 51-56	24.24	VG	C							R		R								T									R		R			R		R			
5H-CC, 25-30	43.58	VG	C									R				T	T			T														R			R		
7H-CC, 65-70	62.52	VG	C							R			R			T																							
9H-CC, 33-38	81.50	VG	C							R			R																T										
11H-CC, 25-30	100.39	VG	C							R		R									T															R			
13H-CC, 48-53	119.66	VG	C							R		R				T					T	T			T				T						R				
15H-CC, 25-30	138.50	VG	C							R		R				T					T																		
17H-CC, 26-31	155.80	VG	R						R	R							T																						
181-1119C-																																							
16H-8, 60-61	150.87	G	C							F		F				T				R	T														R				
17H-CC, 39-44	160.96	G	R									T								T						T			T									T	
18X-CC, 34-39	169.38	VG	C							R		F				T				R	R			T	T		T								R	T	R	R	
19X-CC, 42-47	176.57	VG	C						R	R			F		T	T					T			T		T									R		R		R	
25X-2, 33-37	228.23	VG	A							F		F						T		R					T	T			R						T		R	R	
25X-2, 123-126	229.13	VG	A	T	T	R	T					T	R		T				T					T		T			R				T		T	T		R	
25X-2, 140-146	229.30	VG	R					T															T																
25X-5, 31-33	232.71	VG	C							F		R				T				T	T					T									R		R	T	
25X-5, 34-38	232.74	G	R							F		R								T									R						R				
25X-5, 113-119	233.53	G	F					T		F		R								T						T			R						T				
25X-6, 56-58	234.46	G	C									T							T			R			T			T										
25X-6, 70-75	234.60	VG	C							F		F			T					R					T	T			R					T	R	T	F	R	
25X-CC, 30-35	235.70	VG	C							F		F															T		T					T	F				R	
28X-CC, 95-100	264.87	VG	C							F		F				T				R	T			T		T			R					T	R		R			
31X-CC, 29-34	293.73	VG	C							F		F								T					T												T		T	
35X-CC, 24-29	331.96	G	F																	T									T										T	
36X-CC, 23-33	338.78	G	C							F		R									T			T		T			T					T		F			
38X-1, 64-68	351.74	M	A					T		T		F								R				R	T		T		T	T		T			R		R	R	
38X-2, 100-107	353.60	G	F							R		R												T		T			T								F		
39X-CC, 22-32	363.39	G	F																																				
41X-CC, 29-34	382.24	G	F			T						F				T								R							T					F	R	
45X-CC, 13-18	419.37	G	C			T																										T							
47X-CC, 14-19	447.47	VG	F							R		F															T		T					T				T	
48X-CC, 39-44	456.95	VG	F									F									T			T	T									T				R	
50X-CC, 27-32	476.02	VG	F							F		F									T			T		T			R									R	
52X-CC, 18-28	494.62	VG	F							R	F	F				R								T		T			R						T		R		R	

Table T7. Identification and abundance of diatoms observed at Site 1119. (See table note. Continued on next page.)

Core, section, interval (cm)	Depth (mbsf)	Group abundance	*Achnanthes* sp.	*Actinocyclus ingens* var. *ovalis*	*Actinocyclus ingens* var. *planus*	*Actinoptychus senarius*	*Actinoptychus splendens*	*Aulacoseira granulata*	*Azpeitia tabularis*	*Cavitatus lanceolatus*	*Chaetoceros* resting spores	*Cocconeis* sp.	*Coscinodiscus asteromphalus*	*Coscinodiscus marginatus*	*Coscinodiscus radiatus*	*Cyclotella striata*	Diatom fragments	*Diploneis* sp.	*Eunotia* sp.	*Grammatophora* sp.	*Hemidiscus cuneiformis*	*Hyalodiscus ?scotticus*	*Hyalodiscus* sp.	*Navicula directa*	*Navicula* sp.	*Nitzschia barronii*	*Nitzschia bicapitata*	*Nitzschia kerguelensis*	*Nitzschia kolaczeckii*	*Nitzschia panduriformis*	*Nitzschia praeinterfrigidaria*	*Nitzschia pseudokerguelenis*	*Nitzschia ritscherii*	*Nitzschia weaveri*	*Paralia sulcata*	*Pleurosigma* sp.	*Proboscia alata*	*Rhaphoneis amphiceros*	*Rhaphoneis surirelloides*	*Rhizosolenia hebetata* f. *hiemalis*	*Rhizosolenia styliformis*	Sponge spicules	*Stephanopyxis* sp.	*Stephanopyxis turris intermedia*	*Stephanopyxis turris turris*	*Symbolophora* sp.	*Thalassionema nitzschioides*	*Thalassionema nitzschioides* var. *parva*	*Thalassiosira burckliana*	*Thalassiosira gracilis*	*Thalassiosira lentiginosa*	*Thalassiosira leptopus*	*Thalassiosira oestrupii*	*Thalassiothrix longissima*	*Xanthiopyxis ovalis*	*Xanthiopyxis* sp.
181-1119A-																																																								
1H-CC, 18-23	5.96	T															R					R																				C														
181-1119B-																																																								
1H-1, 0-1	0	B															R																									C														
1H-CC, 10-15	4.68	T															R																									C														
2H-CC, 11-16	14.53	T															R					T																				C														
3H-CC, 51-56	24.24	T															R					T											R									C														
4H-CC, 47-52	30.84	R																				R																				C														
5H-CC, 25-30	43.58	F													R							R		T				T		C					F				C			C													R	
6H-CC, 30-35	52.92	T																				T						T														C														
7H-CC, 65-70	62.52	T																																								C														
8H-CC, 27-32	72.09	R																				T						F		C					F				C			C													R	
9H-CC, 33-38	81.50	T																				T																				C														
10H-CC, 31-36	90.93	R								F												T					T															C														
11H-CC, 25-30	100.39	T																				T																				C														
12H-CC, 29-34	109.91	B																				T																				C														
13H-CC, 48-53	119.66	R																				R																				C														
14H-CC, 33-38	128.98	F																				R																				C														
15H-CC, 25-30	138.50	C				R	T		R													R		R				R		C					R	T			F		T	C			T			T			T	T	C	R		
16H-CC, 36-41	147.95	C			F													R		T		T						F		F					R		R		R	R		C		F	C								R		T	
181-1119C-																																																								
16H-8, 60-61	150.87	A	T		F				R		R					R		R				R		T		F		R		C			F				T		R			C					R	R								
17H-CC, 39-44	160.96	C			R	R			R		R				R	F		T						R						F			C						A			C			T										R	R
18X-CC, 34-39	169.38	A	T		F		R		R		F		R		T	T						R		R				R		C			F		R		R	R	C	T		C					R	R			T			R	R	R
19X-CC, 42-47	176.23	F			F																												F									C														
20X-CC, 33-38	187.69	F																																																						
21X-CC, 45-50	196.52	C			R	T			R	F	R											R								F					F							C												F	R	
22X-CC, 24-29	206.83	F								F	F																	R												T		C									T			F	R	
23X-CC, 37-42	217.15	B																																																						
25X-2, 31-33	228.21	T												T																												F														
25X-2, 138-140	229.28	T														T	R																									R														
25X-5, 31-33	232.71	F																																			T				T	F		R	T		R	F							R	
25X-5, 111-113	233.51	C				T																				F				F									R			F		C	T		C						R			
25X-6, 68-70	234.58	B																																								F														
25X-CC, 30-35	235.70	B																																																						
26X-CC, 72-77	245.91	T																																																						
27X-CC, 50-55	254.63	F								F					T				T																							C												F		

Table T7 (continued).

Core, section, interval (cm)	Depth (mbsf)	Group abundance	*Achnanthes* sp.	*Actinocyclus ingens* var. *ovalis*	*Actinocyclus ingens* var. *planus*	*Actinoptychus senarius*	*Actinoptychus splendens*	*Aulacoseira granulata*	*Azpeitia tabularis*	*Cavitatus lanceolatus*	*Chaetoceros* resting spores	*Cocconeis* sp.	*Coscinodiscus asteromphalus*	*Coscinodiscus marginatus*	*Coscinodiscus radiatus*	*Cyclotella striata*	*Diatom fragments*	*Diploneis* sp.	*Eunotia* sp.	*Grammatophora* sp.	*Hemidiscus cuneiformis*	*Hyalodiscus ?scotticus*	*Hyalodiscus* sp.	*Navicula directa*	*Navicula* sp.	*Nitzschia barronii*	*Nitzschia bicapitata*	*Nitzschia kerguelenis*	*Nitzschia kolackzeckii*	*Nitzschia panduriformis*	*Nitzschia praeinterfrigidaria*	*Nitzschia pseudokerguelenis*	*Nitzschia ritscherii*	*Nitzschia weaveri*	*Paralia sulcata*	*Pleurosigma* sp.	*Proboscia alata*	*Rhaphoneis amphiceros*	*Rhaphoneis surirelloides*	*Rhizosolenia hebetata* f. *hiemalis*	*Rhizosolenia styliformis*	*Sponge spicules*	*Stephanopyxis* sp.	*Stephanopyxis turris intermedia*	*Stephanopyxis turris turris*	*Symbolophora* sp.	*Thalassionema nitzschioides*	*Thalassionema nitzschioides* var. *parva*	*Thalassiosira burckliana*	*Thalassiosira gracilis*	*Thalassiosira lentiginosa*	*Thalassiosira leptopus*	*Thalassiosira oestrupii*	*Thalassiothrix longissima*	*Xanthiopyxis ovalis*	*Xanthiopyxis* sp.
28X-CC, 95-100	264.87	A								C	R															T				R					R							C			T									R		
30X-CC, 50-55	284.00	T						T																																		C													R	
31X-CC, 29-34	293.73	F								F								T				T																				F					F		T							
32X-CC, 39-44	303.19	A		T		T	R			F	R					R						T				F				F					R			T	F		T	F					F					T	R		F	
34X-CC, 26-31	319.17	T															T																		T							R														
35X-CC, 24-29	331.96	A				R			T	R	R	T				R		T								F																C		T	R	T	F						T	F	F	
36X-CC, 23-33	338.78	A							T			T						T			R									T					R							F			R	T	F							R	R	F
37X-CC, 16-26	343.16	R																																	R							F												R		
38X-CC, 28-38	360.12	A	T			R		R		R	F				R			R				F				C		T		F	F	T			R	R						F					C				R		R	T	F	F
39X-CC, 22-32	363.39	T															T																									F														
40X-CC, 20-30	373.46	B																																								R														
41X-CC, 29-34	382.24	B																																								R														
42X-CC, 19-29	396.24	B																																								R														
43X-CC, 29-34	402.59	B																																								C														
44X-CC, 38-43	418.85	R								T								R																								A			R											
45X-CC, 13-18	419.37	B																																								F														
46X-CC, 114-115	433.84	T																																																						
46X-CC, 57-62	437.77	R																T		T			T		T										T							R														
47X-CC, 14-19	447.47	R															T	T																	R							F														
48X-CC, 39-44	456.95	F						T									T			R														T	R							F													R	
49X-CC, 27-32	465.52	F																R							T										R							F													F	
50X-CC, 27-32	476.02	T																																	T							F														
51X-CC, 23-33	483.56	T																																	T							F														
52X-CC, 18-28	494.62	F	T															F							R										F							C			T						T				R	

Note: Total (group) and relative abundance of diatoms: A = abundant, C = common, F = few, R = rare, T = trace, and B = barren.

Table T8. Identification and abundance of radiolarians. (**See table note.** Continued on next page.)

Core, section, interval (cm)	Depth (mbsf)	Preservation	Group abundance	*Actinomma* sp.	*Antarctissa cylindrica*	*Antarctissa denticulata*	*Antarctissa* sp.	*Antarctissa strelkovi*	*Botryostrobus auritus/australis* group	*Carpocanistrum* sp.	*Ceratocyrtis* sp.	*Cycladophora bicornis*	*Cycladophora davisiana*	*Cycladophora pliocenica*	*Cycladophora* sp.	*Euchitonia* sp.	*Eucyrtidium calvertense*	*Larcopyle* sp.	*Lithelius nautiloides*	*Peripbaena* sp.	*Phormocium clevei*	*Pterocanium* sp.	*Pterocanium trilobum*	*Pylospira* sp.	*Spongaster* sp.	*Spongoplegma antarcticum*	*Spongotrochus glacialis*	*Spumellaria* form A	*Stylodictya* sp.	*Triceraspyris antarctica*	*Triceraspyris* sp.	Numbers of specimens per slide
181-1119A-																																
1H-CC, 18-23	5.96	G	T															T														4
181-1119B-																																
1H-CC, 10-15	4.68	G	T												R			R			T			T	T						T	8
2H-CC, 11-16	14.53	G	R					T													R				T							4
3H-CC, 51-56	24.24	G	R											T							R											5
4H-CC, 47-52	30.84	G	R											R	T				R						R							12
5H-CC, 25-30	43.58	M	R		T		T							R							R				R	T						11
6H-CC, 30-35	52.92	M	T					T													R				R							7
7H-CC, 65-70	62.52		B																													0
8H-CC, 27-32	72.09	G	T	T														T							R			T				6
9H-CC, 33-38	81.50	M	R												T										R							3
10H-CC, 31-36	90.93		B																													0
11H-CC, 25-30	100.39	M	R																T		T				F							16
12H-CC, 29-34	109.91	M	R																						R							4
13H-CC, 48-53	119.66	M	F	T															T						C					T		26
14H-CC, 33-38	128.98	G	R						T				R																			4
15H-CC, 25-30	138.50	M	R	T																					R					T		7
16H-CC, 36-41	147.95	M	R																						R							3
17H-CC, 26-31	155.80	M	R		T		T																		R							7
181-1119C-																																
1H-CC, 10-15	8.22	G	T																T													1
2H-CC, 15-20	17.60		B																													0
3H-CC, 36-41	27.83	G	T								R																					1
16H-8, 60-61	150.87	M	R	R				T										F	T		T				F		R					20
17H-CC, 39-44	160.96		B																													0
18X-CC, 34-39	169.38		B																													0
19X-CC, 42-47	176.57	P	R																						R							5
20X-CC, 33-38	187.69	M	T																T						T							2
21X-CC, 45-50	196.52	M	T		T																				R							4
22X-CC, 24-29	206.83	M	R							T								R							R				T			9
23X-CC, 37-42	217.15		B																													0
25X-2, 31-33	228.21		B																													0
25X-2, 138-140	229.28		B																													0
25X-5, 31-33	232.71	M	R															R							R		T		T	T		14
25X-5, 111-113	233.51	M	C	T		T												F	T		R		T		C		F			T		50
25X-6, 68-70	234.58		B																													0
25X-CC, 30-35	235.70		B																													0
26X-CC, 72-77	245.91	M	R																						R							2
27X-CC, 50-55	254.63		B																													0
28X-CC, 95-100	264.87	M	F															R	R	T	R	T		T	C				T			28
29X-CC, 47-52	274.42		B																													0
30X-CC, 50-55	284.00		B																													0
31X-CC, 29-34	293.73	M	R												T				R						R				R			18
32X-CC, 39-44	303.19		B																													0
33X-CC, 49-54	312.83	M	R															T							R				T			4
34X-CC, 26-31	319.17		B																													0
35X-CC, 24-29	331.96	P	T															T							T							1
36X-CC, 23-33	338.78	P	R													T									T							2
37X-CC, 16-26	343.16		B																													0
38X-1, 70-72	351.80		B																													0
38X-2, 110-111	353.70	M	R					T									T	T									T					4
38X-CC, 28-38	360.12		B																													0
39X-CC, 22-32	363.39		B																													0
40X-CC, 20-30	373.46		B																													0
41X-CC, 29-34	382.24		B																													0
42X-CC, 19-29	396.24		B																													0

Table T8 (continued).

Core, section, interval (cm)	Depth (mbsf)	Preservation	Group abundance	*Actinomma* sp.	*Antarctissa cylindrica*	*Antarctissa denticulata*	*Antarctissa* sp.	*Antarctissa strelkovi*	*Botryostrobus auritus/australis* group	*Carpocanistrum* sp.	*Ceratocyrtis* sp.	*Cycladophora bicornis*	*Cycladophora davisiana*	*Cycladophora pliocenica*	*Cycladophora* sp.	*Euchitonia* sp.	*Eucyrtidium calvertense*	*Larcopyle* sp.	*Lithelius nautiloides*	*Peripbaena* sp.	*Phorticium clevei*	*Pterocanium* sp.	*Pterocanium trilobum*	*Pylospira* sp.	*Spongodiscus* sp.	*Spongoplegma antarcticum*	*Spongotrochus glacialis*	*Spumellaria* form A	*Stylodictya* sp.	*Triceraspyris antarctica*	*Triceraspyris* sp.	Numbers of specimens per slide
43X-CC, 29-34	402.59		B																													0
44X-CC, 38-43	418.85		B																													0
45X-CC, 13-18	419.37		B																													0
46X-CC, 57-62	437.77	P	R																						R							2
47X-CC, 14-19	447.47		B																													0
48X-CC, 39-44	456.95	P	R	T																					T							2
49X-CC, 27-32	465.52		B																													0
50X-CC, 27-32	476.02		B																													0
51X-CC, 23-33	483.56		B																													0
52X-CC, 18-28	494.62	P	R																						T				T			2

Note: Preservation: G = good, M = moderate, and P = poor; total (group) and relative abundance of radiolarians: C = common, F = few, R = rare, T = trace, and B = barren.

Table T9. List of fossil mollusks from Site 1119.

Taxon	Hole, core, section, interval (cm)
Bivalvia	
Nuculana sp.	1119C-52X-5, 76-77
Neilo australis (Quoy and Gaimard)	1119C-23X-6, 118
Limopsis peteri Beu	1119C-25X-6, 54
Zygochlamys delicatula (Hutton)	1119C-3H-1, 115-120
Tawera spissa (Deshayes)	1119C-1H-5, 20
Tawera spissa (Deshayes)	1119B-7H-6, 66-68
Tawera spissa (Deshayes)	1119C-7H-7, 94
Tawera spissa (Deshayes)	1119B-7H-8, 20-22
Tawera spissa (Deshayes)	1119B-10H-1, 47-48
Gastropoda	
Stiracolpus sp.	1119C-23X-6, 118
Falsilunatia ambigua (Suter)	1119C-9H-3, 32-33
Falsilunatia ambigua (Suter)	1119C-9H-7, 48
Falsilunatia ambigua (Suter)	1119B-11H-5, 9-10
Falsilunatia ambigua (Suter)	1119C-11H-CC, 0-1
Falsilunatia ambigua (Suter)	1119B-13H-2, 55-56
Falsilunatia ambigua (Suter)	1119C-19X-1, 120-121
Friginatica conjuncta (Dell)	1119B-11H-1, 127-128
Pliconacca denticulifera (Marwick)	1119C-14H-4, 32-33
Pliconacca denticulifera (Marwick)	1119C-17H-1, 14-15
Pliconacca denticulifera (Marwick)	1119C-25X-2, 77-78
Pliconacca denticulifera (Marwick)	1119C-29X-6, 25-26
Cominella (*Josepha*) cf. *onokeana* (King)	1119C-15H-6, 22-23
Cominella (*Eucominia*) *alertae* (Dell)	1119B-6H-2, 29-30
Cominella (*Eucominia*) cf. *elegantula* (Finlay)	1119C-27X-1, 132-133
Aeneator elegans (Suter)	1119C-5H-4, 90-92
A*eneator* (*Ellicea*) *recens* (Dell)	1119C-23X-6, 118
Marginella sp.	1119C-52X-5, 76-77
Amalda (*Gracilispira*) cf. *novaezelandiae* (Sowerby)	1119C-9H-4, 53-54
Amalda (*Gracilispira*) cf. *novaezelandiae* (Sowerby)	1119B-12H-CC,12-13
Provocator mirabilis (Finlay)	1119B-6H-2, 7-9
Antimelatoma buchanani (Hutton)	1119C-9H-5, 36-37
Antimelatoma buchanani (Hutton)	1119C-22X-6A, 92-93
Splendrillia majorina Beu	1119C-15H-5, 16-17
Bathytoma (*Micantapex*) *murdochi* Finlay	1119B-6H-2, 35-37

Note: Identifications by R.M. Carter and A. Beu.

Table T10. Composite depth section. (See table note. Continued on next seven pages.)

Leg	Site	Hole	Core	Type	Section	Section length	Depth (mbsf)	Offset	Composite depth (mcd)
181	1119	A	1	H	1	1.33	0	0	0
181	1119	A	1	H	2	1.5	1.33	0	1.33
181	1119	A	1	H	3	1.5	2.83	0	2.83
181	1119	A	1	H	4	1.32	4.33	0	4.33
181	1119	A	1	H	5	0.13	5.65	0	5.65
181	1119	A	1	H	CC	0.23	5.78	0	5.78
181	1119	B	1	H	1	1.5	0	0.04	0.04
181	1119	B	1	H	2	1.5	1.5	0.04	1.54
181	1119	B	1	H	3	1.3	3	0.04	3.04
181	1119	B	1	H	4	0.28	4.3	0.04	4.34
181	1119	B	1	H	CC	0.15	4.58	0.04	4.62
181	1119	B	2	H	1	1.5	4.7	0.24	4.94
181	1119	B	2	H	2	1.5	6.2	0.24	6.44
181	1119	B	2	H	3	1.5	7.7	0.24	7.94
181	1119	B	2	H	4	1.5	9.2	0.24	9.44
181	1119	B	2	H	5	1.5	10.7	0.24	10.94
181	1119	B	2	H	6	1.5	12.2	0.24	12.44
181	1119	B	2	H	7	0.72	13.7	0.24	13.94
181	1119	B	2	H	CC	0.16	14.42	0.24	14.66
181	1119	B	3	H	1	1.5	14.2	1.24	15.44
181	1119	B	3	H	2	1.5	15.7	1.24	16.94
181	1119	B	3	H	3	1.5	17.2	1.24	18.44
181	1119	B	3	H	4	1.5	18.7	1.24	19.94
181	1119	B	3	H	5	1.5	20.2	1.24	21.44
181	1119	B	3	H	6	0.8	21.7	1.24	22.94
181	1119	B	3	H	7	0.8	22.5	1.24	23.74
181	1119	B	3	H	8	0.43	23.3	1.24	24.54
181	1119	B	3	H	CC	0.56	23.73	1.24	24.97
181	1119	B	4	H	1	1.5	23.7	1.24	24.94
181	1119	B	4	H	2	1.5	25.2	1.24	26.44
181	1119	B	4	H	3	1.5	26.7	1.24	27.94
181	1119	B	4	H	4	1	28.2	1.24	29.44
181	1119	B	4	H	5	0.56	29.2	1.24	30.44
181	1119	B	4	H	6	0.61	29.76	1.24	31
181	1119	B	4	H	CC	0.52	30.37	1.24	31.61
181	1119	B	5	H	1	1.53	33.2	1.31	34.51
181	1119	B	5	H	2	1.5	34.73	1.31	36.04
181	1119	B	5	H	3	1.5	36.23	1.31	37.54
181	1119	B	5	H	4	1.43	37.73	1.31	39.04
181	1119	B	5	H	5	1.55	39.16	1.31	40.47
181	1119	B	5	H	6	1.55	40.71	1.31	42.02
181	1119	B	5	H	7	1.07	42.26	1.31	43.57
181	1119	B	5	H	CC	0.3	43.33	1.31	44.64
181	1119	B	6	H	1	1.5	42.7	2.98	45.68
181	1119	B	6	H	2	1.5	44.2	2.98	47.18
181	1119	B	6	H	3	1.5	45.7	2.98	48.68
181	1119	B	6	H	4	1.5	47.2	2.98	50.18
181	1119	B	6	H	5	1.5	48.7	2.98	51.68
181	1119	B	6	H	6	1.5	50.2	2.98	53.18
181	1119	B	6	H	7	0.92	51.7	2.98	54.68
181	1119	B	6	H	CC	0.35	52.62	2.98	55.6
181	1119	B	7	H	1	1.5	52.2	3.78	55.98
181	1119	B	7	H	2	1.5	53.7	3.78	57.48
181	1119	B	7	H	3	1.5	55.2	3.78	58.98
181	1119	B	7	H	4	1.4	56.7	3.78	60.48
181	1119	B	7	H	5	1.5	58.1	3.78	61.88
181	1119	B	7	H	6	1.5	59.6	3.78	63.38
181	1119	B	7	H	7	0.5	61.1	3.78	64.88
181	1119	B	7	H	8	0.27	61.6	3.78	65.38
181	1119	B	7	H	CC	0.7	61.87	3.78	65.65
181	1119	B	8	H	1	1.5	61.7	5.3	67
181	1119	B	8	H	2	1.5	63.2	5.3	68.5
181	1119	B	8	H	3	1.5	64.7	5.3	70
181	1119	B	8	H	4	1.55	66.2	5.3	71.5
181	1119	B	8	H	5	1.5	67.75	5.3	73.05
181	1119	B	8	H	6	1.5	69.25	5.3	74.55

Table T10 (continued).

Leg	Site	Hole	Core	Type	Section	Section length	Depth (mbsf)	Offset	Composite depth (mcd)
181	1119	B	8	H	7	1.07	70.75	5.3	76.05
181	1119	B	8	H	CC	0.32	71.82	5.3	77.12
181	1119	B	9	H	1	1.5	71.2	6.01	77.21
181	1119	B	9	H	2	1.5	72.7	6.01	78.71
181	1119	B	9	H	3	1.5	74.2	6.01	80.21
181	1119	B	9	H	4	1.4	75.7	6.01	81.71
181	1119	B	9	H	5	1.5	77.1	6.01	83.11
181	1119	B	9	H	6	1.5	78.6	6.01	84.61
181	1119	B	9	H	7	1.07	80.1	6.01	86.11
181	1119	B	9	H	CC	0.38	81.17	6.01	87.18
181	1119	B	10	H	1	1.42	80.7	8.2	88.9
181	1119	B	10	H	2	1.5	82.12	8.2	90.32
181	1119	B	10	H	3	1.5	83.62	8.2	91.82
181	1119	B	10	H	4	1.5	85.12	8.2	93.32
181	1119	B	10	H	5	1.5	86.62	8.2	94.82
181	1119	B	10	H	6	1.5	88.12	8.2	96.32
181	1119	B	10	H	7	1	89.62	8.2	97.82
181	1119	B	10	H	CC	0.36	90.62	8.2	98.82
181	1119	B	11	H	1	1.5	90.2	9.44	99.64
181	1119	B	11	H	2	1.5	91.7	9.44	101.14
181	1119	B	11	H	3	1.5	93.2	9.44	102.64
181	1119	B	11	H	4	1.5	94.7	9.44	104.14
181	1119	B	11	H	5	1.5	96.2	9.44	105.64
181	1119	B	11	H	6	1.5	97.7	9.44	107.14
181	1119	B	11	H	7	0.94	99.2	9.44	108.64
181	1119	B	11	H	CC	0.3	100.14	9.44	109.58
181	1119	B	12	H	1	1.5	99.7	10.02	109.72
181	1119	B	12	H	2	1.5	101.2	10.02	111.22
181	1119	B	12	H	3	1.5	102.7	10.02	112.72
181	1119	B	12	H	4	1.5	104.2	10.02	114.22
181	1119	B	12	H	5	1.5	105.7	10.02	115.72
181	1119	B	12	H	6	1.5	107.2	10.02	117.22
181	1119	B	12	H	7	0.92	108.7	10.02	118.72
181	1119	B	12	H	CC	0.34	109.62	10.02	119.64
181	1119	B	13	H	1	1.5	109.2	11.48	120.68
181	1119	B	13	H	2	1.5	110.7	11.48	122.18
181	1119	B	13	H	3	1.5	112.2	11.48	123.68
181	1119	B	13	H	4	1.5	113.7	11.48	125.18
181	1119	B	13	H	5	1.5	115.2	11.48	126.68
181	1119	B	13	H	6	1.5	116.7	11.48	128.18
181	1119	B	13	H	7	0.98	118.2	11.48	129.68
181	1119	B	13	H	CC	0.53	119.18	11.48	130.66
181	1119	B	14	H	1	1.5	118.7	12.16	130.86
181	1119	B	14	H	2	1.5	120.2	12.16	132.36
181	1119	B	14	H	3	1.5	121.7	12.16	133.86
181	1119	B	14	H	4	1.55	123.2	12.16	135.36
181	1119	B	14	H	5	1.5	124.75	12.16	136.91
181	1119	B	14	H	6	1.5	126.25	12.16	138.41
181	1119	B	14	H	7	0.9	127.75	12.16	139.91
181	1119	B	14	H	CC	0.38	128.65	12.16	140.81
181	1119	B	15	H	1	1.5	128.2	13.97	142.17
181	1119	B	15	H	2	1.5	129.7	13.97	143.67
181	1119	B	15	H	3	1.5	131.2	13.97	145.17
181	1119	B	15	H	4	1.5	132.7	13.97	146.67
181	1119	B	15	H	5	1.5	134.2	13.97	148.17
181	1119	B	15	H	6	1.5	135.7	13.97	149.67
181	1119	B	15	H	7	1.05	137.2	13.97	151.17
181	1119	B	15	H	CC	0.3	138.25	13.97	152.22
181	1119	B	16	H	1	1.5	137.7	17.75	155.45
181	1119	B	16	H	2	1.5	139.2	17.75	156.95
181	1119	B	16	H	3	1.5	140.7	17.75	158.45
181	1119	B	16	H	4	1.5	142.2	17.75	159.95
181	1119	B	16	H	5	1.5	143.7	17.75	161.45
181	1119	B	16	H	6	1.5	145.2	17.75	162.95
181	1119	B	16	H	7	0.89	146.7	17.75	164.45
181	1119	B	16	H	CC	0.41	147.59	17.75	165.34
181	1119	B	17	H	1	1.5	147.2	18.1	165.3
181	1119	B	17	H	2	1.5	148.7	18.1	166.8

Table T10 (continued).

Leg	Site	Hole	Core	Type	Section	Section length	Depth (mbsf)	Offset	Composite depth (mcd)
181	1119	B	17	H	3	1.53	150.2	18.1	168.3
181	1119	B	17	H	4	1.5	151.73	18.1	169.83
181	1119	B	17	H	5	1.5	153.23	18.1	171.33
181	1119	B	17	H	6	0.81	154.73	18.1	172.83
181	1119	B	17	H	CC	0.31	155.54	18.1	173.64
181	1119	C	1	H	1	1.5	0	0.16	0.16
181	1119	C	1	H	2	1.5	1.5	0.16	1.66
181	1119	C	1	H	3	1.5	3	0.16	3.16
181	1119	C	1	H	4	1.5	4.5	0.16	4.66
181	1119	C	1	H	5	1.5	6	0.16	6.16
181	1119	C	1	H	6	0.62	7.5	0.16	7.66
181	1119	C	1	H	CC	0.15	8.12	0.16	8.28
181	1119	C	2	H	1	1.5	8.3	–0.24	8.06
181	1119	C	2	H	2	1.5	9.8	–0.24	9.56
181	1119	C	2	H	3	1.5	11.3	–0.24	11.06
181	1119	C	2	H	4	1.5	12.8	–0.24	12.56
181	1119	C	2	H	5	1.5	14.3	–0.24	14.06
181	1119	C	2	H	6	1.3	15.8	–0.24	15.56
181	1119	C	2	H	7	0.35	17.1	–0.24	16.86
181	1119	C	2	H	CC	0.2	17.45	–0.24	17.21
181	1119	C	3	H	1	1.5	17.8	–0.28	17.52
181	1119	C	3	H	2	1.5	19.3	–0.28	19.02
181	1119	C	3	H	3	1.5	20.8	–0.28	20.52
181	1119	C	3	H	4	1.5	22.3	–0.28	22.02
181	1119	C	3	H	5	1.5	23.8	–0.28	23.52
181	1119	C	3	H	6	1.5	25.3	–0.28	25.02
181	1119	C	3	H	7	0.67	26.8	–0.28	26.52
181	1119	C	3	H	CC	0.41	27.47	–0.28	27.19
181	1119	C	4	H	1	1.5	27.3	0.04	27.34
181	1119	C	4	H	2	1.5	28.8	0.04	28.84
181	1119	C	4	H	3	1.5	30.3	0.04	30.34
181	1119	C	4	H	4	1.5	31.8	0.04	31.84
181	1119	C	4	H	5	1.5	33.3	0.04	33.34
181	1119	C	4	H	6	1.5	34.8	0.04	34.84
181	1119	C	4	H	7	1.19	36.3	0.04	36.34
181	1119	C	4	H	CC	0.35	37.49	0.04	37.53
181	1119	C	5	H	1	1.5	36.8	1	37.8
181	1119	C	5	H	2	1.5	38.3	1	39.3
181	1119	C	5	H	3	1.5	39.8	1	40.8
181	1119	C	5	H	4	1.5	41.3	1	42.3
181	1119	C	5	H	5	1.5	42.8	1	43.8
181	1119	C	5	H	6	1.5	44.3	1	45.3
181	1119	C	5	H	7	0.9	45.8	1	46.8
181	1119	C	5	H	CC	0.42	46.7	1	47.7
181	1119	C	6	H	1	1.5	46.3	2.26	48.56
181	1119	C	6	H	2	1.5	47.8	2.26	50.06
181	1119	C	6	H	3	1.5	49.3	2.26	51.56
181	1119	C	6	H	4	1.5	50.8	2.26	53.06
181	1119	C	6	H	5	1.5	52.3	2.26	54.56
181	1119	C	6	H	6	1.5	53.8	2.26	56.06
181	1119	C	6	H	7	0.9	55.3	2.26	57.56
181	1119	C	6	H	CC	0.5	56.2	2.26	58.46
181	1119	C	7	H	1	0.74	55.8	2.96	58.76
181	1119	C	7	H	2	1.5	56.54	2.96	59.5
181	1119	C	7	H	3	1.5	58.04	2.96	61
181	1119	C	7	H	4	1.5	59.54	2.96	62.5
181	1119	C	7	H	5	1.5	61.04	2.96	64
181	1119	C	7	H	6	1.5	62.54	2.96	65.5
181	1119	C	7	H	7	1.37	64.04	2.96	67
181	1119	C	7	H	CC	1.06	65.41	2.96	68.37
181	1119	C	8	H	1	1.4	65.3	5	70.3
181	1119	C	8	H	2	1.5	66.7	5	71.7
181	1119	C	8	H	3	1.5	68.2	5	73.2
181	1119	C	8	H	4	1.42	69.7	5	74.7
181	1119	C	8	H	5	1.44	71.12	5	76.12
181	1119	C	8	H	6	1.5	72.56	5	77.56
181	1119	C	8	H	7	0.87	74.06	5	79.06
181	1119	C	8	H	CC	0.4	74.93	5	79.93

Table T10 (continued).

Leg	Site	Hole	Core	Type	Section	Section length	Depth (mbsf)	Offset	Composite depth (mcd)
181	1119	C	9	H	1	1.5	74.8	4.7	79.5
181	1119	C	9	H	2	1.5	76.3	4.7	81
181	1119	C	9	H	3	1.34	77.8	4.7	82.5
181	1119	C	9	H	4	1.5	79.14	4.7	83.84
181	1119	C	9	H	5	1.5	80.64	4.7	85.34
181	1119	C	9	H	6	1.5	82.14	4.7	86.84
181	1119	C	9	H	7	0.96	83.64	4.7	88.34
181	1119	C	9	H	CC	0.52	84.6	4.7	89.3
181	1119	C	10	H	1	1.37	84.3	5.94	90.24
181	1119	C	10	H	2	1.5	85.67	5.94	91.61
181	1119	C	10	H	3	1.5	87.17	5.94	93.11
181	1119	C	10	H	4	1.5	88.67	5.94	94.61
181	1119	C	10	H	5	1.5	90.17	5.94	96.11
181	1119	C	10	H	6	1.5	91.67	5.94	97.61
181	1119	C	10	H	7	0.79	93.17	5.94	99.11
181	1119	C	10	H	CC	0.36	93.96	5.94	99.9
181	1119	C	11	H	1	0.24	93.8	9.06	102.86
181	1119	C	11	H	2	1.5	94.04	9.06	103.1
181	1119	C	11	H	3	1.5	95.54	9.06	104.6
181	1119	C	11	H	4	1.5	97.04	9.06	106.1
181	1119	C	11	H	5	1.5	98.54	9.06	107.6
181	1119	C	11	H	6	1.5	100.04	9.06	109.1
181	1119	C	11	H	7	1.5	101.54	9.06	110.6
181	1119	C	11	H	8	0.89	103.04	9.06	112.1
181	1119	C	11	H	CC	0.37	103.93	9.06	112.99
181	1119	C	12	H	1	1.5	103.3	9.58	112.88
181	1119	C	12	H	2	1.5	104.8	9.58	114.38
181	1119	C	12	H	3	1.5	106.3	9.58	115.88
181	1119	C	12	H	4	1.5	107.8	9.58	117.38
181	1119	C	12	H	5	1.5	109.3	9.58	118.88
181	1119	C	12	H	6	1.5	110.8	9.58	120.38
181	1119	C	12	H	7	0.86	112.3	9.58	121.88
181	1119	C	12	H	CC	0.33	113.16	9.58	122.74
181	1119	C	13	H	1	1.5	112.8	10.58	123.38
181	1119	C	13	H	2	1.5	114.3	10.58	124.88
181	1119	C	13	H	3	1.5	115.8	10.58	126.38
181	1119	C	13	H	4	1.5	117.3	10.58	127.88
181	1119	C	13	H	5	1.5	118.8	10.58	129.38
181	1119	C	13	H	6	1.5	120.3	10.58	130.88
181	1119	C	13	H	7	0.89	121.8	10.58	132.38
181	1119	C	13	H	CC	0.42	122.69	10.58	133.27
181	1119	C	14	H	1	0.26	122.3	11.85	134.15
181	1119	C	14	H	2	1.5	122.56	11.85	134.41
181	1119	C	14	H	3	1.5	124.06	11.85	135.91
181	1119	C	14	H	4	1.5	125.56	11.85	137.41
181	1119	C	14	H	5	1.5	127.06	11.85	138.91
181	1119	C	14	H	6	1.5	128.56	11.85	140.41
181	1119	C	14	H	7	1.5	130.06	11.85	141.91
181	1119	C	14	H	8	0.89	131.56	11.85	143.41
181	1119	C	14	H	CC	0.38	132.45	11.85	144.3
181	1119	C	15	H	1	1.5	131.8	14.01	145.81
181	1119	C	15	H	2	1.5	133.3	14.01	147.31
181	1119	C	15	H	3	1.5	134.8	14.01	148.81
181	1119	C	15	H	4	1.5	136.3	14.01	150.31
181	1119	C	15	H	5	1.5	137.8	14.01	151.81
181	1119	C	15	H	6	1.5	139.3	14.01	153.31
181	1119	C	15	H	7	0.91	140.8	14.01	154.81
181	1119	C	15	H	CC	0.37	141.71	14.01	155.72
181	1119	C	16	H	1	0.93	141.3	14.35	155.65
181	1119	C	16	H	2	1.12	142.23	14.35	156.58
181	1119	C	16	H	3	1.21	143.35	14.35	157.7
181	1119	C	16	H	4	1.27	144.56	14.35	158.91
181	1119	C	16	H	5	1.44	145.83	14.35	160.18
181	1119	C	16	H	6	1.5	147.27	14.35	161.62
181	1119	C	16	H	7	1.5	148.77	14.35	163.12
181	1119	C	16	H	8	0.86	150.27	14.35	164.62
181	1119	C	16	H	CC	0.33	151.13	14.35	165.48
181	1119	C	17	H	1	1.5	150.8	18.75	169.55

Table T10 (continued).

Leg	Site	Hole	Core	Type	Section	Section length	Depth (mbsf)	Offset	Composite depth (mcd)
181	1119	C	17	H	2	1.5	152.3	18.75	171.05
181	1119	C	17	H	3	1.5	153.8	18.75	172.55
181	1119	C	17	H	4	1.5	155.3	18.75	174.05
181	1119	C	17	H	5	1.38	156.8	18.75	175.55
181	1119	C	17	H	6	1.5	158.18	18.75	176.93
181	1119	C	17	H	7	0.89	159.68	18.75	178.43
181	1119	C	17	H	CC	0.44	160.57	18.75	179.32
181	1119	C	18	X	1	1.5	160.3	18.75	179.05
181	1119	C	18	X	2	1.35	161.8	18.75	180.55
181	1119	C	18	X	3	1.34	163.15	18.75	181.9
181	1119	C	18	X	4	1.4	164.49	18.75	183.24
181	1119	C	18	X	5	1.43	165.89	18.75	184.64
181	1119	C	18	X	6	1.26	167.32	18.75	186.07
181	1119	C	18	X	7	0.46	168.58	18.75	187.33
181	1119	C	18	X	CC	0.39	169.04	18.75	187.79
181	1119	C	19	X	1	1.5	168.7	18.75	187.45
181	1119	C	19	X	2	1.45	170.2	18.75	188.95
181	1119	C	19	X	3	1.29	171.65	18.75	190.4
181	1119	C	19	X	4	1.5	172.94	18.75	191.69
181	1119	C	19	X	5	1.37	174.44	18.75	193.19
181	1119	C	19	X	CC	0.47	175.81	18.75	194.56
181	1119	C	20	X	1	1.5	178.3	18.75	197.05
181	1119	C	20	X	2	1.5	179.8	18.75	198.55
181	1119	C	20	X	3	1.43	181.3	18.75	200.05
181	1119	C	20	X	4	1.5	182.73	18.75	201.48
181	1119	C	20	X	5	1.39	184.23	18.75	202.98
181	1119	C	20	X	6	1.5	185.62	18.75	204.37
181	1119	C	20	X	7	0.24	187.12	18.75	205.87
181	1119	C	20	X	CC	0.38	187.36	18.75	206.11
181	1119	C	21	X	1	1.5	187.9	18.75	206.65
181	1119	C	21	X	2	1.5	189.4	18.75	208.15
181	1119	C	21	X	3	1.5	190.9	18.75	209.65
181	1119	C	21	X	4	1.5	192.4	18.75	211.15
181	1119	C	21	X	5	1.5	193.9	18.75	212.65
181	1119	C	21	X	6	0.67	195.4	18.75	214.15
181	1119	C	21	X	CC	0.5	196.07	18.75	214.82
181	1119	C	22	X	1	0.29	197.6	18.75	216.35
181	1119	C	22	X	2	1.5	197.89	18.75	216.64
181	1119	C	22	X	3	1.5	199.39	18.75	218.14
181	1119	C	22	X	4	1.5	200.89	18.75	219.64
181	1119	C	22	X	5	1.5	202.39	18.75	221.14
181	1119	C	22	X	6	1.5	203.89	18.75	222.64
181	1119	C	22	X	7	1.2	205.39	18.75	224.14
181	1119	C	22	X	CC	0.29	206.59	18.75	225.34
181	1119	C	23	X	1	0.52	207.2	18.75	225.95
181	1119	C	23	X	2	1.5	207.72	18.75	226.47
181	1119	C	23	X	3	1.5	209.22	18.75	227.97
181	1119	C	23	X	4	1.5	210.72	18.75	229.47
181	1119	C	23	X	5	1.5	212.22	18.75	230.97
181	1119	C	23	X	6	1.23	213.72	18.75	232.47
181	1119	C	23	X	7	1.5	214.95	18.75	233.7
181	1119	C	23	X	8	0.33	216.45	18.75	235.2
181	1119	C	23	X	CC	0.42	216.78	18.75	235.53
181	1119	C	25	X	1	1.5	226.4	18.75	245.15
181	1119	C	25	X	2	1.5	227.9	18.75	246.65
181	1119	C	25	X	3	1.5	229.4	18.75	248.15
181	1119	C	25	X	4	1.5	230.9	18.75	249.65
181	1119	C	25	X	5	1.5	232.4	18.75	251.15
181	1119	C	25	X	6	1.5	233.9	18.75	252.65
181	1119	C	25	X	CC	0.35	235.4	18.75	254.15
181	1119	C	26	X	1	1.5	236	18.75	254.75
181	1119	C	26	X	2	1.5	237.5	18.75	256.25
181	1119	C	26	X	3	1.5	239	18.75	257.75
181	1119	C	26	X	4	1.5	240.5	18.75	259.25
181	1119	C	26	X	5	1.5	242	18.75	260.75
181	1119	C	26	X	6	1.18	243.5	18.75	262.25
181	1119	C	26	X	7	0.51	244.68	18.75	263.43
181	1119	C	26	X	CC	0.77	245.19	18.75	263.94

Table T10 (continued).

Leg	Site	Hole	Core	Type	Section	Section length	Depth (mbsf)	Offset	Composite depth (mcd)
181	1119	C	27	X	1	1.5	245.6	18.75	264.35
181	1119	C	27	X	2	1.5	247.1	18.75	265.85
181	1119	C	27	X	3	1.5	248.6	18.75	267.35
181	1119	C	27	X	4	1.5	250.1	18.75	268.85
181	1119	C	27	X	5	1.5	251.6	18.75	270.35
181	1119	C	27	X	6	1.03	253.1	18.75	271.85
181	1119	C	27	X	CC	0.55	254.13	18.75	272.88
181	1119	C	28	X	1	1.5	255.2	18.75	273.95
181	1119	C	28	X	2	1.5	256.7	18.75	275.45
181	1119	C	28	X	3	1.5	258.2	18.75	276.95
181	1119	C	28	X	4	1.5	259.7	18.75	278.45
181	1119	C	28	X	5	1.5	261.2	18.75	279.95
181	1119	C	28	X	6	1.22	262.7	18.75	281.45
181	1119	C	28	X	CC	1	263.92	18.75	282.67
181	1119	C	29	X	1	1.5	264.8	18.75	283.55
181	1119	C	29	X	2	1.5	266.3	18.75	285.05
181	1119	C	29	X	3	1.5	267.8	18.75	286.55
181	1119	C	29	X	4	1.5	269.3	18.75	288.05
181	1119	C	29	X	5	1.5	270.8	18.75	289.55
181	1119	C	29	X	6	1.5	272.3	18.75	291.05
181	1119	C	29	X	7	0.15	273.8	18.75	292.55
181	1119	C	29	X	CC	0.52	273.95	18.75	292.7
181	1119	C	30	X	1	1.5	274.5	18.75	293.25
181	1119	C	30	X	2	1.5	276	18.75	294.75
181	1119	C	30	X	3	1.5	277.5	18.75	296.25
181	1119	C	30	X	4	1.5	279	18.75	297.75
181	1119	C	30	X	5	1.5	280.5	18.75	299.25
181	1119	C	30	X	6	1.5	282	18.75	300.75
181	1119	C	30	X	CC	0.55	283.5	18.75	302.25
181	1119	C	31	X	1	0.47	284.1	18.75	302.85
181	1119	C	31	X	2	1.5	284.57	18.75	303.32
181	1119	C	31	X	3	1.5	286.07	18.75	304.82
181	1119	C	31	X	4	1.5	287.57	18.75	306.32
181	1119	C	31	X	5	1.5	289.07	18.75	307.82
181	1119	C	31	X	6	1.5	290.57	18.75	309.32
181	1119	C	31	X	7	1.37	292.07	18.75	310.82
181	1119	C	31	X	CC	0.34	293.44	18.75	312.19
181	1119	C	32	X	1	1.5	293.8	18.75	312.55
181	1119	C	32	X	2	1.5	295.3	18.75	314.05
181	1119	C	32	X	3	1.5	296.8	18.75	315.55
181	1119	C	32	X	4	1.5	298.3	18.75	317.05
181	1119	C	32	X	5	1.5	299.8	18.75	318.55
181	1119	C	32	X	6	1.5	301.3	18.75	320.05
181	1119	C	32	X	CC	0.44	302.8	18.75	321.55
181	1119	C	33	X	1	1.5	303.4	18.75	322.15
181	1119	C	33	X	2	1.5	304.9	18.75	323.65
181	1119	C	33	X	3	1.24	306.4	18.75	325.15
181	1119	C	33	X	4	1.5	307.64	18.75	326.39
181	1119	C	33	X	5	1.5	309.14	18.75	327.89
181	1119	C	33	X	6	1.5	310.64	18.75	329.39
181	1119	C	33	X	7	0.2	312.14	18.75	330.89
181	1119	C	33	X	CC	0.54	312.34	18.75	331.09
181	1119	C	34	X	1	1.5	313	18.75	331.75
181	1119	C	34	X	2	1.39	314.5	18.75	333.25
181	1119	C	34	X	3	1.5	315.89	18.75	334.64
181	1119	C	34	X	4	1.52	317.39	18.75	336.14
181	1119	C	34	X	CC	0.31	318.91	18.75	337.66
181	1119	C	35	X	1	1.5	322.3	18.75	341.05
181	1119	C	35	X	2	1.5	323.8	18.75	342.55
181	1119	C	35	X	3	1.5	325.3	18.75	344.05
181	1119	C	35	X	4	1.5	326.8	18.75	345.55
181	1119	C	35	X	5	1.5	328.3	18.75	347.05
181	1119	C	35	X	6	1.5	329.8	18.75	348.55
181	1119	C	35	X	7	0.42	331.3	18.75	350.05
181	1119	C	35	X	CC	0.29	331.72	18.75	350.47
181	1119	C	36	X	1	1.5	331.9	18.75	350.65
181	1119	C	36	X	2	1.5	333.4	18.75	352.15
181	1119	C	36	X	3	1.5	334.9	18.75	353.65

Table T10 (continued).

Leg	Site	Hole	Core	Type	Section	Section length	Depth (mbsf)	Offset	Composite depth (mcd)
181	1119	C	36	X	4	1.5	336.4	18.75	355.15
181	1119	C	36	X	5	0.65	337.9	18.75	356.65
181	1119	C	36	X	CC	0.33	338.55	18.75	357.3
181	1119	C	37	X	1	1.5	341.5	18.75	360.25
181	1119	C	37	X	CC	0.26	343	18.75	361.75
181	1119	C	37	X	1	1.5	351.1	18.75	369.85
181	1119	C	38	X	2	1.5	352.6	18.75	371.35
181	1119	C	38	X	3	1.5	354.1	18.75	372.85
181	1119	C	38	X	4	1.5	355.6	18.75	374.35
181	1119	C	38	X	5	1.5	357.1	18.75	375.85
181	1119	C	38	X	6	1.24	358.6	18.75	377.35
181	1119	C	38	X	CC	0.38	359.84	18.75	378.59
181	1119	C	39	X	1	1.5	360.8	18.75	379.55
181	1119	C	39	X	2	0.87	362.3	18.75	381.05
181	1119	C	39	X	CC	0.32	363.17	18.75	381.92
181	1119	C	40	X	1	1.5	370.5	18.75	389.25
181	1119	C	40	X	2	1.26	372	18.75	390.75
181	1119	C	40	X	CC	0.3	373.26	18.75	392.01
181	1119	C	41	X	1	1.5	380.1	18.75	398.85
181	1119	C	41	X	2	0.35	381.6	18.75	400.35
181	1119	C	41	X	CC	0.34	381.95	18.75	400.7
181	1119	C	42	X	1	1.5	389.8	18.75	408.55
181	1119	C	42	X	2	1.5	391.3	18.75	410.05
181	1119	C	42	X	3	1.5	392.8	18.75	411.55
181	1119	C	42	X	4	1.5	394.3	18.75	413.05
181	1119	C	42	X	5	0.25	395.8	18.75	414.55
181	1119	C	42	X	CC	0.29	396.05	18.75	414.8
181	1119	C	43	X	1	1.5	399.4	18.75	418.15
181	1119	C	43	X	2	1.4	400.9	18.75	419.65
181	1119	C	43	X	CC	0.34	402.3	18.75	421.05
181	1119	C	44	X	1	1.5	409	18.75	427.75
181	1119	C	44	X	2	1.5	410.5	18.75	429.25
181	1119	C	44	X	3	1.5	412	18.75	430.75
181	1119	C	44	X	4	1.5	413.5	18.75	432.25
181	1119	C	44	X	5	1.5	415	18.75	433.75
181	1119	C	44	X	6	1.5	416.5	18.75	435.25
181	1119	C	44	X	7	0.47	418	18.75	436.75
181	1119	C	44	X	CC	0.43	418.47	18.75	437.22
181	1119	C	45	X	1	0.64	418.6	18.75	437.35
181	1119	C	45	X	CC	0.18	419.24	18.75	437.99
181	1119	C	46	X	1	1.5	428.2	18.75	446.95
181	1119	C	46	X	2	1.5	429.7	18.75	448.45
181	1119	C	46	X	3	1.5	431.2	18.75	449.95
181	1119	C	46	X	4	1.5	432.7	18.75	451.45
181	1119	C	46	X	5	1.5	434.2	18.75	452.95
181	1119	C	46	X	6	1.5	435.7	18.75	454.45
181	1119	C	46	X	CC	0.62	437.2	18.75	455.95
181	1119	C	47	X	1	1.5	437.9	18.75	456.65
181	1119	C	47	X	2	1.5	439.4	18.75	458.15
181	1119	C	47	X	3	1.5	440.9	18.75	459.65
181	1119	C	47	X	4	1.5	442.4	18.75	461.15
181	1119	C	47	X	5	1.5	443.9	18.75	462.65
181	1119	C	47	X	6	1.5	445.4	18.75	464.15
181	1119	C	47	X	7	0.43	446.9	18.75	465.65
181	1119	C	47	X	CC	0.19	447.33	18.75	466.08
181	1119	C	48	X	1	1.5	447.2	18.75	465.95
181	1119	C	48	X	2	1.5	448.7	18.75	467.45
181	1119	C	48	X	3	1.5	450.2	18.75	468.95
181	1119	C	48	X	7	1.5	451.7	18.75	470.45
181	1119	C	48	X	5	1.5	453.2	18.75	471.95
181	1119	C	48	X	6	1.5	454.7	18.75	473.45
181	1119	C	48	X	7	0.36	456.2	18.75	474.95
181	1119	C	48	X	CC	0.44	456.56	18.75	475.31
181	1119	C	49	X	1	1.5	456.8	18.75	475.55
181	1119	C	49	X	2	1.5	458.3	18.75	477.05
181	1119	C	49	X	3	1.5	459.8	18.75	478.55
181	1119	C	49	X	7	1.5	461.3	18.75	480.05
181	1119	C	49	X	8	1.5	462.8	18.75	481.55

Table T10 (continued).

Leg	Site	Hole	Core	Type	Section	Section length	Depth (mbsf)	Offset	Composite depth (mcd)
181	1119	C	49	X	9	0.95	464.3	18.75	483.05
181	1119	C	49	X	CC	0.32	465.25	18.75	484
181	1119	C	50	X	1	1.5	466.4	18.75	485.15
181	1119	C	50	X	2	1.5	467.9	18.75	486.65
181	1119	C	50	X	3	1.5	469.4	18.75	488.15
181	1119	C	50	X	4	1.5	470.9	18.75	489.65
181	1119	C	50	X	5	1.5	472.4	18.75	491.15
181	1119	C	50	X	6	1.5	473.9	18.75	492.65
181	1119	C	50	X	7	0.35	475.4	18.75	494.15
181	1119	C	50	X	CC	0.32	475.75	18.75	494.5
181	1119	C	51	X	1	1.5	475.6	18.75	494.35
181	1119	C	51	X	2	1.5	477.1	18.75	495.85
181	1119	C	51	X	3	1.5	478.6	18.75	497.35
181	1119	C	51	X	4	1.5	480.1	18.75	498.85
181	1119	C	51	X	5	1.5	481.6	18.75	500.35
181	1119	C	51	X	6	0.23	483.1	18.75	501.85
181	1119	C	51	X	CC	0.33	483.33	18.75	502.08
181	1119	C	52	X	1	1.5	485.2	18.75	503.95
181	1119	C	52	X	2	1.5	486.7	18.75	505.45
181	1119	C	52	X	3	1.5	488.2	18.75	506.95
181	1119	C	52	X	4	1.5	489.7	18.75	508.45
181	1119	C	52	X	5	1.5	491.2	18.75	509.95
181	1119	C	52	X	6	1.5	492.7	18.75	511.45
181	1119	C	52	X	7	0.24	494.2	18.75	512.95
181	1119	C	52	X	CC	0.28	494.44	18.75	513.19

Note: This table is also available in **ASCII format.**

Table T11. Splice tie points, Site 1119.

Site	Hole	Core	Type	Section	Depth in section (cm)	Depth (mbsf)	Depth (mcd)		Site	Hole	Core	Type	Section	Depth in section (cm)	Depth (mbsf)	Depth (mcd)
1119	B	1	H	3	76	3.76	3.80	Tie to	1119	C	1	H	3	64.0	3.64	3.80
1119	C	1	H	5	136	7.36	7.52	Tie to	1119	B	2	H	2	108.0	7.28	7.52
1119	B	2	H	6	100	13.20	13.44	Tie to	1119	C	2	H	4	88.0	13.68	13.44
1119	C	2	H	6	100	16.80	16.56	Tie to	1119	B	3	H	1	112.0	15.32	16.56
1119	B	3	H	4	56	19.26	20.50	Tie to	1119	C	3	H	2	148.0	20.78	20.50
1119	C	3	H	6	52	25.82	25.54	Tie to	1119	B	4	H	1	60.0	24.30	25.54
1119	B	4	H	4	8	28.28	29.52	Tie to	1119	C	4	H	2	68.0	29.48	29.52
1119	C	4	H	7	60	36.90	36.94	Tie to	1119	B	5	H	2	87.0	35.63	36.94
1119	B	5	H	6	40	41.11	42.42	Tie to	1119	C	5	H	4	12.0	41.42	42.42
1119	C	5	H	6	92	45.22	46.22	Tie to	1119	B	6	H	1	53.0	43.24	46.22
1119	B	6	H	4	92	48.12	51.10	Tie to	1119	C	6	H	2	104.0	48.84	51.10
1119	C	6	H	6	116	54.96	57.22	Tie to	1119	B	7	H	1	122.0	53.44	57.22
1119	B	7	H	5	44	58.54	62.32	Tie to	1119	C	7	H	3	132.0	59.36	62.32
1119	C	7	H	7	88	64.92	67.88	Tie to	1119	B	8	H	1	88.0	62.58	67.88
1119	B	8	H	6	120	70.45	75.75	Tie to	1119	C	8	H	4	97.5	70.75	75.75
1119	C	8	H	6	56	73.12	78.12	Tie to	1119	B	9	H	1	90.5	72.11	78.12
1119	B	9	H	5	96	78.06	84.07	Tie to	1119	C	9	H	4	22.5	79.37	84.07
1119	C	9	H	7	68	84.32	89.02	Tie to	1119	B	10	H	1	10.0	80.82	89.02
1119	B	10	H	3	140	85.02	93.22	Tie to	1119	C	10	H	3	10.5	87.28	93.22
1119	C	10	H	7	64	93.81	99.75	Tie to	1119	B	11	H	1	10.5	90.31	99.75
1119	B	11	H	5	124	97.44	106.88	Tie to	1119	C	11	H	4	77.0	97.82	106.88
1119	C	11	H	7	124	102.78	111.84	Tie to	1119	B	12	H	2	61.0	101.82	111.84
1119	B	12	H	6	68	107.88	117.90	Tie to	1119	C	12	H	4	52.0	108.32	117.90
1119	C	12	H	6	144	112.24	121.82	Tie to	1119	B	13	H	1	113.0	110.34	121.82
1119	B	13	H	4	44	114.14	125.62	Tie to	1119	C	13	H	2	73.0	115.04	125.62
1119	C	13	H	6	64	120.94	131.52	Tie to	1119	B	14	H	1	65.0	119.36	131.52
1119	B	14	H	5	4	124.79	136.95	Tie to	1119	C	14	H	3	104.0	125.10	136.95
1119	C	14	H	7	140	131.46	143.31	Tie to	1119	B	15	H	1	113.0	129.34	143.31
1119	B	15	H	5	88	135.08	149.05	Tie to	1119	C	15	H	3	24.0	135.04	149.05
1119	C	15	H	7	80	141.6	155.61	Tie to	1119	B	16	H	1	16.0	137.86	155.61
1119	B	16	H	3	32	141.02	158.77	Tie to	1119	C	16	H	3	106.5	144.42	158.77
1119	C	16	H	8	76	151.03	165.38	Tie to	1119	B	17	H	1	8.0	147.28	165.38
1119	B	17	H	5	24	153.47	171.57	Tie to	1119	C	17	H	2	52.0	152.82	171.57
1119	C	17	H	7	88	160.56	179.31									

Note: This table is also available in **ASCII format.**

Table T12. Composition of interstitial waters, Site 1119.

Core, section, interval (cm)	Depth (mbsf)	Depth (mcd)	Salinity	Cl^- (mM)	pH	Alkalinity (mM)	Na^+ (mM)	Mg^{2+} (mM)	Ca^{2+} (mM)	SO_4^{2-} (mM)	HPO_4^{2-} (µM)	NH_4^+ (mM)	H_4SiO_4 (µM)	K^+ (mM)	Li^+ (µM)	Sr^{2+} (µM)
181-1119B-																
1H-2, 145-150	2.95	2.99	34.0	552	7.60	2.18	470	53.1	10.8	28.6	4.5	0.07	281	11.3	30	94
2H-4, 145-150	10.65	10.89	33.0	553	7.89	19.41	456	46.5	5.9	9.8	145	2.19	682	10.0	21	60
3H-4, 145-150	20.15	21.39	32.5	551	7.70	27.73	449	40.7	3.5	0.0	99	4.35	653	9.4	26	55
4H-5, 55-60	29.65	29.99	32.5	550	7.85	26.71	453	38.0	3.6	0.0	209	4.88	640	9.5	24	64
5H-4, 138-143	39.05	40.42	32.0	549	7.72	24.26	457	34.9	3.5	0.0	125	5.05	633	9.6	24	70
6H-4, 145-150	48.65	51.63	32.0	549	7.83	19.35	464	32.0	3.2	0.2	8.9	4.87	636	9.9	31	78
7H-4, 135-140	58.05	61.83	32.0	547	7.98	18.73	464	31.0	3.3	0.0	17.3	4.68	682	10.0	27	80
8H-4, 140-155	67.60	72.90	32.0	548	8.09	17.90	467	29.6	3.3	0.0	18.3	4.64	697	10.1	27	87
9H-4, 135-140	77.00	83.06	31.5	545	7.99	18.16	468	27.3	3.4	0.0	7.5	4.65	690	10.2	33	98
10H-4, 140-150	86.60	94.72	31.5	548		15.83	478	23.5	3.7	0.0	9.1	5.05	710	10.0	41	125
11H-4, 140-150	96.10	105.54	31.0	547	7.99	14.86	474	25.7	3.5	0.0	7.7	4.57	717	9.9	36	111
14H-4, 150-155	124.70	136.86	31.0	551	7.83	14.93	483	22.3	3.7	0.0	5.3	5.60	787	10.1	55	150
17H-4, 140-150	153.10	171.23	31.5	550	7.77	14.33	484	20.7	3.7	0.0	7.7	6.31	754	10.1	62	179
181-1119C-																
17H-4, 140-150	156.70	175.45	31.5	551	7.65	15.12	486	21.0	3.8	0.0	8.7	5.73	745	9.8	62	184
20X-4, 140-150	184.20	202.88	31.5	550	7.79	13.56	488	18.9	3.7	0.0	5.7	6.03	769	9.6	68	214
23X-4, 140-150	213.10	230.87	31.5	555	7.80	12.46	493	18.8	4.1	0.3	5.5	6.46	813	9.5	74	314
26X-4, 140-150	241.90	260.65	31.5	552	7.59	11.82	491	17.6	4.3	0.0	3.1	7.40	839	9.2	74	424
29X-4, 140-150	270.70	289.45	31.5	556	7.60	10.28	495	17.2	4.5	0.0	1.9	7.67	826	8.9	75	582
32X-4, 140-150	299.70	318.45	31.5	556	7.63	10.33	494	17.4	5.0	0.0	2.5	7.61	850	8.7	75	716
35X-4, 140-150	328.20	346.95	31.5	558	7.63	9.27	497	18.4	4.8	1.1	2.9	7.32	944	8.5	65	794
38X-4, 140-150	357.00	375.75	31.5	557	7.65	8.20	489	20.5	5.6	0.9	1.1	8.23	885	8.1	80	969
41X-1, 140-150	381.50	400.25	31.5	559	7.58	6.37	488	21.8	7.4	2.4	1.1	7.92	723	8.0	123	1141
44X-4, 140-150	414.90	433.65	32.0	558	7.53	5.47	483	21.5	9.4	1.4	1.1	7.02	763	7.6	164	1218
47X-4, 140-150	443.80	462.55	32.0	560	7.56	6.45	478	22.0	12.4	0.8	1.3	6.77	868	6.6	172	1359
50X-4, 140-150	472.30	491.05	32.0	562	7.53	5.41	475	24.3	13.3	1.6	1.1	7.21	743	6.5	184	1395

Note: This table is also available in **ASCII format.**

Table T13. Inorganic carbon, carbonate, total carbon, total organic carbon, total nitrogen, total sulfur, and atomic organic carbon/nitrogen values for sediments from Holes 1119B and 1119C. (**See table note.** Continued on next two pages.)

Core, section interval (cm)	Depth (mbsf)	IC (%)	$CaCO_3$ (%)	TC (%)	TOC (%)	TN (%)	TS (%)	$[C/N]_a$
181-1119B-								
1H-2, 45-46	1.95	1.09	9.1					
1H-3, 45-46	3.45	0.78	6.5	1.08	0.29	0.07	0.25	4.9
2H-2, 45-46	6.65	0.06	0.5					
2H-4, 45-46	9.65	0.10	0.8	0.53	0.43	0.07	0.23	7.3
2H-6, 45-46	12.65	0.29	2.4					
3H-1, 100-101	15.20	0.39	3.2					
3H-2, 76-77	16.46	2.87	23.9					
3H-3, 120-121	18.40	0.18	1.5	0.57	0.40	0.07	0.00	6.6
3H-7, 50-51	23.00	0.27	2.2					
4H-1, 105-106	24.75	0.16	1.4					
4H-3, 60-61	27.30	0.18	1.5	0.54	0.36	0.06	0.00	6.5
4H-6, 35-36	30.11	0.18	1.5					
5H-2, 110-111	35.83	0.28	2.3					
5H-4, 75-76	38.48	0.31	2.6	0.75	0.44	0.09	0.00	6.1
5H-5, 145-146	40.61	0.10	0.8					
6H-1, 26-27	42.96	3.76	31.3					
6H-2, 135-136	45.55	3.09	25.8					
6H-5, 30-31	49.00	0.20	1.7	0.69	0.49	0.08	0.44	7.5
7H-3, 69-70	55.89	0.13	1.1	0.48	0.35	0.07	0.26	5.7
7H-3, 110-111	56.30	0.11	0.9					
7H-8, 15-16	61.75	2.31	19.2					
8H-1, 73-74	62.43	0.17	1.4	0.33	0.16	0.08	0.18	2.4
8H-2, 138-139	64.58	2.38	19.9					
8H-6, 106-107	70.31	0.21	1.7					
9H-5, 10-11	77.20	0.17	1.4	0.30	0.13	0.07	0.29	2.3
9H-6, 65-66	79.25	1.47	12.3					
9H-6, 122-123	79.82	3.33	27.7					
10H-4, 58-59	85.70	4.14	34.5					
10H-5, 42-43	87.04	1.28	10.6	1.55	0.27	0.07	0.05	4.6
10H-7, 70-71	90.32	0.38	3.1					
11H-1, 20-21	90.40	0.33	2.7	0.75	0.42	0.08	0.53	6.0
11H-5, 31-32	96.51	4.82	40.1					
11H-5, 108-109	97.28	0.82	6.8					
12H-1, 30-31	100.00	0.43	3.6	0.62	0.19	0.08	0.32	2.8
12H-4, 88-89	105.08	1.47	12.2					
12H-7, 30-31	109.00	1.68	14.0					
13H-1, 40-41	109.60	0.41	3.5	0.63	0.22	0.08	0.42	3.0
13H-3, 40-41	112.60	1.63	13.6					
14H-2, 45-46	120.65	7.24	60.3					
14H-4, 45-46	123.65	0.46	3.9	0.84	0.37	0.07	0.38	6.0
14H-6, 45-46	126.70	0.99	8.2					
15H-2, 45-46	130.15	1.61	13.4					
15H-4, 45-46	133.15	0.51	4.2	0.72	0.21	0.09	0.51	2.9
15H-6, 45-46	136.15	1.34	11.2					
16H-2, 69-70	139.89	0.13	1.1					
16H-3, 128-129	141.98	2.94	24.5	3.28	0.35	0.08	0.40	4.8
16H-6, 70-71	145.90	1.28	10.7					
17H-1, 20-21	147.40	1.66	13.9	2.15	0.49	0.11	0.47	5.3
17H-2, 109-110	149.79	0.37	3.1					
17H-4, 86-87	152.59	5.89	49.1					
181-1119C-								
17H-2, 20-21	152.50	0.35	2.9					
17H-5, 20-21	157.00	0.59	4.9	0.63	0.04	0.08	0.30	0.6
17H-CC, -0-21	160.77	2.54	21.1					
18X-1, 60-61	160.90	0.45	3.8					
18X-3, 78-79	163.93	0.59	4.9	1.03	0.44	0.09	0.26	5.9
18X-7, 16-17	168.74	3.34	27.8					
19X-2, 72-73	170.92	0.24	2.0					
19X-4, 41-42	173.35	0.25	2.1	0.67	0.42	0.08	0.32	6.0
19X-5, 30-31	174.74	0.26	2.2					
20X-2, 31-32	180.11	0.49	4.1					
20X-4, 86-87	183.59	6.56	54.6					
20X-6, 84-85	186.46	0.50	4.2	0.58	0.08	0.08	0.25	1.3
21X-1, 67-68	188.57	0.29	2.4					

Table T13 (continued).

Core, section interval (cm)	Depth (mbsf)	IC (%)	$CaCO_3$ (%)	TC (%)	TOC (%)	TN (%)	TS (%)	$[C/N]_a$
21X-3, 88-89	191.78	0.82	6.8					
21X-4, 68-69	193.08	0.28	2.3	0.51	0.23	0.09	0.58	3.0
22X-4, 130-131	202.19	1.04	8.6					
22X-6, 71-72	204.60	3.34	27.8	3.61	0.26	0.07	0.33	4.5
22X-7, 40-41	205.79	0.94	7.8					
23X-7, 104-105	215.99	0.20	1.6	0.28	0.08	0.07	0.15	1.3
23X-7, 110-111	216.05	0.65	5.4					
25X-2, 113-114	229.03	0.63	5.3					
25X-6, 37-38	234.27	6.19	51.6	6.44	0.25	0.08	0.43	3.9
25X-6, 130-131	235.20	0.48	4.0					
26X-1, 30-32	236.30	0.32	2.6					
26X-3, 120-122	240.20	0.67	5.6	1.12	0.45	0.09	0.24	6.2
26X-6, 20-22	243.70	4.41	36.7					
27X-1, 6-7	245.66	0.95	7.9					
27X-1, 136-137	246.96	5.19	43.2					
27X-3, 100-101	249.60	3.59	29.9	4.24	0.66	0.12	0.61	6.2
28X-2, 130-131	258.00	0.39	3.2					
28X-3, 110-111	259.30	2.49	20.8	3.04	0.55	0.09	0.32	7.3
28X-5, 80-81	262.00	5.69	47.4					
29X-2, 100-102	267.30	5.06	42.2					
29X-4, 100-101	270.30	1.53	12.7	1.76	0.24	0.08	0.54	3.4
29X-6, 99-100	273.29	2.12	17.6					
30X-1, 102-103	275.52	0.59	4.9					
30X-2, 112-113	277.12	0.72	6.0	1.12	0.40	0.08	0.44	5.9
30X-4, 109-110	280.09	3.17	26.4					
31X-2, 99-101	285.56	2.17	18.1					
31X-4, 99-101	288.56	0.37	3.1	0.74	0.37	0.09	0.52	5.0
31X-7, 99-101	293.06	0.30	2.5					
32X-1, 80-81	294.60	0.23	2.0					
32X-3, 80-81	297.60	0.36	3.0					
32X-6, 130-131	302.60	2.26	18.8					
33X-1, 30-31	303.70	8.16	68.0					
33X-3, 84-85	307.24	1.63	13.6					
33X-5, 108-109	310.22	1.97	16.4					
34X-1, 69-70	313.69	1.56	13.0					
34X-3, 103-104	316.92	5.20	43.3	5.71	0.51	0.08	0.22	7.7
34X-4, 83-84	318.22	8.72	72.7					
35X-1, 89-90	323.19	2.76	23.0	3.18	0.41	0.08	0.15	5.9
35X-3, 89-90	326.19	0.56	4.7					
35X-5, 89-90	329.19	1.83	15.3					
36X-1, 100-101	332.90	0.74	6.1	0.98	0.24	0.09	0.66	3.2
36X-4, 100-101	337.40	7.37	61.4					
36X-5, 50-51	338.40	7.19	59.9					
37X-1, 110-111	342.60	7.33	61.0	7.59	0.26	0.08	0.21	3.8
38X-1, 33-34	351.43	8.40	69.9					
38X-3, 82-83	354.92	0.65	5.4					
38X-6, 104-105	359.64	0.20	1.6	0.41	0.21	0.08	0.19	3.3
39X-1, 54-55	361.34	0.45	3.7	0.6	0.15	0.09	0.19	1.9
39X-2, 74-75	363.04	6.66	55.4					
40X-1, 70-71	371.20	0.88	7.4	1.18	0.3	0.08	0.25	4.5
40X-2, 77-78	372.77	8.32	69.3					
41X-1, 36-37	380.46	1.95	16.2	1.97	0.03	0.1	0.38	0.3
41X-1, 113-114	381.23	1.34	11.2					
42X-1, 123-124	391.03	2.18	18.1					
42X-3, 102-103	393.82	6.05	50.4					
43X-1, 70-71	400.10	1.12	9.4	1.25	0.12	0.09	0.40	1.7
44X-1, 120-121	410.20	1.05	8.7					
44X-5, 20-21	415.20	3.36	28.0					
44X-7, 16-17	418.16	3.39	28.3	3.99	0.60	0.08	0.12	8.3
46X-1, 101-102	429.21	0.79	6.6					
46X-3, 72-73	431.92	0.43	3.6					
46X-6, 128-129	436.98	0.29	2.4	0.81	0.52	0.08	0.58	7.2
47X-3, 33-34	441.23	0.61	5.1					
47X-4, 45-46	442.85	0.44	3.7					
47X-6, 89-90	446.29	0.41	3.4	0.86	0.44	0.08	0.49	6.5
49X-3, 18-19	459.98	0.79	6.6					
49X-3, 108-109	460.88	0.86	7.2					
49X-5, 91-92	463.71	0.99	8.2	1.51	0.52	0.09	0.00	5.5
50X-4, 77-78	471.67	1.19	9.9					

Table T13 (continued).

Core, section interval (cm)	Depth (mbsf)	IC (%)	$CaCO_3$ (%)	TC (%)	TOC (%)	TN (%)	TS (%)	$[C/N]_a$
51X-3, 1-2	478.61	0.53	4.4					
51X-4, 49-50	480.59	0.79	6.6	1.37	0.58	0.09	0.00	7.6
52X-1, 85-86	486.05	0.95	7.9					
52X-4, 76-77	490.46	1.48	12.3					
52X-6, 73-74	493.43	1.85	15.4	2.56	0.71	0.08	0.30	10.4

Note: Carbonate is calculated assuming that all inorganic carbon is calcite. This table is also available in **ASCII format.**

Table T14. List of index properties measured from Holes 1119B and 1119C. (See table note. Continued on next two pages.)

Leg	Hole	Core	Section	Interval (cm)	Depth (mbsf)	Wet-water content (%)	Dry-water content (%)	Wet-bulk density (g/cm^3)	Dry density (g/cm^3)	Grain density (g/cm^3)	Porosity (%)	Void ratio
181	1119B	1H	1	131-133	1.31	32.6	48.4	1.774	1.195	2.747	56.5	1.299
181	1119B	1H	3	113-115	4.13	34.1	51.7	1.741	1.148	2.729	57.9	1.378
181	1119B	2H	1	122-124	5.92	31.2	45.4	1.821	1.252	2.814	55.5	1.247
181	1119B	2H	3	108-110	8.78	30.9	44.7	1.824	1.261	2.803	55	1.223
181	1119B	2H	5	108-110	11.78	30.5	43.9	1.822	1.266	2.77	54.3	1.189
181	1119B	2H	7	48-50	14.18	28.8	40.4	1.871	1.333	2.81	52.6	1.108
181	1119B	3H	1	138-140	15.58	28.6	40	1.863	1.33	2.773	52	1.084
181	1119B	3H	3	118-120	18.38	27	36.9	1.904	1.39	2.788	50.1	1.005
181	1119B	3H	5	122-124	21.42	27.4	37.8	1.893	1.373	2.787	50.7	1.029
181	1119B	3H	8	8-10	23.38	25.9	35	1.932	1.432	2.801	48.9	0.956
181	1119B	4H	1	124-126	24.94	26.8	36.5	1.895	1.388	2.749	49.5	0.981
181	1119B	4H	3	123-125	27.93	26.4	35.8	1.911	1.407	2.77	49.2	0.97
181	1119B	4H	5	41-43	29.61	27.4	37.7	1.886	1.37	2.762	50.4	1.016
181	1119B	5H	1	120-122	34.4	29.6	42	1.843	1.298	2.773	53.2	1.136
181	1119B	5H	3	134-136	37.57	28.3	39.5	1.87	1.34	2.777	51.7	1.072
181	1119B	5H	5	142-144	40.58	28.4	39.7	1.854	1.328	2.733	51.4	1.058
181	1119B	5H	7	76-78	43.02	28.9	40.7	1.854	1.318	2.768	52.4	1.1
181	1119B	6H	1	125-127	43.95	27.9	38.7	1.865	1.345	2.735	50.8	1.034
181	1119B	6H	3	115-117	46.85	27.4	37.7	1.862	1.352	2.695	49.8	0.993
181	1119B	6H	5	142-144	50.12	26.7	36.4	1.902	1.394	2.766	49.6	0.984
181	1119B	6H	7	80-82	52.5	25.9	35	1.922	1.424	2.774	48.7	0.948
181	1119B	7H	1	139-141	53.59	27	37	1.902	1.388	2.787	50.2	1.007
181	1119B	7H	3	132-134	56.52	25.4	34.1	1.937	1.445	2.78	48	0.925
181	1119B	7H	5	134-136	59.44	26.4	35.8	1.914	1.409	2.779	49.3	0.972
181	1119B	7H	7	26-28	61.36	27.3	37.5	1.905	1.385	2.812	50.7	1.03
181	1119B	8H	1	132-134	63.02	26.3	35.6	1.928	1.422	2.813	49.4	0.978
181	1119B	8H	3	124-126	65.94	24.5	32.4	1.963	1.483	2.793	46.9	0.883
181	1119B	8H	5	112-114	68.87	26.2	35.5	1.918	1.415	2.779	49.1	0.964
181	1119B	8H	7	88-90	71.63	26.4	35.9	1.908	1.404	2.764	49.2	0.969
181	1119B	9H	1	132-134	72.52	26.5	36	1.918	1.41	2.795	49.5	0.982
181	1119B	9H	3	128-130	75.48	30.7	44.3	1.796	1.245	2.695	53.8	1.165
181	1119B	9H	5	133-135	78.43	26.4	36	1.931	1.42	2.833	49.9	0.995
181	1119B	9H	7	100-102	81.1	25	33.4	1.943	1.456	2.775	47.5	0.906
181	1119B	10H	1	126-128	81.96	28.2	39.4	1.85	1.327	2.71	51	1.042
181	1119B	10H	3	143-145	85.05	28.8	40.5	1.84	1.309	2.718	51.8	1.076
181	1119B	10H	5	137-139	87.99	24.8	33	1.942	1.46	2.756	47	0.887
181	1119B	10H	7	80-82	90.42	26.3	35.7	1.921	1.416	2.794	49.3	0.973
181	1119B	11H	1	130-132	91.5	25.4	34.1	1.936	1.444	2.78	48	0.925
181	1119B	11H	3	126-128	94.46	24.9	33.1	1.942	1.459	2.763	47.2	0.894
181	1119B	11H	5	138-140	97.58	24	31.6	1.97	1.497	2.781	46.2	0.857
181	1119B	11H	7	78-80	99.98	25.4	34.1	1.938	1.445	2.786	48.1	0.928
181	1119B	12H	1	142-144	101.12	28.7	40.2	1.862	1.329	2.774	52.1	1.088
181	1119B	12H	3	109-111	103.79	27	37	1.891	1.38	2.754	49.9	0.995
181	1119B	12H	5	136-138	107.06	27.9	38.7	1.875	1.352	2.762	51.1	1.043
181	1119B	12H	7	69-71	109.39	29.9	42.6	1.814	1.272	2.699	52.9	1.122
181	1119B	13H	1	128-130	110.48	28.5	39.9	1.868	1.335	2.783	52	1.085
181	1119B	13H	3	144-146	113.64	25.1	33.5	1.936	1.45	2.76	47.5	0.903
181	1119B	13H	5	120-122	116.4	25.9	34.9	1.93	1.431	2.791	48.7	0.951
181	1119B	13H	7	82-84	119.02	27	37	1.899	1.387	2.777	50.1	1.002
181	1119B	14H	1	125-127	119.95	28	38.8	1.885	1.358	2.8	51.5	1.061
181	1119B	14H	3	138-140	123.08	25.5	34.2	1.931	1.439	2.77	48.1	0.925
181	1119B	14H	5	120-122	125.95	26.2	35.5	1.918	1.416	2.778	49	0.962
181	1119B	14H	7	84-86	128.59	26.5	36.1	1.905	1.399	2.764	49.4	0.975
181	1119B	15H	1	116-118	129.36	29.5	41.8	1.834	1.294	2.741	52.8	1.118
181	1119B	15H	3	143-145	132.63	29	40.8	1.863	1.323	2.798	52.7	1.116
181	1119B	15H	5	106-108	135.26	30.2	43.3	1.815	1.266	2.729	53.6	1.155
181	1119B	15H	7	89-91	138.09	25.2	33.6	1.938	1.45	2.768	47.6	0.908
181	1119B	16H	1	126-128	138.96	25.2	33.7	1.953	1.461	2.813	48.1	0.926
181	1119B	16H	3	135-137	142.05	24	31.5	1.97	1.498	2.78	46.1	0.856
181	1119B	16H	5	124-126	144.94	27.6	38.1	1.905	1.379	2.832	51.3	1.053
181	1119B	16H	7	4-6	146.74	25.1	33.4	1.963	1.471	2.83	48	0.924
181	1119B	17H	1	128-130	148.48	27.3	37.6	1.905	1.384	2.816	50.9	1.035
181	1119B	17H	3	147-149	151.67	27.5	37.9	1.886	1.368	2.769	50.6	1.024
181	1119B	17H	4	75-77	152.48	26.6	36.2	1.915	1.406	2.796	49.7	0.988
181	1119B	17H	5	124-126	154.47	26.2	35.4	1.931	1.426	2.814	49.3	0.973
181	1119C	21X	1	130-132	189.2	26.7	36.5	1.885	1.381	2.721	49.2	0.97
181	1119C	21X	3	125-127	192.15	27.1	37.2	1.899	1.384	2.783	50.3	1.011

Table T14 (continued).

Leg	Hole	Core	Section	Interval (cm)	Depth (mbsf)	Wet-water content (%)	Dry-water content (%)	Wet-bulk density (g/cm^3)	Dry density (g/cm^3)	Grain density (g/cm^3)	Porosity (%)	Void ratio
181	1119C	21X	5	130-132	195.2	27.6	38.2	1.9	1.375	2.82	51.2	1.051
181	1119C	22X	2	130-132	199.19	29.5	41.9	1.84	1.297	2.762	53	1.129
181	1119C	22X	4	135-137	202.24	27.7	38.4	1.884	1.362	2.779	51	1.041
181	1119C	22X	6	130-132	205.19	27.8	38.5	1.873	1.352	2.75	50.8	1.034
181	1119C	23X	2	130-132	209.02	28.2	39.2	1.854	1.332	2.719	51	1.042
181	1119C	23X	4	130-132	212.02	28.3	39.4	1.866	1.338	2.763	51.6	1.064
181	1119C	23X	7	130-132	216.25	25.3	33.8	1.924	1.438	2.739	47.5	0.905
181	1119C	26X	1	130-132	237.3	27.3	37.6	1.9	1.381	2.8	50.7	1.028
181	1119C	26X	3	130-132	240.3	26.4	35.8	1.9	1.399	2.74	49	0.959
181	1119C	26X	5	130-132	243.3	28.6	40.1	1.853	1.323	2.744	51.8	1.075
181	1119C	27X	1	130-132	246.9	25.5	34.2	1.917	1.429	2.73	47.7	0.911
181	1119C	27X	3	130-132	249.9	28.4	39.7	1.847	1.322	2.711	51.2	1.05
181	1119C	27X	5	130-132	252.9	26.8	36.5	1.893	1.386	2.744	49.5	0.979
181	1119C	28X	1	130-132	256.5	25.7	34.6	1.92	1.426	2.754	48.2	0.931
181	1119C	28X	3	130-132	259.5	26.3	35.6	1.899	1.4	2.73	48.7	0.95
181	1119C	28X	5	130-132	262.5	25.6	34.4	1.902	1.415	2.699	47.6	0.907
181	1119C	29X	3	130-132	269.1	27.2	37.4	1.901	1.383	2.8	50.6	1.024
181	1119C	29X	5	130-132	272.1	28.5	39.8	1.853	1.326	2.735	51.5	1.063
181	1119C	30X	1	130-132	275.8	23.6	30.9	1.975	1.508	2.77	45.6	0.837
181	1119C	30X	3	130-132	278.8	26.7	36.4	1.881	1.379	2.706	49	0.961
181	1119C	30X	5	130-132	281.8	28.9	40.7	1.851	1.316	2.758	52.3	1.096
181	1119C	31X	2	130-132	285.87	30.2	43.3	1.826	1.274	2.761	53.8	1.167
181	1119C	31X	4	130-132	288.87	25.2	33.7	1.933	1.446	2.758	47.6	0.908
181	1119C	31X	6	130-132	291.87	24.6	32.7	1.939	1.461	2.739	46.6	0.874
181	1119C	32X	1	133-135	295.13	26.3	35.7	1.905	1.403	2.75	49	0.96
181	1119C	32X	3	130-132	298.1	27.1	37.1	1.891	1.38	2.758	50	0.999
181	1119C	32X	5	130-132	301.1	25.9	34.9	1.928	1.429	2.788	48.7	0.951
181	1119C	33X	1	130-132	304.7	22.1	28.4	2.005	1.562	2.754	43.3	0.763
181	1119C	33X	3	110-112	307.5	28.3	39.5	1.855	1.33	2.73	51.3	1.052
181	1119C	33X	5	130-132	310.44	29.7	42.3	1.828	1.285	2.737	53	1.129
181	1119C	34X	2	120-122	315.7	27.8	38.5	1.877	1.355	2.766	51	1.041
181	1119C	34X	4	130-132	318.69	25.4	34.1	1.944	1.45	2.801	48.2	0.932
181	1119C	35X	1	100-102	323.3	26.3	35.7	1.906	1.405	2.75	48.9	0.958
181	1119C	35X	3	100-102	326.3	26.8	36.5	1.902	1.393	2.77	49.7	0.989
181	1119C	35X	5	130-132	329.6	28	38.9	1.889	1.36	2.812	51.6	1.068
181	1119C	36X	1	120-122	333.1	30	42.9	1.86	1.302	2.862	54.5	1.198
181	1119C	36X	3	120-122	336.1	26.2	35.5	1.891	1.395	2.704	48.4	0.938
181	1119C	36X	5	30-32	338.2	26.5	36.1	1.899	1.395	2.745	49.2	0.968
181	1119C	37X	1	140-142	342.9	24.4	32.3	1.934	1.461	2.712	46.1	0.856
181	1119C	38X	1	120-122	352.3	25.1	33.5	1.947	1.458	2.787	47.7	0.911
181	1119C	38X	3	130-132	355.4	26	35.2	1.911	1.413	2.749	48.6	0.945
181	1119C	38X	5	130-132	358.4	25.1	33.5	1.954	1.464	2.811	47.9	0.921
181	1119C	39X	2	80-82	363.1	23.3	30.3	1.968	1.511	2.731	44.7	0.808
181	1119C	40X	1	110-112	371.6	28.1	39.1	1.881	1.353	2.795	51.6	1.066
181	1119C	41X	1	110-112	381.2	27.6	38.1	1.88	1.361	2.759	50.6	1.026
181	1119C	42X	1	130-132	391.1	25.3	33.9	1.945	1.453	2.798	48.1	0.925
181	1119C	42X	3	130-132	394.1	26.4	35.8	1.901	1.4	2.744	49	0.96
181	1119C	43X	1	130-132	400.7	27.2	37.4	1.902	1.384	2.801	50.6	1.024
181	1119C	44X	2	130-132	411.8	26	35.2	1.924	1.423	2.785	48.9	0.957
181	1119C	44X	4	130-132	414.8	25.4	34	1.924	1.436	2.743	47.6	0.91
181	1119C	45X	1	40-42	419	26	35.2	1.909	1.413	2.744	48.5	0.942
181	1119C	46X	2	130-132	431	20.8	26.3	2.018	1.598	2.712	41.1	0.698
181	1119C	46X	4	115-116	433.85	3.8	4	2.65	2.549	2.829	9.9	0.11
181	1119C	46X	4	125-127	433.95	9.5	10.4	2.435	2.204	2.844	22.5	0.29
181	1119C	46X	6	50-52	436.2	14.5	17	2.231	1.907	2.792	31.7	0.464
181	1119C	47X	1	130-132	439.2	24.2	31.9	1.96	1.486	2.765	46.2	0.86
181	1119C	47X	3	130-132	442.2	24.6	32.6	1.971	1.487	2.819	47.3	0.897
181	1119C	47X	5	130-132	445.2	23.9	31.3	1.966	1.497	2.763	45.8	0.846
181	1119C	48X	1	130-132	448.5	23.1	30	1.988	1.529	2.77	44.8	0.812
181	1119C	48X	3	130-132	451.5	22.7	29.4	1.991	1.539	2.755	44.2	0.791
181	1119C	48X	5	130-132	454.5	24.9	33.2	1.942	1.457	2.765	47.3	0.897
181	1119C	49X	3	130-132	461.1	26.7	36.4	1.908	1.399	2.783	49.7	0.989
181	1119C	49X	5	128-130	464.08	24.9	33.1	1.948	1.463	2.778	47.3	0.898
181	1119C	50X	1	128-130	467.68	27	37	1.915	1.398	2.824	50.5	1.02
181	1119C	50X	3	131-133	470.71	24.8	33	1.959	1.473	2.801	47.4	0.902
181	1119C	50X	5	130-132	473.7	24.2	32	1.975	1.496	2.809	46.8	0.878
181	1119C	51X	1	130-132	476.9	25.6	34.4	1.932	1.437	2.783	48.4	0.936
181	1119C	51X	3	129-131	479.89	26.6	36.2	1.931	1.418	2.841	50.1	1.003

Table T14 (continued).

Leg	Hole	Core	Section	Interval (cm)	Depth (mbsf)	Wet-water content (%)	Dry-water content (%)	Wet-bulk density (g/cm^3)	Dry density (g/cm^3)	Grain density (g/cm^3)	Porosity (%)	Void ratio
181	1119C	52X	1	126-128	486.46	26.1	35.2	1.929	1.426	2.802	49.1	0.964
181	1119C	52X	3	132-134	489.52	25	33.3	1.93	1.448	2.735	47.1	0.889
181	1119C	52X	5	127-129	492.47	25.2	33.7	1.937	1.448	2.77	47.7	0.913

Note: This table is also available in **ASCII format.**